

# Chapter 2

## Application of MATLAB/SIMULINK in Solar PV Systems

### Learning Objectives

On completion of this chapter, the reader will have knowledge on:

- Basic components of Solar PV system and its merits and demerits.
- Involvement of power electronic devices in Solar PV components.
- MATLAB/SIMULINK model of different control strategies of power conditioning unit.
- Importance of MATLAB/SIMULINK model in improving the efficiency of the overall solar PV system.
- Characteristics of Solar PV panel and its MATLAB/SIMULINK model.
- Characteristics and MATLAB/SIMULINK model of Solar PV power conditioning unit.

MATLAB and Power electronics application ranges from power supplies to robotic controls, industrial automation, automotive, industrial drives, power quality, and renewable energy systems. In particular, before the installation of power plant, MATLAB finds applications in selecting the system based on the requirements and to choose particular components for the Solar PV application. This chapter is to explore the role and possibility of MATLAB along with its tool boxes in Solar PV Systems to promote Modeling, and Simulation with emphasis on Analysis, and Design. In renewable energy systems applications, MATLAB helps for selecting the matrix manipulations in the converters to grid inverter, plotting of functions and data, implementation of MPPT algorithms, creation of user interfaces for monitoring the Solar PV modules and for interfacing with inverters and converters, wherein which control algorithms would be written in other languages. As a result of the MATLAB simulation of the components of the solar PV system one can benefit from this model as a photovoltaic generator in the framework of the MATLAB/SIMULINK toolbox in the field of solar PV power conversion systems. In addition,

such models discussed in this chapter would provide a tool to predict the behavior of solar PV cell, module and array, charge controller, SOC battery, inverter, and MPPT, under climate and physical parameters changes.

## 2.1 Basics of Solar PV

A photovoltaic system is made up of several photovoltaic solar cells. An individual small PV cell is capable of generating about 1 or 2 W of power approximately depends of the type of material used. For higher power output, PV cells can be connected together to form higher power modules. In the market the maximum power capacity of the module is 1 kW, even though higher capacity is possible to manufacture, it will become cumbersome to handle more than 1 kW module. Depending upon the power plant capacity or based on the power generation, group of modules can be connected together to form an array.

Solar PV systems are usually consists of numerous solar arrays, although the modules are from the same manufactures or from the same materials, the module performance characteristics varies and on the whole the entire system performance is based on the efficiency or the performance of the individual components. Apart from the solar PV module the system components comprises a battery charge controller, an inverter, MPPT controller and some of the low voltage switchgear components. Presently in the market, power conditioning unit consists of charge controller, inverter and MPPT controller. A Balance-of-System (BoS) includes components and equipments that convert DC supply from the solar PV module to AC grid supply. In general, BOS of the solar PV system includes all the components of the system except the Solar PV modules. In addition to inverters, this includes the cables/wires, switches, enclosures, fuses, ground fault detectors, surge protectors, etc. BOS applies to all types of solar applications (i.e. commercial, residential, agricultural, public facilities, and solar parks).

In many systems, the cost of BOS equipment can equal or exceed the cost of the PV modules. When examining the costs of PV modules, these costs do not include the cost of BOS equipment. In a typical battery based solar PV system the cost of the modules is 20–30 % of the total while the remaining 70 % is the balance of systems (BOS). Apart from the 50 % of the system BOS costs a lot more maintenance expense is also required for proper maintenance of the BOS. By controlling the balance-of-system components, increase efficiency, and modernize solar PV systems can be maintained. BOS components include the majority of the pieces, which make up roughly 10–50 % of solar purchasing and installation costs, and account for the majority of maintenance requirements. Thus, suitable integration of the BOS is vital for the proper functionality and the reliability of the solar PV system. However it is often completely overlooked and poorly integrated. Costs are steadily decreasing with regard to solar panels and inverters.

As per the statistics, the Solar PV module world market is steadily growing at the rate of 30 % per year. The reasons behind this growth are that the reliable

production of electricity without fuel consumption anywhere there is light and the flexibility of PV systems. Also the solar PV systems using modular technology and the components of Solar PV can be configured for varying capacity, ranging from watts to megawatts. Earlier, large variety of solar PV applications found to be in industries but now it is being used for commercial as well as for domestic needs.

One of the hindrance factor is the efficiency of the solar PV cell, in the commercial market a cell efficiency of up to 18.3 % is currently obtained, depending on the technology that is used. When it is related to the module efficiency, it is slightly lower than the cell efficiency. This is due to the blank spaces between the arrays of solar cells in the module. The overall system efficiency includes the efficiency and the performance of the entire components in the system and also depends on the solar installation. Here there is another numerical drop in value when compared to the module efficiency, this being due to conductance losses, e.g., in cables. In the case of inverter, it converts the DC output from the Solar PV module to the AC grid voltage with a certain degree of efficiency. It depends upon conversion efficiency and the precision and quickness of the MPP tracking called tracking efficiency. MPP tracking which is having an efficiency of 98–99 % is available in the market, each and every MPPT is based on a particular tracking algorithm.

Current research states that all materials have physical limits on the electricity that they can generate. For example, the maximum efficiency of crystalline silicon is only 28 %. But tandem cells provide immense scope for development in coming years. Efficiency of existing laboratory cells has already achieved efficiency values of over 25 %. PV Modules with BOS components known as an entire PV system. This system is usually sufficient to meet a particular energy demand, such as powering a water pump, the appliances and lights in a home, and electrical requirements of a community.

In the cost of PV systems and in consumer acceptance, reliability of PV arrays is a crucial factor. With the help of fault-tolerant circuit design, reliability can be improved using various redundant features in the circuit to control the effect of partial failure on overall module yield and array power degradation. Degradation can be limited by dividing the modules into a number of parallel solar cell networks. This type of design can also improve module losses caused by broken cells. The hot-spots in the Solar PV module can be avoided by having diodes across each cell and that is called as bypass diodes. Practically a solar PV module consists of one bypass diode for 18 cells to mitigate the effects of local cell hot-spots.

## 2.2 PV Module Performance Measurements

Peak watt rating is a key performance measurement of PV module. The peak watt ( $W_p$ ) rating is determined by measuring the maximum power of a PV module under laboratory Standard Test Conditions (STC). These conditions related to the maximum power of the PV module are not practical. Hence, researchers must use the

NOCT (Nominal Operating Cell Temperature) rating. In reality, either of the methods is designed to indicate the performance of a solar module under realistic operating conditions. Another method is to consider the whole day rather than “peak” sunshine hours and it is based on some of the factors like light levels, ambient temperature, and air mass and also based on a particular application.

Solar arrays can provide specific amount of electricity under certain conditions. In order to determine array performance, following factors to be considered: (i) characterization of solar cell electrical performance (ii) degradation factors related to array design (iii) assembly, conversion of environmental considerations into solar cell operating temperatures and (iv) array power output capability. The following performance criteria determines the amount of PV output.

**Power Output** Power output is represented in watts and it is the power available at the charge controller/regulator specified either as peak power or average power produced during one day.

**Energy Output** Energy Output indicates the amount of energy produced during a certain period of time and it is represented in Wh/m<sup>2</sup>.

**Conversion Efficiency** It is defined as energy output from array to the energy input from sun. It is also referred as power efficiency and it is equal to power output from array to the power input from sun. Power is typically given in units of watts (W), and energy is typical in units of watt-hours (Wh).

To ensure the consistency, safety and quality of Solar PV system components and to increase consumer confidence in system performance IEEE, Underwriters Laboratories (UL), International Electrotechnical Commission (IEC), AM0 Spectrum (ASTM) are working on standards and performance criteria for PV systems.

### ***2.2.1 Balance of System and Applicable Standards***

The market access requirements for PV equipment are segmented into safety and performance. UL is a global leader in energy product testing and certification. The focus of the UL standards is in providing requirements for materials, construction and the evaluation of the potential electrical shock, fire safety hazard and also testing and certification according to the appropriate energy standard. UL certifies that PV equipment complies with the safety, environmental and other performance requirements of the appropriate standards.

IEC focus on the requirements in terms and symbols, testing, design qualification and type approval. UL supports manufacturers with the compliance to both the UL and the IEC requirements. In addition, UL provides balance of systems equipment certification to the standards identified in the diagram. These certifications include materials (such as polymeric used for back sheets, encapsulates, and adhesives), components (like junction boxes and connectors) and end-products (for example, inverters and meters). Even though the design of solar PV system

**Table 2.1** UL standards used for the BOS components

Description	UL standards
PV modules testing and certification	UL 1703
	IEC/EN 61215, IEC/EN 61646
	IEC 61730/UL 790 (Fire Test)
	UL-SU 8703 (CPV)
Mounting system	UL-SU 1703 –A
Tracking system	UL-SU 9703
Combiner box	UL 1741
Inverter	UL 1741
	IEC 62109
Batteries	UL 1989, UL 2054
	UL-SU 2580, UL-SU 1973

components can be done with the help of mathematical calculations or by using dedicated software, there are certain protocols and standards in selecting the BOS components which should be adhered to while installing a PV system. The UL standards used for the corresponding BOS components of the Solar PV system are as shown in Table 2.1 above.

As these issues might seem insignificant during the installation, they affect the system performance, efficiency, reliability, maintenance cost and aesthetics in the long run. The BOS components can be divided into the following categories based on their basic functions: (i) Mounting Structure (ii) Power Conditioning Units (iii) Cables/Protection devices and (iv) Storage devices.

**2.2.1.1 Mounting Structure**

The PV module should be designed in such a way that it can withstand rain, hail, wind and other adverse conditions. The common made mistakes in selection of the mounting structures are (i) Durability of the design (ii) Tilt angle (iii) Orientation and (iv) PV array shading. Tilting angle optimally varies the efficiency of the solar PV module so, the mounting structure also serves as a PV module tilting structure which tilts the PV arrays at an angle determined by the latitude of the site location, to maximize the solar insolation falling on the panels. The optimum tilt angle required to maximize the solar insolation changes as the position of the sun varies every month.

Similarly, shading has a significant effect on PV generation. Partial shading can reduce the system production up to 90 %. Thus, it is essential that the PV arrays to be installed at a suitable location without any difficulties. To identify the shading levels at any location, software and online tools are available. Some of commonly used tools are – Sun path, Eco tech, Celeste lite etc. For PV array installation with multiple rows the shading de-rate factor should account for losses that may occur when a row shades an adjacent row.

### **2.2.1.2 Power Conditioners**

In the off-grid inverter in a battery based PV system, it is important to review the efficiency and the self-power consumption of the inverter along with the capacity, power quality and surge rating. Generally inverter is normally sized to support the load, power factor and surge. For the efficient operation of the inverter, it should have low self consumption to increase the battery life. A high self consumption inverter, continuously drains the battery which results in lower back up and decrease the battery life cycle due to increased discharge. Further, as the efficiency of the inverter changes with respect to the load, it is good practice to design the load on average efficiency rather than the peak efficiency. In a typical inverter, the peak efficiency is mostly between 20 % and 30 % of the total capacity.

### **2.2.1.3 Cables and Protection Devices**

The main purpose of cabling is to allow a safe passage of current. Appropriate cable sizing allows the current to be transferred within an acceptable loss limit to ensure optimal system performance. In order to establish connection between solar PV modules, charge controller, battery etc., cables are needed. The size of the cable determined based on the transmission length, voltage, flowing current and the conductor. The commonly found mistakes in installation sites are the undersized or inappropriate selection of cables. The cables can be appropriately sized with the help of several tools – such as mathematical formula, voltage drop tables and online calculators. In addition to the appropriate sizing, selection of relevant type of wire is also important in the case of solar PV application. For outdoor applications UV stabilized cable must be used, while normal residential cables can be used in indoors. This ensures the long term functioning of the cable and hence reduction in the system ongoing maintenance.

### **2.2.1.4 Storage**

For off-grid and critical applications, storage systems are required, the most common medium of storage are the lead acid batteries. Presently researches are going on in the field of Li-ion batteries and to implement the concept of fuel cells in Solar PV Systems. One of the most expensive components in the PV system is the battery. Under sizing the batteries will become more costly as the battery life cycle is significantly reduced at higher Depth of Discharge (DOD%). At a higher depth of discharge, expected average number of charge–discharge cycles of a battery reduced. Further, a higher current discharge than the rating will dramatically reduce the battery life. This can be avoided by carefully sizing of the battery according to the ‘C-rating’ during the system design. It signifies the maximum amount of current that can be safely withdrawn from the battery to provide adequate back up and without causing any damage. A discharge more than the C-ratings, may cause

irreversible capacity loss due to the fact that the rate of chemical reactions taking place in the batteries cannot keep pace with the current being drawn from them.

The de-rating factor of the BOS plays a significance role in boosting up the overall efficiency of the solar PV system. The de-rating factor can be calculated by multiplying the BOS components de-rate factor. As per the survey, the overall de-rating factor is 84.5 % at STC. With good selection and installation practice the overall losses from BOS can be limited to 15.5 % at STC. With poor practice the overall de-rate factor can be 54.7 % or even less, which means the losses can account for more than 46 %.

### 2.2.2 Photovoltaic Systems Total Costs Overview

The PV industry is drawing attention because of worldwide environmental concerns and of its immense energy production potential due to the widely available free solar resource. It is important to understand the factors that directly and indirectly affect the system costs and viability (Table 2.2).

**Table 2.2** Factors affecting PV system costs and feasibility

Factors	Facts
Grid connection	Grid-connected systems do not need batteries which reduces initial capital costs
	For a comparable load, grid-tied systems use smaller PV arrays than stand-alone systems
Distance to nearest utility grid	Stand-alone systems tend to become feasible in locations which are far from electrical distribution networks
	Grid extensions can cost thousands of dollars per mile of transmission line
Solar resource	Solar resource will not affect capital costs but the availability of solar energy does affect the cost of producing energy, hence the payback period for the investment
	Location is considered the second important factor affecting PV system cost performance. It can have influence on shading patterns, soiling, operating temperature and solar resource variations
BOS (tracking)	Balance of system components is estimated to represent 30–50 % of the total costs of a PV system
	Local safety codes or regulations can require additional balance of system costs for the installation
Type of installation, mounting, size and space	Commercial and industrial clients prefer horizontal Installation to maximize flat roof utilization and to lower mounting expenses
	Retrofit installations tend to be more expensive than those planned for new buildings
	Large scale systems tend to be less expensive on a per watt basis
	Due to capital cost restrictions, stand-alone systems tend to be smaller or used for smaller loads
	Grid-tied systems tend to be larger because they provide lower capital costs and energy costs for larger loads
	Typically larger systems tend to have lower cost per kW

(continued)

**Table 2.2** (continued)

Factors	Facts
Module technology	Modules account for 40–50 % of total system costs. These determine the total area needed to install the system. Less area per watt is desired to maximize roof or land use
O&M	Grid tied PV systems do not have notable O&M costs
	Most small scale grid-tied systems do not have moving parts and therefore maintenance is minimal
	Large-scale systems may use tracking systems and therefore may require more work
	Battery assisted systems may require acid refills when valve regulated batteries are not used
	Some arrays will require regular cleaning. This could represent additional costs especially for large scale systems
Energy use and cost	System size depends mostly on energy use, solar resource and component efficiency
	Reducing energy consumption greatly reduces the initial capital cost investment necessary
	PV systems can be cost competitive in locations with high energy prices and Net metering programs. The assumption that PV is expensive is therefore relative to the solar resource and utility energy prices in a location
Indirect benefits	Emissions reductions provide a wide range of economic, environmental and health benefits. These are difficult to quantify, yet they cannot be ignored

## 2.3 Types of PV Systems

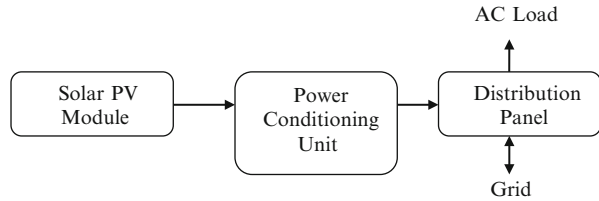
Based on the electric energy production, PV modules can be arranged into arrays to increase electric output. Solar PV systems are generally classified based on their functional and operational requirements, their component configurations. It can be classified into grid-connected and stand-alone systems.

### 2.3.1 *Grid-Connected Solar PV System*

The primary component of grid-connected PV systems is power conditioning unit (PCU). The PCU converts the DC power produced by the PV array into AC power as per the voltage and power quality requirements of the utility grid. A bi-directional interface is made between the PV system AC output circuits and the electric utility network, typically at an on-site distribution panel or service entrance. This allows the AC power produced by the PV system to either supply on-site electrical loads or to back-feed the grid when the PV system output is greater than the on-site load demand. This safety feature is required in all grid-connected



**Fig. 2.1** Block diagram of grid-connected solar PV system



PV systems, and ensures that the PV system will not continue to operate and feed back into the utility grid when the grid is down for maintenance or during grid failure state. Figure 2.1 shows the general block diagram of the grid connected solar PV system. In grid-connected systems, switching of AC power from the standby generator and the inverter to the service bus or the connected load is accomplished by internal or external automatic transfer switches.

One of the important components of a grid-connected system is *net metering*. Standard service meters are odometer-type counting wheels that record power consumption at a service point by means of a rotating disc, which is connected to the counting mechanism. The rotating discs operate by an electro physical principle called *eddy current*. Digital electric meters make use of digital electronic technology that registers power measurement by solid-state current and voltage-sensing devices that convert analog measured values into binary values that are displayed on the meter using liquid crystal display (LCD) readouts.

Inverters are the main difference between a grid-connected system and a stand-alone system. Inverters must have line frequency synchronization capability to deliver the excess power to the grid. Net meters have a capability to record consumed or generated power in an exclusive summation format. The recorded power registration is the net amount of power consumed—the total power used minus the amount of power that is produced by the solar power cogeneration system. Net meters are supplied and installed by utility companies that provide grid-connection service systems. Net metered solar PV power plants are subject to specific contractual agreements and are subsidized by state and municipal governmental agencies.

### 2.3.2 Stand-Alone Solar PV System

Stand-alone PV systems or direct coupled PV systems are designed and sized to supply DC and/or AC electrical loads. It is called direct coupled systems because, the DC output of a PV module or array is directly connected to a DC load. There is no electrical energy storage (batteries) in direct-coupled systems as because of that, the load only operates during sunlight hours. The maximum power point tracker

**Fig. 2.2** Direct coupled solar PV system

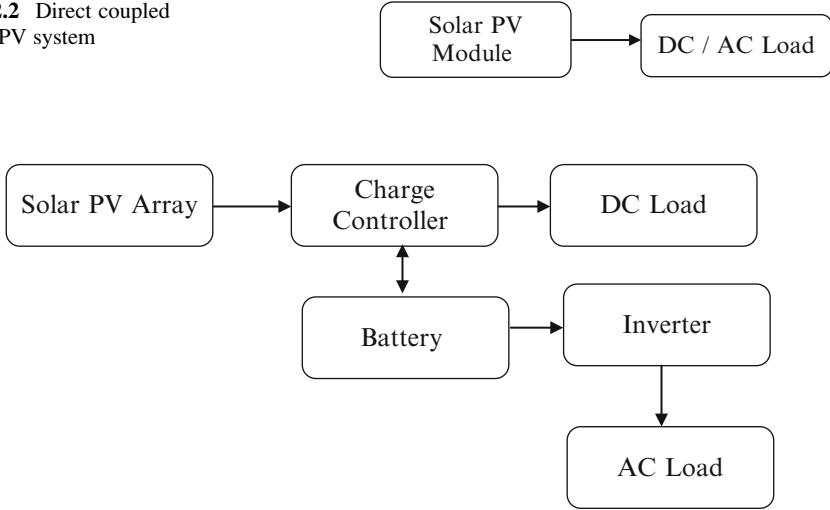


**Fig. 2.3** Block diagram of stand-alone PV system with battery storage

(MPPT) is used between the array and load to help better utilize the available array maximum power output and also for matching the impedance of the electrical load to the maximum power output of the PV array. Figure 2.2 shows the general block diagram of the stand alone solar PV system.

An example of direct coupled solar PV systems is in agriculture applications, solar PV module can be directly connected to run the pump. Depending upon the capacity of the pump, the module can be connected in series/parallel configurations. In such application, surge protector is needed to be connected between the positive and negative supply provides protection against lightning surges. Batteries are used for energy storage in many stand-alone PV systems. Figure 2.3 shows the block diagram of a typical stand-alone PV system powering DC and AC loads with battery storage option.

The solar PV array configuration, a DC load with battery backup, is essentially the same as the one without the battery except that there are a few additional components that are required to provide battery charge stability. PV panels are connected in series to obtain the desired increase in DC voltage, such as 12, 24, or 48 V. The charge controller regulates the current output and prevents the voltage level from exceeding the maximum value for charging the batteries. The output of the charge controller is connected to the battery bank by means of a dual DC cutoff disconnect. Apart from this a cutoff switch can be provided, when turned off for safety measures, disconnects the load and the PV arrays simultaneously.

During the sunshine hours, the load is supplied with DC power while simultaneously charging the battery. The controller will ensure that the DC power output

from the PV arrays should be adequate to sustain the connected load while sizing the batteries. Battery bank sizing depends on a number of factors, such as the duration of an uninterrupted power supply to the load when there is less or no radiation from the sun. The battery bank produces a 20–30 % power loss due to heat when in operation, which also must be taken into consideration. When designing a solar PV system with a battery backup, the designer must determine the appropriate location for the battery racks and room ventilation.

### ***2.3.3 PV-Hybrid Systems***

Hybrid systems generally refers to the combination of any two input sources, here solar PV can be integrated with Diesel Generator, Wind Turbines, Bio-mass or any other renewable on non-renewable energy sources. Solar PV systems will generally use battery bank to store energy output from the panels to accommodate a pre-defined period of insufficient sunshine, there may still be exceptional periods of poor weather when an alternative source is required to guarantee power production. PV-hybrid systems combine a PV module with another power sources - typically a diesel generator, but occasionally another renewable supply such as a wind turbine. The PV generator would usually be sized to meet the base load demand, with the alternate supply being called into action only when essential. This arrangement offers all the benefits of PV in respect of low operation and maintenance costs, but additionally ensures a secure supply.

Hybrid systems can also be sensible approach in situations where occasional demand peaks are significantly higher than the base load demand. It makes little sense to size a system to be able to meet demand entirely with PV if, for example, the normal load is only 10 % of the peak demand. By the same token, a diesel generator-set sized to meet the peak demand would be operating at inefficient part-load for most of the time. In such a situation a PV-diesel hybrid would be a good compromise. Figure 2.4 shows the block diagram of Solar PV hybrid system.

### ***2.3.4 Stand-Alone Hybrid AC Solar Power System with Generator and Battery Backup***

A stand-alone hybrid solar PV configuration is essentially identical to the DC solar power system. In this alternating current inverters are used to convert DC into AC. The output of inverter is square waves, which are filtered and shaped into sinusoidal AC waveforms. Any waveform, when analyzed, essentially consists of the superimposition of many sinusoidal waveforms known as harmonics. The first

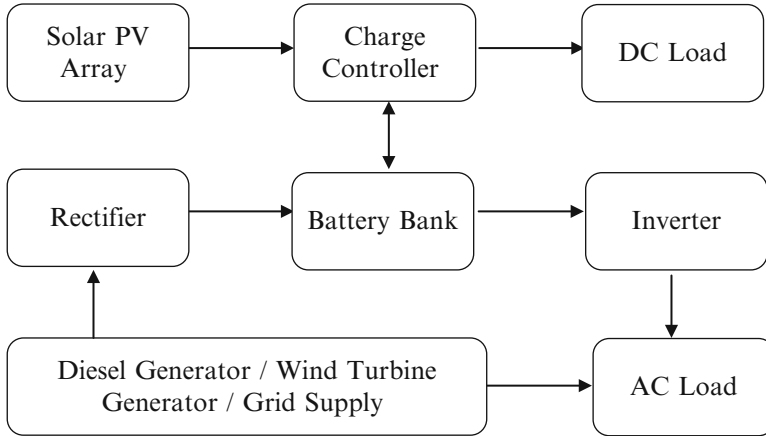


**Fig. 2.4** Block diagram of photovoltaic hybrid system

harmonic represents a pure sinusoidal waveform. Additional waveforms with higher frequencies, when superimposed on the base waveform, add or subtract from the amplitude of the base sinusoidal waveform.

The combination of base waveform and higher harmonics produce a distorted wave shape that resembles a distorted sinusoidal wave. Converted DC output, derived from the solar power, is considered to be a numerous superimposition of odd and even numbers of harmonics. To obtain a relatively clean sinusoidal output, most inverters employ electronic circuitry to filter a large number of harmonics. Filter circuits consist of specially designed inductive and capacitor circuits to block certain unwanted harmonics. In general, DC-to-AC inverters are intricate electronic power conversion equipment designed to convert direct current to a single or three-phase current that replicates the regular electrical services provided by utilities.

Most inverters, in addition to PV module input power, accept auxiliary input power to form a standby generator, used to provide power when battery voltage is dropped to a minimum level. A special type of inverter, referred to as the *grid-connected* type, incorporates synchronization circuitry that allows the production of sinusoidal waveforms in harmony with the electrical service grid. When the inverter is connected to the electrical service grid, it can effectively act as an AC power generation source. Grid-type inverters used in grid-connected solar power systems are strictly regulated by utility agencies that provide net metering. Some inverters incorporate an internal AC transfer switch that is capable of accepting an output from an AC-type standby generator. In such designs, the inverters include special electronics that transfer power from the generator to the load.

### 2.4 MATLAB Model of Solar PV

As shown in Fig. 2.5, the solar system configuration consists of a required number of solar photovoltaic cells, commonly referred to as PV modules, connected in series or in parallel to attain the required voltage output.

The basic equation from the theory of semiconductors that mathematically describes the  $I-V$  characteristic of the ideal PV cell is

$$I = I_{pv,cell} - I_{0,cell} \left[ \exp\left(\frac{qV}{\alpha kT}\right) - 1 \right] \tag{2.1}$$

The basic (2.1) of the elementary PV cell does not represent the  $I-V$  characteristic of a practical PV array. Cells connected in parallel increase the current and cells connected in series provide greater output voltages. Practical arrays are composed of several connected PV cells and the observation of the characteristics at the

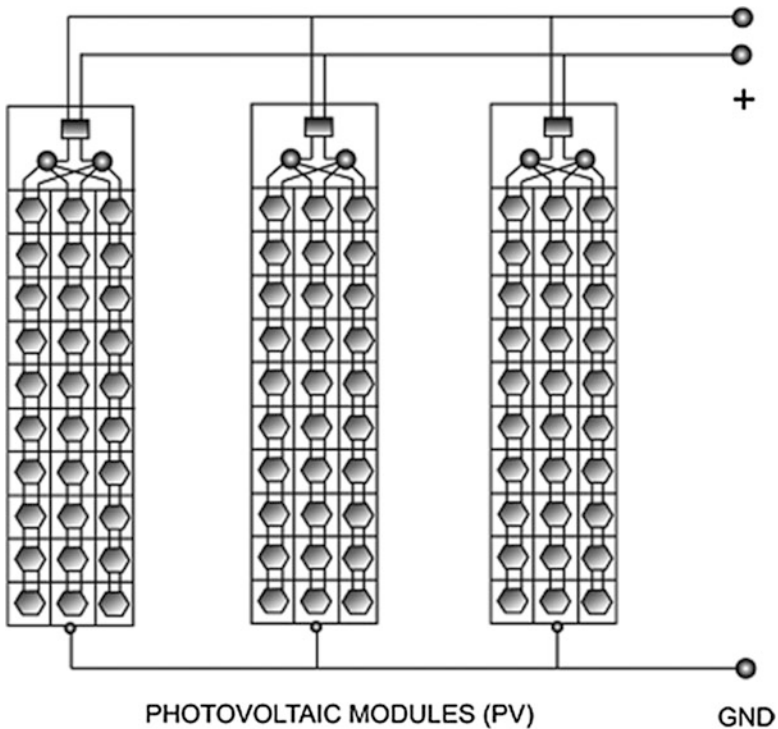


Fig. 2.5 Solar array diagram

terminals of the PV array requires the inclusion of additional parameters to the basic equation

$$I = I_{pv} - I_0 \left[ \exp \left( \frac{V + R_s I}{V_t \alpha} \right) - 1 \right] - \frac{V + R_s I}{R_p} \quad (2.2)$$

All PV array datasheets bring basically the nominal open-circuit voltage ( $V_{oc,n}$ ), the nominal short-circuit current ( $I_{sc,n}$ ), the voltage at the MPP ( $V_{mp}$ ), the current at the MPP ( $I_{mp}$ ), the open-circuit voltage/temperature coefficient ( $K_V$ ), the short circuit current/temperature coefficient ( $K_I$ ), and the maximum experimental peak output power ( $P_{max,e}$ ). This information is always provided with reference to the nominal condition or standard test conditions (STC's) of temperature and solar irradiation. The practical PV device has a series resistance  $R_s$  whose influence is stronger when the device operates in the voltage source region and a parallel resistance  $R_p$  with stronger influence in the current source region of operation.

The assumption  $I_{sc} \approx I_{pv}$  is generally used in the modeling of PV devices because in practical devices the series resistance is low and the parallel resistance is high. The diode saturation current is given by

$$I_0 = \frac{I_{sc,n} + K_I \Delta T}{\exp \left( \frac{V_{oc,n} + K_V \Delta T}{\alpha V_t} \right) - 1} \quad (2.3)$$

The saturation current  $I_0$  is strongly dependent on the temperature so that the net effect of the temperature is the linear variation of the open-circuit voltage according to the practical voltage/temperature coefficient. This equation simplifies the model and cancels the model error at the vicinities of the open-circuit voltages, and consequently, at other regions of the  $I$ - $V$  curve.

$$I_{pv} = (I_{pv,n} + K_I \Delta T) \frac{G}{G_n} \quad (2.4)$$

The relation between  $R_s$  and  $R_p$ , the only unknowns of (2.2) may be found by making  $P_{max,m} = P_{max,e}$  and solving the resulting equation for  $R_s$ , as shown

$$\begin{aligned} P_{max,m} &= V_{mp} \left\{ I_{pv} - I_0 \left[ \exp \left( \frac{q V_{mp} + R_s I_{mp}}{kT \alpha N_s} \right) - 1 \right] - \frac{V_{mp} + R_s I_{mp}}{R_p} \right\} \\ &= P_{max,e} \end{aligned} \quad (2.5)$$

$$R_p = \frac{V_{mp} + I_{mp} R_s}{\left\{ V_{mp} I_{pv} - V_{mp} I_0 \exp \left[ \frac{(V_{mp} + I_{mp} R_s) q}{N_s \alpha} \right] + V_{mp} I_0 - P_{max,e} \right\}} \quad (2.6)$$

Equation 2.6 means that for any value of  $R_s$  there will be a value of  $R_p$  that makes the mathematical  $I$ - $V$  curve cross the experimental ( $V_{mp}$ ,  $I_{mp}$ ) point. The goal is to

find the value of  $R_s$  (and hence,  $R_p$ ) that makes the peak of the mathematical  $P-V$  curve coincide with the experimental peak power at the  $(V_{mp}, I_{mp})$  point. This requires several iterations until  $P_{\max,m} = P_{\max,e}$ . Each iteration updates  $R_s$  and  $R_p$  toward the best model solution.

$$I_{pv,n} = \frac{R_p + R_s}{R_p} I_{sc,n} \tag{2.7}$$

The initial value of  $R_s$  may be zero. The initial value of  $R_p$  may be given by

$$R_{p,\min} = \frac{V_{mp}}{I_{sc,n} - I_{mp}} - \frac{V_{oc,n} - V_{mp}}{I_{mp}} \tag{2.8}$$

Equation 2.8 determines the minimum value of  $R_p$ , which is the slope of the line segment between the short-circuit and the maximum-power *remarkable points*. Although  $R_p$  is still unknown, it surely is greater than  $R_{p,\min}$  and this is a good initial guess.

According to Tables 2.3 and 2.4, along with Figs. 2.6 to 2.8, the developed model and the experimental data are exactly matched at the nominal *remarkable points* of the  $I-V$  curve (flowchart is shown in Fig. 2.6), and the experimental and

**Table 2.3** Parameters of KC200GT solar array at 25 °C, 1,000 W/m<sup>2</sup>

$I_{mp}$	7.61 A
$V_{mp}$	26.3 V
$P_{\max,e}$	200.143 W
$I_{sc}$	8.21 A
$V_{oc}$	32.9 V
$K_V$	-0.1230 V/K
$K_I$	0.0032 A/K
$N_S$	54

**Table 2.4** Parameters of the adjusted model of the KC200GT solar array at nominal operating conditions

$I_{mp}$	7.61 A
$V_{mp}$	26.3 V
$P_{\max,e}$	200.143 W
$I_{sc}$	8.21 A
$V_{oc}$	32.9 V
$I_{0,n}$	$9.825 \cdot 10^{-8}$ A
$I_{pv}$	8.214 A
$\alpha$	1.3
$R_p$	415.405 $\Omega$
$R_s$	0.221 $\Omega$

**Fig. 2.6** Algorithm of the method used to adjust the  $I-V$  model

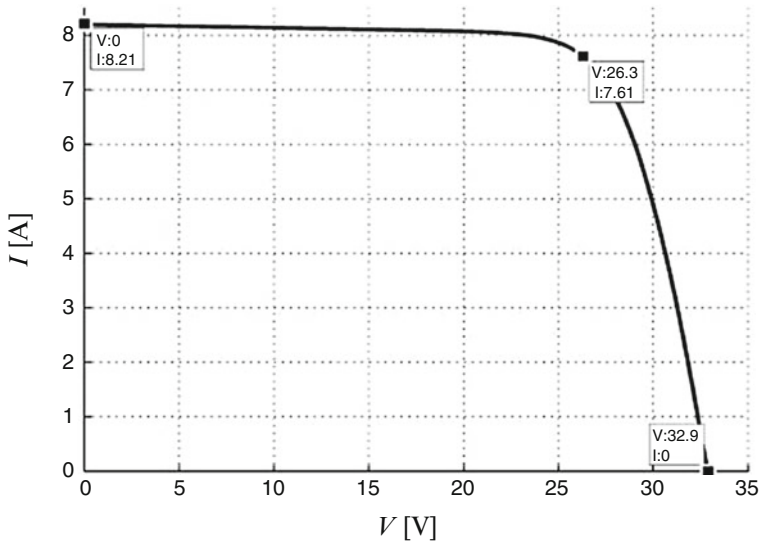
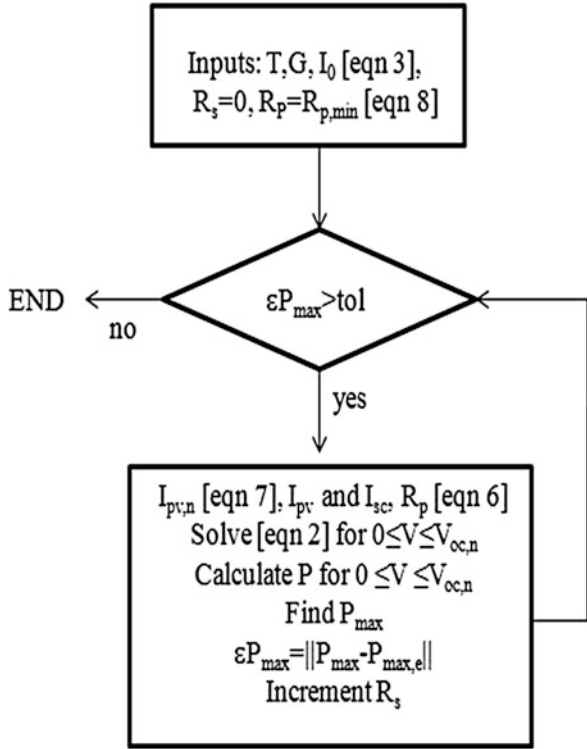


**Fig. 2.7**  $I-V$  curve adjusted to three remarkable points



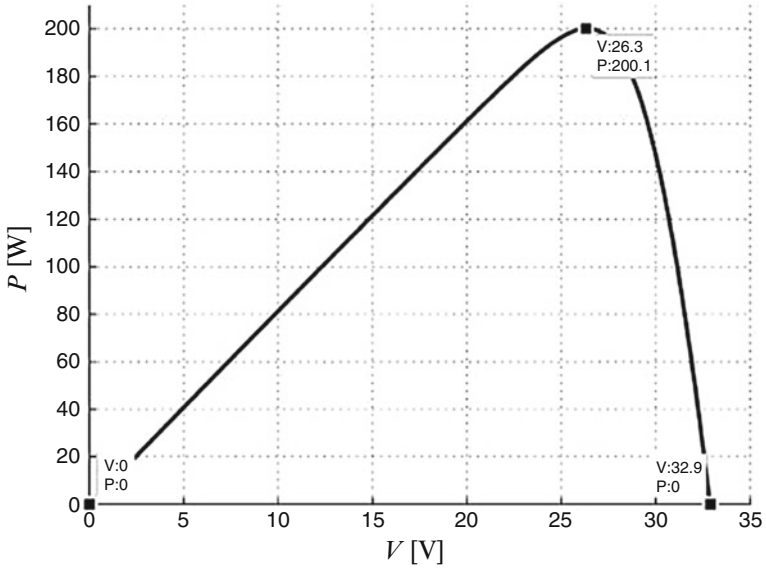


Fig. 2.8 P-V curve adjusted to three remarkable points

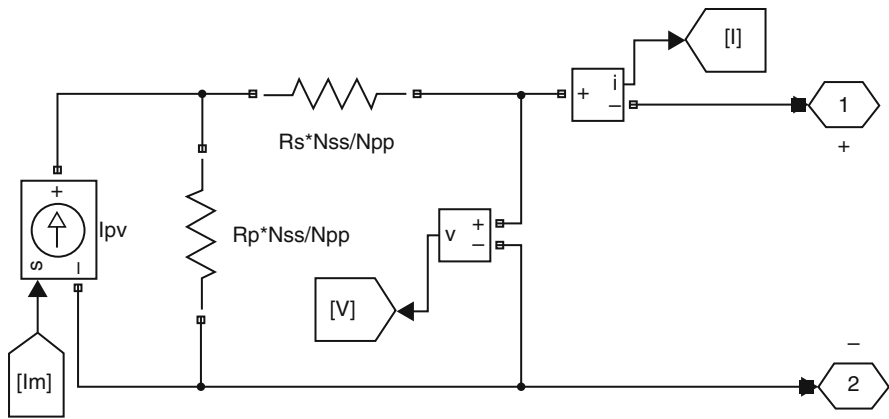
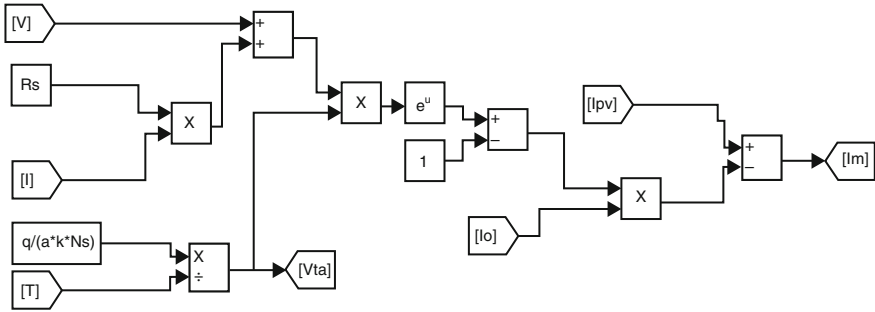


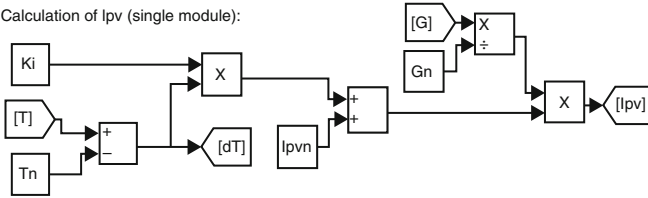
Fig. 2.9 Basic SIMULINK model of equivalent PV module

mathematical maximum peak powers coincide. The objective of adjusting the mathematical  $I-V$  curve at the three *remarkable points* was successfully achieved. The PV array can be simulated with an equivalent circuit model based on the PV model of Fig. 2.9. The circuit model composed of only one current source. The value of the current is obtained by numerically solving the  $I-V$  equation. For every value of  $V$ , a corresponding  $I$  that satisfy the  $I-V$  (2.2) is obtained.

Calculation of  $I_m = I_{pv} - I_d$  ( $N_{ss} \times N_{pp}$  modules):



Calculation of  $I_{pv}$  (single module):



Calculation of  $I_o$  (single module):

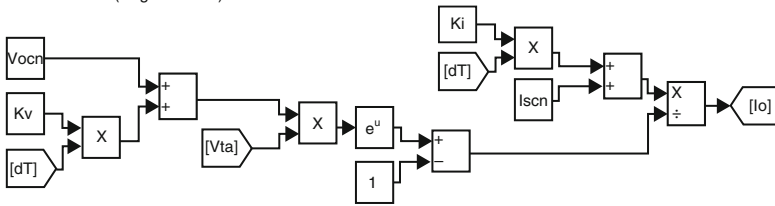


**Fig. 2.10** SIMULINK model of the PV equations

The model of the PV array was designed and the calculation of  $I_m$ ,  $I_{pv}$  and  $I_o$  are presented as separate sub-systems in Fig. 2.10.

The parameters required for simulation are initialized by the following script file

```

%% Information from the KC200GT solar array datasheet
Iscn = 8.21;    %Nominal short-circuit voltage [A]
Vocn = 32.9;   %Nominal array open-circuit voltage [V]
Imp = 7.61;    %Array current @ maximum power point [A]
Vmp = 26.3;   %Array voltage @ maximum power point [V]
Pmax_e = Vmp*Imp; %Array maximum output peak power [W]
Kv = -0.123;  %Voltage/temperature coefficient [V/K]
Ki = 3.18e-3; %Current/temperature coefficient [A/K]
Ns = 36;     %Number of series cells
    
```

```

%% Constants

k = 1.3806503e-23; %Boltzmann [J/K]
q = 1.60217646e-19; %Electron charge [C]
a = 1.3; %Diode constant

%% Nominal values

Gn = 1000; % Nominal irradiance [W/m^2] @ 25oC
Tn = 25 + 273.15; % Nominal operating temperature [K]

%% Adjusting algorithm

% The model is adjusted at the nominal condition
T = 25 + 273.15;
G = 800;

Vtn = k * Tn / q; %Thermal junction voltage (nominal)
Vt = k * T / q; %Thermal junction voltage (current temperature)

Ion = Iscn/(exp(Vocn/a/Ns/Vtn)-1); % Nominal diode saturation current

Io = Ion;

% Reference values of Rs and Rp
Rs_max = (Vocn - Vmp)/ Imp;
Rp_min = Vmp/(Iscn-Imp) - Rs_max;

% Initial guesses of Rp and Rs
Rp = Rp_min;
Rs = 0;

tol = 0.001; % Power mismatch Tolerance

P=(0);

error = Inf; %dummy value

% Iterative process for Rs and Rp until Pmax,model = Pmax,experimental

while (error>tol)

% Temperature and irradiation effect on the current
dT = T-Tn;
Ipn = (Rs+Rp)/Rp * Iscn; % Nominal light-generated current
Ipn = (Ipn + Ki*dT) *G/Gn; % Actual light-generated current
Isc = (Iscn + Ki*dT) *G/Gn; % Actual short-circuit current

% Increments Rs
Rs = Rs + .01;

% Parallel resistance
Rp = Vmp*(Vmp+Imp*Rs)/(Vmp*Ipv-Vmp*Io*exp((Vmp+Imp*Rs)/Vt/Ns/a)+Vmp*Io-Pmax_e);

% Solving the I-V equation for several (V,I) pairs
clear V
clear I

```

```

V = 0:1:50;    % Voltage vector
I = zeros(1,size(V,2)); % Current vector

for j = 1 : size(V,2) %Calculates for all voltage values

% Solves g = I - f(I,V) = 0 with Newtonn-Raphson

g(j) = Ipv-Io*(exp((V(j)+I(j)*Rs)/Vt/Ns/a)-1)-(V(j)+I(j)*Rs)/Rp-I(j);

while (abs(g(j)) > 0.001)

g(j) = Ipv-Io*(exp((V(j)+I(j)*Rs)/Vt/Ns/a)-1)-(V(j)+I(j)*Rs)/Rp-I(j);
glin(j) = -Io*Rs/Vt/Ns/a*exp((V(j)+I(j)*Rs)/Vt/Ns/a)-Rs/Rp-1;
I_(j) = I(j) - g(j)/glin(j);
I(j) = I_(j);

end

end % for j = 1 : size(V,2)

% Calculates power using the I-V equation
P = (Ipv-Io*(exp((V+I.*Rs)/Vt/Ns/a)-1)-(V+I.*Rs)/Rp).*V;

Pmax_m = max(P);

error = (Pmax_m-Pmax_e);

end % while (error>tol)

%% Outputs

fprintf('Model info:\n');
fprintf(' Rp_min = %f,Rp_min);
fprintf('\n Rp = %f,Rp);
fprintf('\n Rs_max = %f,Rs_max);
fprintf('\n Rs = %f,Rs);
fprintf('\n a = %f,a);
fprintf('\n T = %f,T-273.15);
fprintf('\n G = %f,G);
fprintf('\n Pmax,m = %f (model)',Pmax_m);
fprintf('\n Pmax,e = %f (experimental)',Pmax_e);
fprintf('\n tol = %f,tol);
fprintf('\n P_error = %f,error);
fprintf('\n Ipv = %f,Ipv);
fprintf('\n Isc = %f,Isc);
fprintf('\n Ion = %f,Ion);

```

The characteristics of PV cell are a combination of current source and diode. The current source V-I characteristics are considered separately and the diode V-I characteristics are determined separately. Here these two elements are in parallel connection so by adding currents the PV array characteristics are achieved.

The simulation results for the single PV cell are shown  $W/m^2$  in Figs. 2.11 and 2.12. The V-I characteristics and V-P characteristics for different temperatures such as  $25^\circ$ ,  $50^\circ$  and  $75^\circ$  are presented. It is observed that as the temperature increases the open circuit voltage decreases without any considerable change in the short circuit current. As a result, the maximum power from the cell is decreasing. Similarly, the

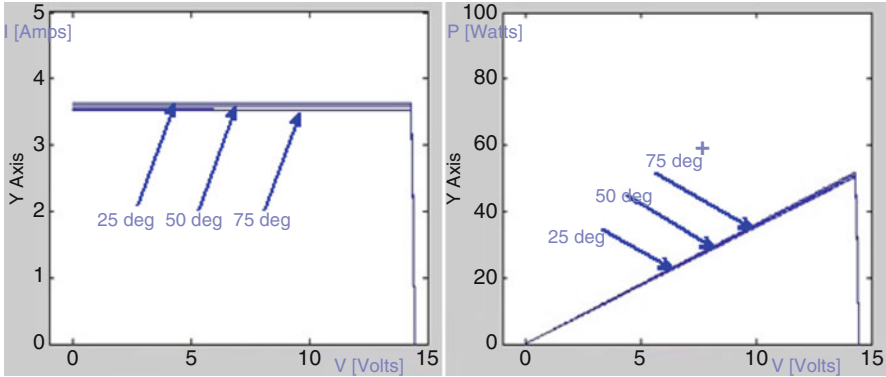


Fig. 2.11 V-I and V-P characteristics to the variation in temperature

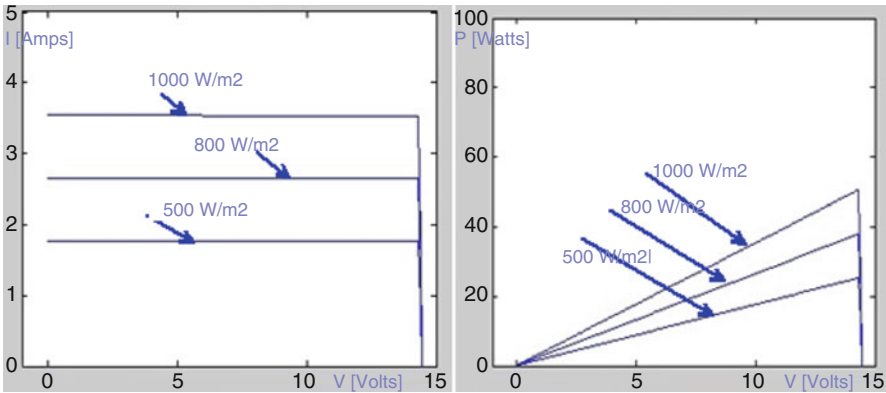


Fig. 2.12 V-I and V-P characteristics to the variation in solar radiations

V-I and V-P characteristics for radiations 500, 800, and 1000 W/m<sup>2</sup> are given. For low values of solar radiations the short circuit current is reducing considerably but the change in open circuit voltage is very less, thus proving that the maximum power from the module is dropping.

### 2.4.1 SIMULINK Model of PV Module

This model contains an external control block permitting an uncomplicated variation of the models’ parameters. In this model, 36 PV cells are interconnected in series to form one module. As a result, the module voltage is obtained by multiplying the cell voltage by the cells number while the total module current is the same as the cell’s current.

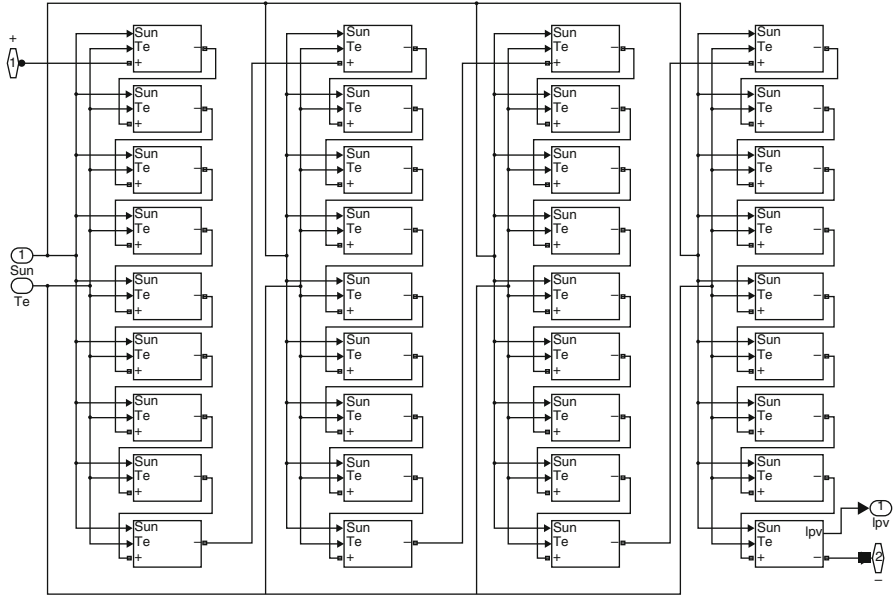


Fig. 2.13 Proposed PV module SIMULINK model

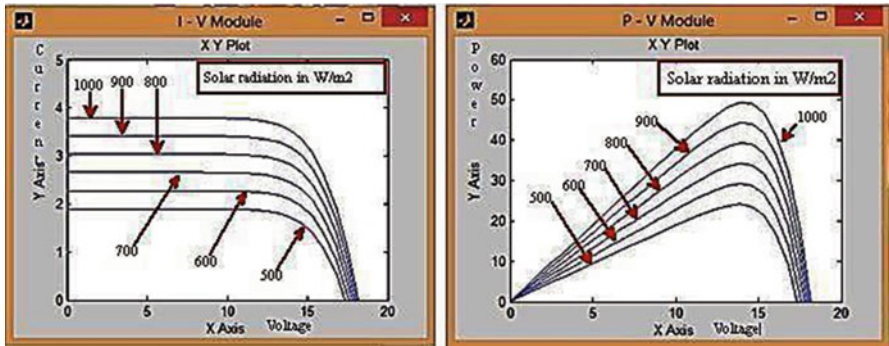


Fig. 2.14 (a) P – V characteristics of PV module (b) I – V characteristics of PV module

Figure 2.13 shows the PV module with 36 cells connected in series in order to obtain an increased voltage level. Each cell is a sub-system based on Figs. 2.9 and 2.10. Simulation results for the proposed PV module based on P-V and I-V characteristics under different solar radiations are shown in Fig. 2.14.

Simulation results for the proposed PV module based on P-V and I-V characteristics for different values of cell temperatures are shown in Fig. 2.15.

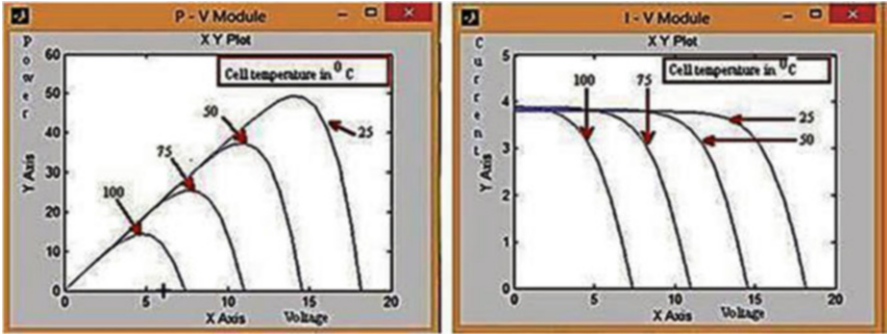


Fig. 2.15 (a) P – V characteristics of PV module (b) I – V characteristics of PV module

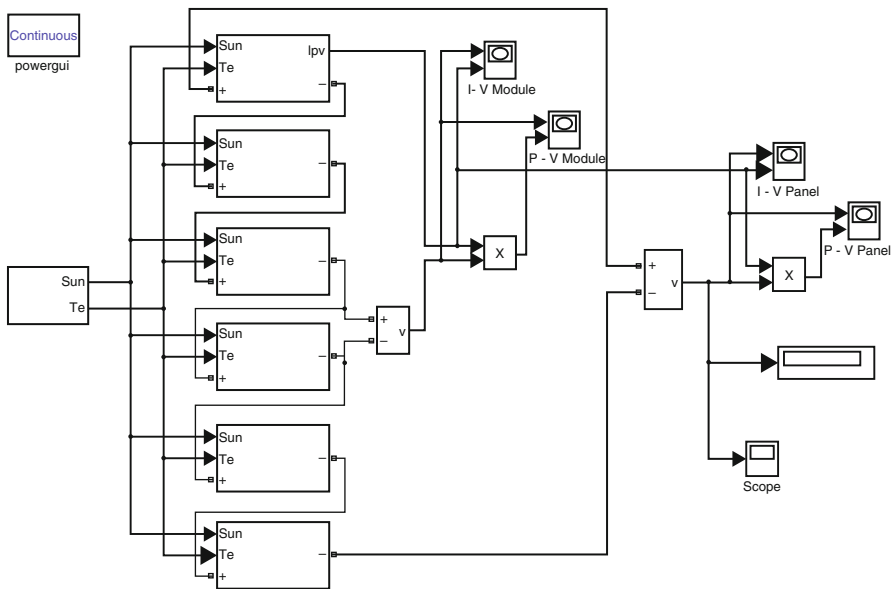


Fig. 2.16 Proposed PV array SIMULINK model

### 2.4.2 SIMULINK Model for PV Array

An array of 6 PV modules has been constructed based on Fig. 2.9. The PV modules were interconnected in series and all of them are connected to the external control block as shown in Fig. 2.16. The PV array model was simulated similarly to the model of the PV module and the results obtained are shown in Figs. 2.17 and 2.18.

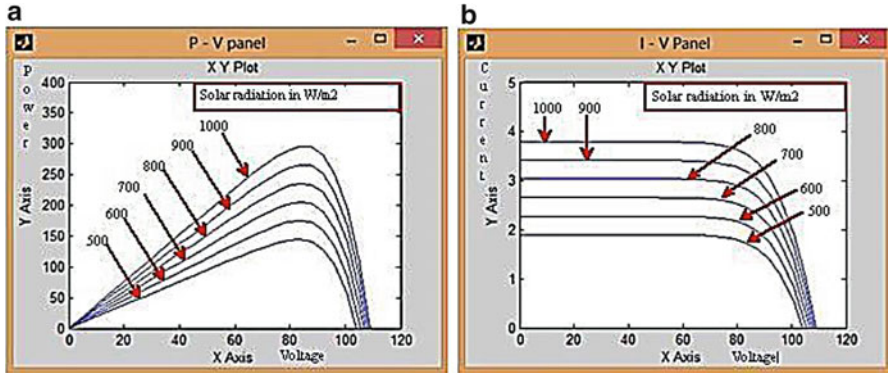


Fig. 2.17 (a) P – V characteristics of PV array (b) I – V characteristics of PV array

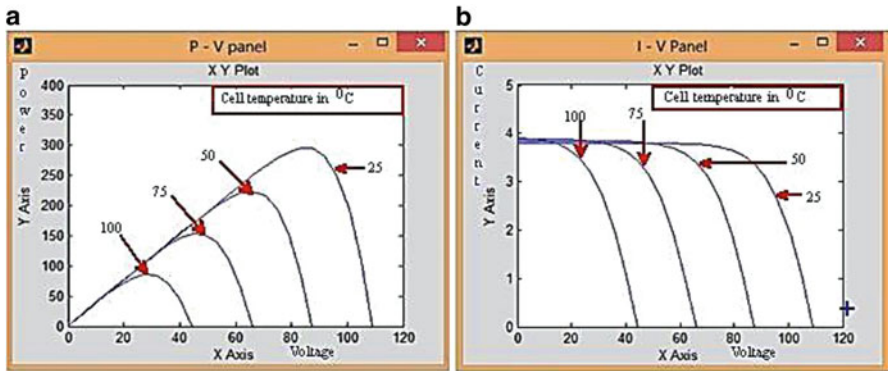


Fig. 2.18 (a) P – V characteristics for PV array (b) I – V characteristics for PV array

### 2.4.3 SIMULINK Model to Find Shading Effect

This section describes the procedure used for simulating the I–V and P–V characteristics of a partially shaded PV array. It is important to understand how the shading pattern and the PV array structure are defined in MATLAB (Fig. 2.19) using the proposed scheme. The PV array is configured as a combination of six series of PV modules connected in three parallel connections. Each set of PV modules operate under different solar radiations and different cell temperatures. The first set is under solar radiation of  $800 \text{ W/m}^2$  and cell temperature of  $750 \text{ }^\circ\text{C}$ , second set is under solar radiation of  $600 \text{ W/m}^2$  and cell temperature of  $250 \text{ }^\circ\text{C}$ , and third set is under solar radiation of  $700 \text{ W/m}^2$  and cell temperature of  $500 \text{ }^\circ\text{C}$ . Based on these conditions the simulations illustrating the PV characteristics is shown in Fig. 2.20 with three different multiple peaks. The maximum peak is called as global peak and the remaining two peaks are called as the local peaks.



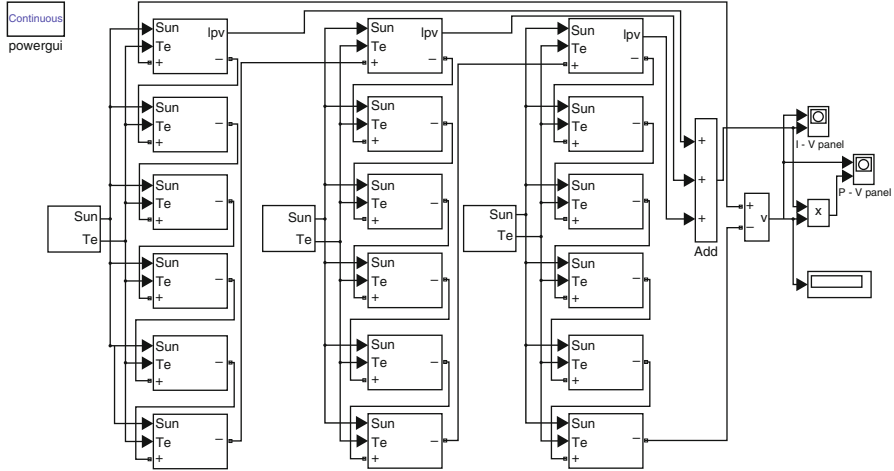


Fig. 2.19 Proposed SIMULINK model PV arrangement to find shading effect

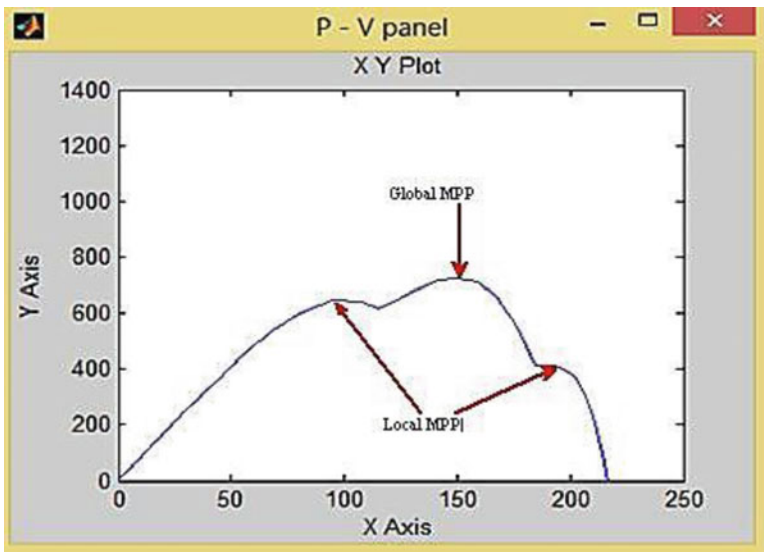


Fig. 2.20 P-V curves under shaded conditions

## 2.5 Charge Controller

A charge controller, charge regulator or battery regulator limits the rate at which electric current is added to or drawn from electric batteries. It prevents overcharging and may prevent against overvoltage, which can reduce battery performance or lifespan, and may pose a safety risk. To protect battery life, charge

controller may prevent battery from deep discharging or it will perform controlled discharges, depending on the battery technology. The terms “charge controller” or “charge regulator” may refer to either a stand-alone device, or to control circuitry integrated within a battery pack, battery-powered device, or battery recharger.

Solar Charge Controllers are the controllers which regulate the power output or the DC output voltage of the solar PV panels to the batteries. Charge controllers take the DC output voltage as the input voltage converts it into same DC voltage required for battery charging. These are mostly used in off grid scenario and uses Maximum Power Point Tracking scheme which maximizes the output efficiency of the Solar PV Panel. In battery charging system, the output voltage regulation is an important factor as batteries require specific charging method with various voltage and current levels for specific stage. These charging processes enhance battery performance and battery life. Standard Charge controllers are used where the solar panel voltage used as input are higher than the output voltage. Thus keeping the current constant, the voltage will be reduced by the controller but it results in loss of power. MPPT based solar charge controllers use microcontrollers based techniques to compute highest possible power output at any given time i.e. voltage will be monitored and regulated without power loss. The Controller will lower the voltage simultaneously increase the current, thereby increasing the power transfer efficiency. To know much about the charge controller, it is better to discuss about the batteries used in the PV system.

### ***2.5.1 Batteries in PV Systems***

Selecting the suitable battery for a PV application depends on many factors. Specific decisions on battery selection depend on physical properties, while other decisions will be much more difficult and may involve making tradeoffs between desirable and undesirable battery features. With the proper application of this knowledge, designers should be able to differentiate among battery types and gain some application experience with batteries they are familiar with. Considerations in battery subsystem design include the number of batteries in series and parallel, over-current and disconnect requirements, and selection of the proper wire sizes and types.

The energy output from the Solar PV systems is generally stored in a battery or in a battery bank deepening upon the requirements of the system. Mostly batteries are used in the stand-alone system and in the case of grid connected system, batteries are used as a backup system. The primary functions of the battery in a PV system are:

- (a) **Energy Storage Capability and Autonomy:** to store electrical energy when it is produced by the PV array and to supply energy to electrical loads as needed or on demand.
- (b) **Voltage and Current Stabilization:** to supply power to electrical loads at stable voltages and currents, by suppressing or ‘smoothing out’ transients that may occur in PV systems.
- (c) **Supply Surge Currents:** to supply surge or high peak operating currents to electrical loads or appliances.

## 2.5.2 *Battery Types and Classifications*

Even batteries from the same manufactures differ in their performance and its characteristics. Different manufacturers have variations in the details of their battery construction, but some common construction features can be described for almost all batteries. Batteries are generally mass produced; it consists of several sequential and parallel processes to construct a complete battery unit. The manufacturing is an intensive, heavy industrial process involving the use of hazardous and toxic materials. After production, initial charge and discharge cycles are conducted on batteries before they are shipped to distributors and consumers.

Different types of batteries are manufactured today, each with specific design for particular applications. Each battery type or design has its individual strengths and weaknesses. In solar PV system predominantly, *lead-acid* batteries are used due to their wide availability in many sizes, low cost and well determined performance characteristics. For low temperature applications *nickel-cadmium* cells are used, but their high initial cost limits their use in most PV systems. The selection of the suitable battery depends upon the application and the designer. In general, electrical storage batteries can be divided into two major categories, *primary* and *secondary* batteries.

### 2.5.2.1 **Primary Batteries**

Primary batteries are non rechargeable but they can store and deliver electrical energy. Typical carbon-zinc and lithium batteries commonly used primary batteries. Primary batteries are not used in PV systems because they cannot be recharged.

### 2.5.2.2 **Secondary Batteries**

Secondary batteries are rechargeable and they can store and deliver electrical energy. Common *lead-acid* batteries used in automobiles and PV systems are secondary batteries.

The batteries can be selected based on their design and performance characteristics. The PV designer should consider the advantages and disadvantages of the batteries based on its characteristics and with respect to the requirements of a particular application. Some of the important parameters to be considered for the selection of battery are lifetime, deep cycle performance, tolerance to high temperatures and overcharge, maintenance and many others.

## 2.5.3 *Battery Charging*

In a stand-alone PV system, the ways in which a battery is charged are generally much different from the charging methods battery manufacturers use to rate battery

performance. The battery charging in PV systems consists of three modes of battery charging; *normal or bulk charge*, *finishing or float charge* and *equalizing charge*.

***Bulk or Normal Charge:*** It is the initial portion of a charging cycle performed at any charge rate and it occurs between 80 % and 90 % state of charge. This will not allow the cell voltage to exceed the gassing voltage.

***Float or Finishing Charge:*** It is usually conducted at low to medium charge rates. When the battery is fully charged, most of the active material in the battery has been converted to its original form, generally voltage/current regulation are required to limit the overcharge supplied to the battery.

***Equalizing Charge:*** It consists of a current-limited charge to higher voltage limits than set for the finishing or float charge. It is done periodically to maintain consistency among individual cells. An equalizing charge is typically maintained until the cell voltages and specific gravities remain consistent for a few hours.

#### 2.5.4 Battery Discharging

***Depth of Discharge (DOD):*** The battery DOD is defined as the percentage of capacity that has been withdrawn from a battery compared to the total fully charged capacity. The two common qualifiers for depth of discharge in PV systems are the *allowable* or *maximum DOD* and the *average daily DOD* and are described as follows:

***Allowable DOD:*** The maximum percentage of full-rated *capacity* that can be withdrawn from a battery is known as its allowable depth of discharge. The allowable DOD is the maximum discharge limit for a battery, generally dictated by the *cut off voltage* and *discharge rate*. In standalone PV systems, the *low voltage load disconnect (LVD)* set point of the battery charge controller dictates the allowable DOD limit at a given discharge rate.

Depending on the type of battery used in a PV system, the design allowable depth of discharge may be as high as 80 % for deep cycle, motive power batteries, to as low as 15–25 %. The allowable DOD is related to the *autonomy*, in terms of the *capacity* required to operate the system loads for a given number of days without energy from the PV array.

***Average Daily DOD:*** The average daily depth of discharge is the percentage of the full-rated *capacity* that is withdrawn from a battery with the *average daily load* profile. If the load varies seasonally, the average daily DOD will be greater in the winter months due to the longer nightly load operation period. For PV systems with a constant daily load, the average daily DOD is generally greater in the winter due to lower battery temperature and lower rated capacity. Depending on the *rated capacity* and the *average daily load* energy, the average daily DOD may vary between only a few percent in systems designed with a lot of autonomy, or as high as 50 % for marginally sized battery systems. The average daily DOD is inversely related to autonomy; meaning that systems designed for longer autonomy periods (more capacity) have a lower average daily DOD.

**State of Charge (SOC):** The state of charge (SOC) is defined as the amount of energy as a percentage of the energy stored in a fully charged battery. Discharging a battery results in a decrease in state of charge, while charging results in an increase in state of charge. A battery that has had three quarters of its capacity removed, or been discharged 75 %, is said to be at 25 % state of charge.

**Autonomy:** Generally autonomy refers to the time a fully charged battery can supply energy to the systems loads when there is no energy supplied by the PV array. Longer autonomy periods generally result in a lower average daily DOD and lower the probability that the allowable (maximum) DOD or minimum load voltage is reached.

**Self-Discharge Rate:** In open-circuit mode without any charge or discharge current, a battery undergoes a reduction in state of charge, due to internal mechanisms and losses within the battery. Different battery types have different self-discharge rates, the most significant factor being the active materials and grid alloying elements used in the design.

**Battery Lifetime:** Battery lifetime is dependent upon a number of design and operational factors, including the components and materials of battery construction, temperature, frequency, depth of discharges, and average state of charge and charging methods.

**Temperature Effects:** For an electrochemical cell such as a battery, temperature has important effects on performance. As the temperature increases by 10 °C, the rate of an electrochemical reaction doubles, resulting in statements from battery manufacturers that battery life decreases by a factor of two for every 10 °C increase in average operating temperature. Higher operating temperatures accelerate corrosion of the positive plate grids, resulting in greater gassing and electrolyte loss. Lower operating temperatures generally increase battery life. However, the capacity is reduced significantly at lower temperatures, particularly for lead-acid batteries. When severe temperature variations from room temperatures exist, batteries are located in an insulated or other temperature-regulated enclosure to minimize battery.

**Effects of Discharge Rates:** The higher the discharge rate or current, the lower the capacity that can be withdrawn from a battery to a specific allowable DOD or cut off voltage. Higher discharge rates also result in the voltage under load to be lower than with lower discharge rates, sometimes affecting the selection of the low voltage load disconnects set point. At the same battery voltage the lower the discharge rates, the lower the battery state of charge compared to higher discharge rates.

**Corrosion:** The electrochemical activity resulting from the immersion of two dissimilar metals in an electrolyte, or the direct contact of two dissimilar metals causing one material to undergo oxidation or lose electrons and causing the other material to undergo reduction, or gain electrons. Corrosion of the grids supporting the active material in a battery is an ongoing process and may ultimately dictate the battery's useful lifetime. Battery terminals may also experience corrosion due to the action of electrolyte gassing from the battery, and generally require periodic cleaning and tightening in flooded lead-acid types. Higher temperatures and the flow of electrical current between two dissimilar metals accelerate the corrosion process.

### 2.5.5 Battery Gassing and Overcharge Reaction

When the battery is nearly fully charged gassing occurs in a battery during charging. At this point, essentially all of the active materials have been converted to their fully charged composition and the cell voltage rises sharply. The gas products are either recombined internal to the cell as in sealed or valve regulated batteries, or released through the cell vents in flooded batteries. In battery, the overcharge or gassing reaction is irreversible and it results in water loss. All gassing reactions consume a portion of the charge current which cannot be delivered on the subsequent discharge, thereby reducing the battery charging efficiency.

### 2.5.6 Charge Controller Types

There are two basic charge controller (i) Shunt Controller and (ii) Series Controller

#### 2.5.6.1 Shunt Controller

Shunt controllers consists of a blocking diode in series between the battery and the shunt element to prevent the battery from short-circuiting when the module is regulating. This type of charge controllers are limited to use in Solar PV systems with PV module currents less than 20 A. Shunt controller require a heat sink to dissipate the power because of the voltage drop between the module and controller and due to wiring and resistance of the shunt element, the module is never entirely short circuited, resulting in some power dissipation within the controller. Figure 2.21 below shows the diagram of shunt controller.

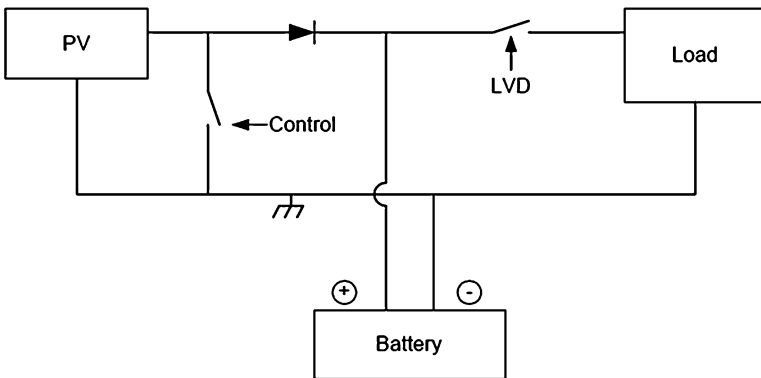


Fig. 2.21 Diagram of shunt controller

### 2.5.6.2 Shunt-Interrupting Design

The shunt-interrupting controller completely disconnects the array current in an interrupting or on-off fashion when the battery reaches the voltage regulation set point. When the battery decreases to the array reconnect voltage, the controller connects the array to resume charging the battery. This cycling between the regulation voltage and array reconnect voltage is why these controllers are often called on-off or pulsing controllers. Shunt-interrupting controllers are widely available and are low cost, however they are generally limited to use in systems with array currents less than 20 A due to heat dissipation requirements. In general, on-off shunt controllers consume less power than series type controllers that use relays, so they are best suited for small systems where even minor parasitic losses become a significant part of the system load. Shunt-interrupting charge controllers can be used on all battery types; however the way in which they apply power to the battery may not be optimal for all battery designs. In general, constant-voltage, PWM or linear controller designs are recommended by manufacturers of gelled and AGM lead-acid batteries. However, shunt-interrupting controllers are simple, low cost and perform well in most small stand-alone PV systems.

### 2.5.6.3 Shunt-Linear Design

Once a battery becomes nearly fully charged, a shunt-linear controller maintains the battery at near a fixed voltage by gradually shunting the array through a semiconductor regulation element. In some designs, a comparator circuit in the controller senses the battery voltage, and makes corresponding adjustments to the impedance of the shunt element, thus regulating the array current. In other designs, simple Zener power diodes are used, which are the limiting factor in the cost and power ratings for these controllers. There is generally more heat dissipation in a shunt-linear controller than in shunt-interrupting types. Shunt-linear controllers are popular for use with sealed VRLA batteries. This algorithm applies power to the battery in a preferential method for these types of batteries, by limiting the current while holding the battery at the regulation voltage.

### 2.5.6.4 Series Controller

In a series controller, a relay or solid-state switch either opens the circuit between the module and the battery to discontinuing charging, or limits the current in a series-linear manner to hold the battery voltage at a high value. In the simpler series interrupting design, the controller reconnects the module to the battery once the battery falls to the module reconnect voltage set point. Figure 2.22 shows the diagram of series controller.

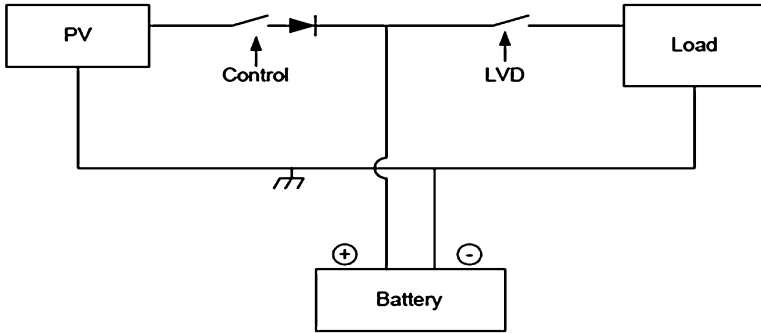


Fig. 2.22 Diagram of series controller

### 2.5.6.5 Series-Interrupting Design

The most simple series controller is the series-interrupting type, involving a one-step control, turning the array charging current either on or off. The charge controller constantly monitors battery voltage, and disconnects or open-circuits the array in series once the battery reaches the regulation voltage set point.

After a pre-set period of time, or when battery voltage drops to the array reconnect voltage set point, the array and battery are reconnected, and the cycle repeats. As the battery becomes more fully charged, the time for the battery voltage to reach the regulation voltage becomes shorter each cycle, so the amount of array current passed through to the battery becomes less each time. In this way, full charge is approached gradually in small steps or pulses, similar in operation to the shunt-interrupting type controller. The principle difference is the series or shunt mode by which the array is regulated. Similar to the shunt-interrupting type controller, the series-interrupting type designs are best suited for use with flooded batteries rather than the sealed VRLA types due to the way power is applied to the battery.

### 2.5.6.6 Series-Interrupting, 2-Step, Constant-Current Design

This type of controller is similar to the series-interrupting type, however when the voltage regulation set point is reached, instead of totally interrupting the array current, a limited constant current remains applied to the battery. This “trickle charging” continues either for a pre-set period of time, or until the voltage drops to the array reconnect voltage due to load demand. Then full array current is once again allowed to flow, and the cycle repeats. Full charge is approached in a continuous fashion, instead of smaller steps as described above for the on-off type controllers. A load pulls down some two-stage controls increase array current immediately as battery voltage. Others keep the current at the small trickle charge level until the battery voltage has been pulled down below some intermediate value (usually 12.5–12.8 V) before they allow full array current to resume.



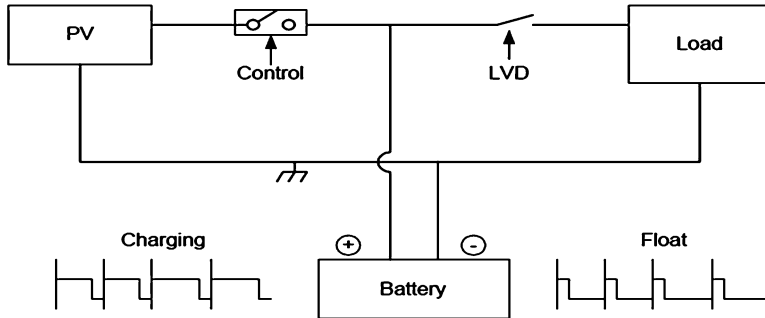


Fig. 2.23 Pulse width modulation (PWM)

### 2.5.6.7 Pulse-Width Modulation (PWM)

This method uses solid state switches to apply pulses of current at a reasonably high frequency (e.g., 300 Hz), but with a varying duty cycle, such that the battery receives a constant voltage charge from the array. This type of controller, shown in a series configuration in Fig. 2.23, can also be configured in the shunt topology. Although similar to the series linear and shunt linear controller in function, power dissipation is reduced with PWM topology compared to series linear control.

### Overcharge Protection

In a 12 V battery system the voltage vary between 10.5 and 14.4 V, depending on the actual state of charge of the battery, charge current, discharge current, type and age of the battery. When a normal full loaded battery and no charging or discharging current is flowing than the battery voltage is about 12.4–12.7 V, when charging current is flowing the voltages jump to a higher level e.g. 13.7 V (depending on the current), when loads are switched on the voltage drops down to a lower lever e.g. 12.0 V or 11.8 V (also depending on the current). The PV module produces energy and the current is flowing into the battery so voltage level increases up to the range of 14.4 V. Then the overcharge protection starts the work. When the battery voltage level is 14.4 V, the charge controller is switched off the charging current or reduced it (by pulse wide modulation). To disconnect the system loads once the battery reaches a low voltage or low state of charge condition.

If the voltage of the system falls below 11.5 V for a period of minimum 20 s than the charge controller will be switched off for minimum 30 s. All loads which are connected to the controller is off. If the battery voltage increase above 12.5 V for more than 20 s than the charge controller will be switched ON the loads again for a minimum time of 30 s. The delay of 30 s is integrated to protect the system against a swinging situation.

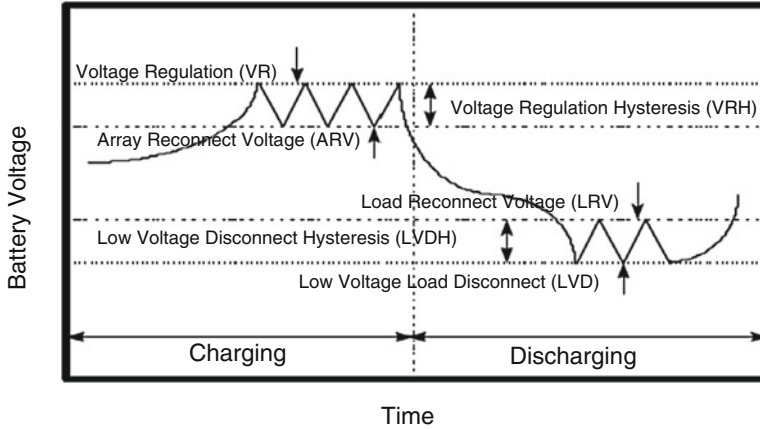


**Fig. 2.24** Charge controller set points

### Charge Controller Set Points

Controller set points are the battery voltage levels at which a charge controller performs control or switching functions. Four basic control set points are defined for most charge controllers that have battery overcharge and over-discharge protection features. The voltage regulation (VR) and the array reconnect voltage (ARV) refer to the voltage set points at which the array is connected and disconnected from the battery. The low voltage load disconnect (LVD) and load reconnect voltage (LRV) refer to the voltage set points at which the load is disconnected from the battery to prevent over discharge. Figure 2.24 shows the basic controller set points on a simplified diagram plotting battery voltage versus time for a charge and discharge cycle. A detailed discussion of each charge controller set point follows.

### High Voltage Disconnect (HVD) Set Point

The high voltages disconnect (HVD) set point is one of the key specifications for charge controllers. The voltage regulation set point is the maximum voltage that the charge controller allows the battery to reach, limiting the overcharge of the battery. Once the controller senses that the battery reaches the voltage regulation set point, the controller will either discontinue battery charging or begin to regulate the amount of current delivered to the battery.

### Array Reconnect Voltage (ARV) Set Point

In interrupting (on-off) type controllers, once the module or array current is disconnected at the voltage regulation set point, the battery voltage will begin

to decrease. If the charge and discharge rates are high, the battery voltage will decrease at a greater rate when the battery voltage decreases to a predefined voltage, the module is again reconnected to the battery for charging. The voltage at which the module is reconnected is defined as the array reconnects voltage (ARV) set point.

### Deep Discharge Protection

When a battery is deeply discharged, the reaction in the battery occurs close to the grids, and weakens the bond between the active materials and the grids. When we deep discharge the battery repeatedly, loss of capacity and life will eventually occur. To protect battery from deep discharge, most charge controllers include an optional feature.

#### **2.5.6.8 Voltage Regulation Hysteresis (VRH)**

The voltage differences between the high voltages disconnect set point and the array reconnect voltage is often called the voltage regulation hysteresis (VRH). The VRH is a major factor which determines the effectiveness of battery recharging for interrupting (on-off) type controller. If the hysteresis is too big, the module current remains disconnected for long periods, effectively lowering the module energy utilization and making it very difficult to fully recharge the battery. If the regulation hysteresis is too small, the module will cycle on and off rapidly. Most interrupting (on-off) type controllers have hysteresis values between 0.4 and 1.4 V for nominal 12 V systems.

#### **2.5.6.9 Low Voltage Load Disconnect (LVD) Set Point**

Deep discharging the battery can make it susceptible to freezing and shorten its operating life. If battery voltage drops too low, due to prolonged bad weather or certain non-essential loads are connected the charge controller disconnected the load from the battery to prevent further discharge. This can be done using a low voltage load disconnect (LVD) device is connected between the battery and non-essential loads. The LVD is either a relay or a solid-state switch that interrupts the current from the battery to the load.

#### **2.5.6.10 Load Reconnect Voltage (LRV) Set Point**

The battery voltage at which a controller allows the load to be reconnected to the battery is called the load reconnect voltage (LRV). After the controller disconnects the load from the battery at the LVD set point, the battery voltage rises to its

open-circuit voltage. When the PV module connected for charging, the battery voltage rises even more. At some point, the controller senses that the battery voltage and state of charge are high enough to reconnect the load, called the load reconnect voltage set point. LRV should be 0.08 V/cell (or 0.5 V per 12 V) higher than the load-disconnection voltage. Typically LVD set points used in small PV systems are between 12.5 and 13.0 V for most nominal 12 V lead-acid battery. If the LRV set point is selected too low, the load may be reconnected before the battery has been charged.

### **2.5.6.11 Low Voltage Load Disconnect Hysteresis (LVLH)**

The voltage difference between the low voltage disconnect set point and the load reconnect voltage is called the low voltage disconnect hysteresis. If the low voltage disconnect hysteresis is too small, the load may cycle on and off rapidly at low battery state-of-charge (SOC), possibly damaging the load or controller, and extending the time it required to charge the battery fully. If the low voltage disconnect hysteresis is too large the load may remain off for extended periods until the array fully recharges the battery.

## ***2.5.7 Charge Controller Selection***

Charge controllers are used in Solar PV systems to allow high rates of charging up to the gassing point, and then limit or disconnect the PV current to prevent overcharge. The highest voltage that batteries are allowed to reach depends on how much gassing occurs. To limit gassing, proper selection of the charge controller voltage regulation set point is critical in PV systems. Both under and overcharging will result in premature battery failure and loss of load in stand-alone PV systems. The selection and sizing of charge controllers in PV systems involves the consideration of several factors, depending on the complexity and control options required. While the primary function is to prevent battery overcharge, many other functions may also be used, including low voltage load disconnect, load regulation and control, control of backup energy sources, diversion of energy to and auxiliary load, and system monitoring. The designer must decide which options are needed to satisfy the requirements of a specific application.

The charge controller must not only be able to handle typical or rated voltages and currents, but must also be sized to handle expected peak or surge conditions from the PV array or required by the electrical loads that may be connected to the controller. It is extremely important that the controller be adequately sized for the intended application. The sizing of the charge controller can be determined by multiplying the short-circuit current of the solar PV module and the safety factor.

### 2.5.8 *Operating Without a Charge Controller*

Charge controller is an essential part in stand-alone PV systems. However there are special circumstances where a charge controller may not be needed in small systems with well-defined loads. By eliminating the need for the sensitive electronic charge controller, the design is simplified, at lower cost and with improved reliability. There are two cases where battery charge regulation may not be required: (1) when a low voltage “self-regulating module” is used in the proper climate; and (2) when the battery is very large compared to the array. Each of these cases are discussed next.

### 2.5.9 *Using Low-Voltage “Self-Regulating” Modules*

A Self-regulating system consists of a low voltage solar PV module, battery and load. Solar PV module is used to charge a 12 V battery. In the case self-regulating modules without battery charge regulation, the array current falls off sharply as the voltage increases above the maximum power point. In a “self-regulating” low voltage PV module, there are generally only 28–30 silicon cells connected in series, resulting in an open-circuit voltage of about 18 V and a maximum power voltage of about 15 V at 25 °C. For every 1 °C increase in temperature, module voltage decreases by 2.3 mV. For self-regulation and no battery overcharge to occur, the following three conditions must be met:

1. ***The load must be used daily.*** Every day the battery will receive excessive charge, even if the module is forced to operate beyond the “knee” at current levels lower than its  $I_{mp}$ . If the load is used daily, then the amp-hours produced by the module are removed from the battery, and this energy can be safely replaced the next day without overcharging the battery. So for a system to be “self-regulating”, the load must be consistent and predictable.
2. ***The climate cannot be too cold.*** If the module stays very cool, the “knee” of the IV curve will not move down in voltage enough, and the expected drop off in current will not occur, even if the battery voltage rises as expected. Often “self-regulating modules” are used in arctic climates for lighting for remote cabins for example, because they are the smallest and therefore least expensive of the power modules, but they are combined with a charge controller or voltage dropping diodes to prevent battery overcharge.
3. ***The climate cannot be too warm.*** If the module heats up too much, then the drop off in current will be too extreme, and the battery may never be properly recharged. The battery will sulfate, and the loads will not be able to operate. A “self-regulating system” design can greatly simplify the design by eliminating the need for a charge controller, however these type of designs are only appropriate for certain applications and conditions. In most common stand-alone PV system designs, a battery charge controller is required.

### 2.5.10 *Using a Large Battery or Small Array*

A charge controller may not be needed if the charge rates delivered by the array to the battery are small enough to prevent the battery voltage from exceeding the gassing voltage limit when the battery is fully charged and the full array current is applied. In certain applications, a long autonomy period may be used, resulting in a large amount of battery storage capacity. In these cases, the charge rates from the array may be very low, and can be accepted by the battery at any time without overcharging. These situations are common in critical application requiring large battery storage, such as telecommunications repeaters in alpine conditions or remote navigational aids. It might also be the case when a very small load and array are combined with a large battery, as in remote telemetry systems. In general a charging rate of  $C/100$  or less is considered low enough to be tolerated for long periods even when the battery is fully charged. This means that even during the peak of the day, the array is charging the battery bank at the 100 h rate or slower, equivalent to the typical trickle charge rate that a controller would produce anyway.

## 2.6 MATLAB Model of SOC

The implementation of State of charge battery using MATLAB/SIMULINK is presented in this section. This simulation focuses on knowing the state of charge of a battery by connecting it to a load with constant charging and discharging.

### Assumptions

- The internal resistance is maintained constant during the charge and the discharge cycles and does not vary with the amplitude of the current.
- The parameters of the model are deduced from discharge characteristics and assumed to be the same for charging.
- The capacity of the battery doesn't change with the amplitude of current (No Peukert effect).
- The model doesn't take the temperature into account.
- The Self-Discharge of the battery is not represented. It can be represented by adding a large resistance in parallel with the battery terminals.
- The battery has no memory effect.

### Limitations

The minimum no-load battery voltage is 0 V and the maximum battery voltage is equal to  $2 \cdot E_0$ . The minimum capacity of the battery is 0 Ah and the maximum capacity is  $Q_{max}$ . The equivalent circuit of a generic dynamic battery model parameterized to represent most popular types of rechargeable batteries is shown in Fig. 2.25.

In this section, Nickel-Cadmium and Nickel-Metal-Hydride model is implemented using SIMULINK. The corresponding equations for charge and discharge model are represented according to the following equations.

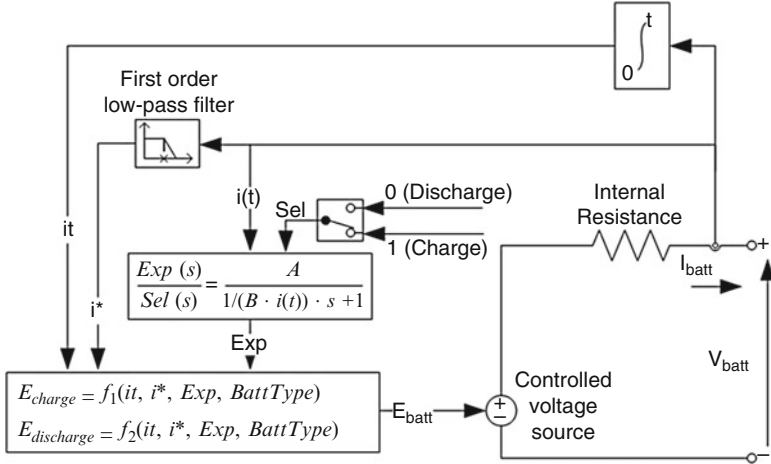


Fig. 2.25 Equivalent circuit of battery

Charge model ( $i^* < 0$ )

$$f_2(it, i^*, i, Exp) = E_0 - K \cdot \frac{Q}{|it| + 0.1Q} \cdot i^* - K \cdot \frac{Q}{Q - it} \cdot it + Laplace^{-1} \left( \frac{Exp(s)}{Sel(s)} \cdot \frac{1}{s} \right) \tag{2.9}$$

Discharge model ( $i^* > 0$ )

$$f_1(it, i^*, i, Exp) = E_0 - K \cdot \frac{Q}{Q - it} \cdot i^* - K \cdot \frac{Q}{Q - it} \cdot it + Laplace^{-1} \left( \frac{Exp(s)}{Sel(s)} \cdot 0 \right) \tag{2.10}$$

where

$E_0$  = Constant voltage (V)

$Exp(s)$  = Exponential zone dynamics (V)

$Sel(s)$  = Represents the battery mode.  $Sel(s) = 0$  during battery discharge,  $Sel(s) = 1$  during battery charging.

$K$  = Polarization constant ( $Ah^{-1}$ ) or Polarization resistance (Ohms)

$i^*$  = Low frequency current dynamics (A)

$i$  = Battery current (A)

$it$  = Extracted capacity (Ah)

$Q$  = Maximum battery capacity (Ah)

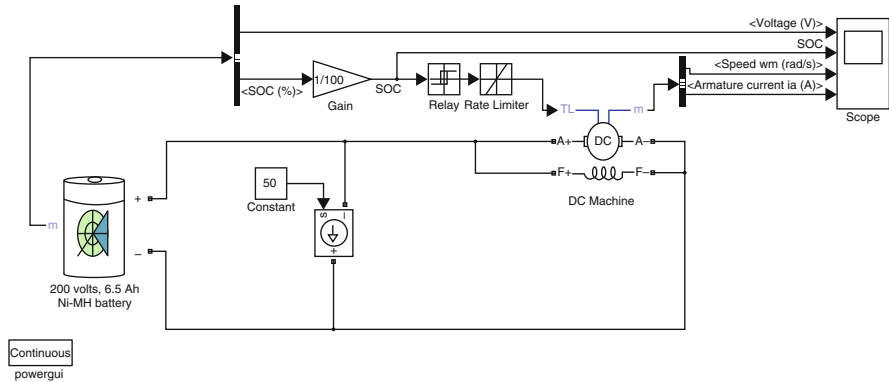


Fig. 2.26 SIMULINK model of state of charge estimation of a battery

### 2.6.1 SIMULINK Model

The power battery example illustrates a 200 V, 6.5 Ah NiMH battery connected to a constant load of 50 A as shown in Fig. 2.26. The DC machine is connected in parallel with the load and operates at no load torque. When the State-Of-Charge (SOC) of the battery goes under 0.4 (40 %), a negative load torque of 200 Nm is applied to the machine so it acts as a generator to recharge the battery. When the SOC goes over 80 %, the load torque is removed so only the battery supplies the 50 amps load.

The battery is discharged by the constant DC load of 50 A. When the SOC drops under 0.4, a mechanical torque of  $-200$  Nm is applied so the machine acts as a generator and provides a current of 100 amps, among which 50 amps is consumed by the load and 50 amps consumed to recharge the battery. When the SOC goes over 0.8, the mechanical torque is removed and the machine operates freely to repeat the cycle of operation.

#### 2.6.1.1 Blockset Used

The dialog box and the parameters for the battery model are shown in Fig. 2.27.

##### Battery Type

Provides a set of predetermined charge behavior for four types of battery such as Lead-Acid, Lithium-Ion, Nickel-Cadmium, and Nickel-Metal-Hydride.

##### Nominal Voltage (V)

The nominal voltage ( $V_{nom}$ ) of the battery (volts). The nominal voltage represents the end of the linear zone of the discharge characteristics.

##### Rated Capacity (Ah)

The rated capacity ( $Q_{rated}$ ) of the battery in ampere-hour. The rated capacity is the minimum effective capacity of the battery.



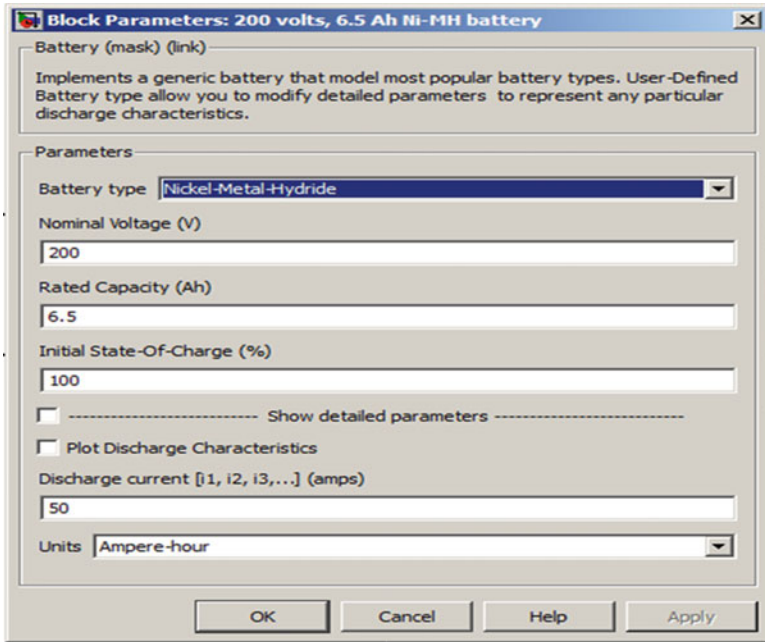


Fig. 2.27 Block parameters for Ni-MH battery

**Initial State-of-Charge (%)**

The initial State-Of-Charge (SOC) of the battery. 100 % indicates a fully charged battery and 0 % indicates an empty battery. This parameter is used as an initial condition for the simulation and does not affect the discharge curve (when the option **Plot Discharge Characteristics** is used).

**Use Parameters Based on Battery Type and Nominal Values**

Load the corresponding parameters in the entries of the dialog box, depending on the selected **Battery type**, the **Nominal Voltage** and the **Rated Capacity**. When a preset model is used, the detailed parameters cannot be modified. If the user wants to modify the discharge curve, select the desired battery type to load the default parameters, and then uncheck the **Use parameters based on Battery type and nominal values** checkbox to access the detailed parameters.

**Discharge Characteristics**

The simulation result of the SOC model for Ni-MH battery is shown in Fig. 2.28. Here the first graph represents the battery terminal voltage under charge and discharge conditions of the battery. The second graph represents the state of charge of the battery, due to the presence of the generator when state of charge crosses below the 40 % mark, the battery is charged by the generator and when it drops below the 80 % mark, the battery starts to discharge as indicated by the

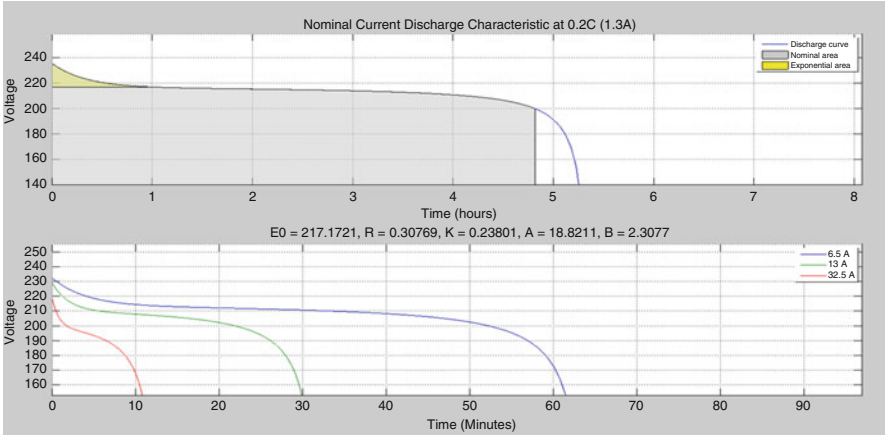


Fig. 2.28 Discharge characteristics of battery

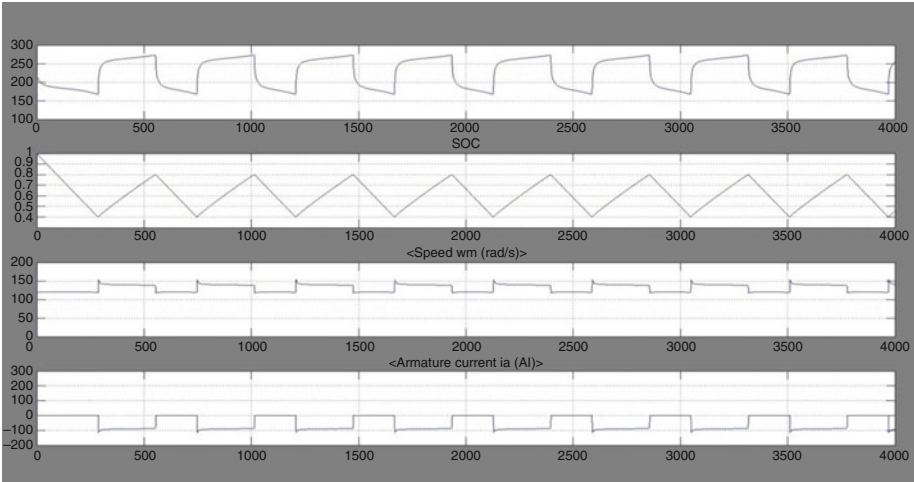
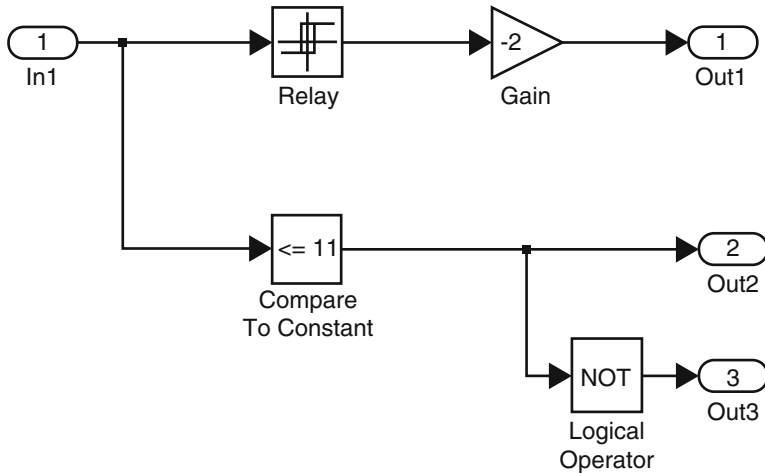


Fig. 2.29 Simulation results for Ni-MH SOC battery

graph. The third graph represents the speed of the DC machine which alters with respects to charge and discharge of the battery. The final graph shown in Fig. 2.29 represents the armature current output of the machine.

## 2.7 MATLAB Model of Charge Controller

The main function of a charge controller in a PV system is to regulate the voltage and current from PV solar panels into a rechargeable battery. The minimum function of a PV charge controller is to disconnect the array when the battery is



**Fig. 2.30** Internal circuit of charge controller

fully charged and keep the battery fully charged without damage. A charge controller is important to prevent battery overcharging, excessive discharging, reverse current flow at night and to protect the life of the batteries in a PV system. Power electronics circuit is used in a PV charge-controller to get highest efficiency, availability and reliability. The use of power electronics circuits such as various DC to DC converters topologies like buck converter, boost converter, buck-boost converter and others converter topology as power conditioning circuitry enables the effective flow of desired current to charge the battery.

A PV array with 17 subsystems was developed to implement the charge controller model. The charge controller unit is designed according to Fig. 2.30 based on the battery voltage level, which was considered to be 12 V and with a current level of 1 Amphr. The function of charge controller is as follows: if the battery voltage reaches the more than 13 V, battery disconnected from the PV-array, and if the voltage drops lesser than 10 V then it has to be connected to PV array, so if voltage of battery in between 10 and 13 V then only connection between PV-array and battery exist. This logic is implemented by taking considering the hysteresis relay. If the voltage of battery is between 11 and 13 V, normal load is connected else dummy load is connected to battery. The block parameters of the SIMULINK blocks used in this example are shown in Figs. 2.31 and 2.32.

The complete circuit involving the PV array, charge controller and battery is illustrated in Fig. 2.33. The battery voltage and the load voltage are represented in the form of waveforms in Fig. 2.34.

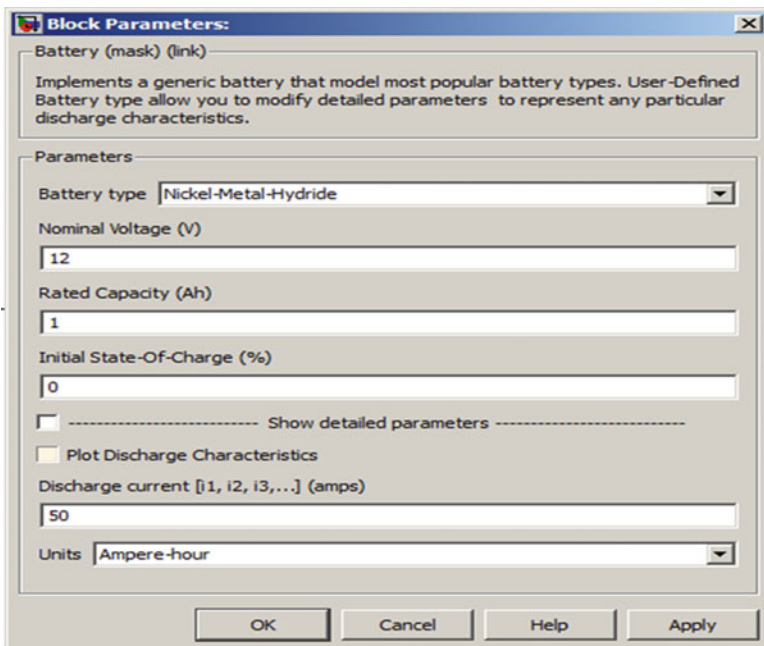


Fig. 2.31 Block parameters of Ni-MH battery

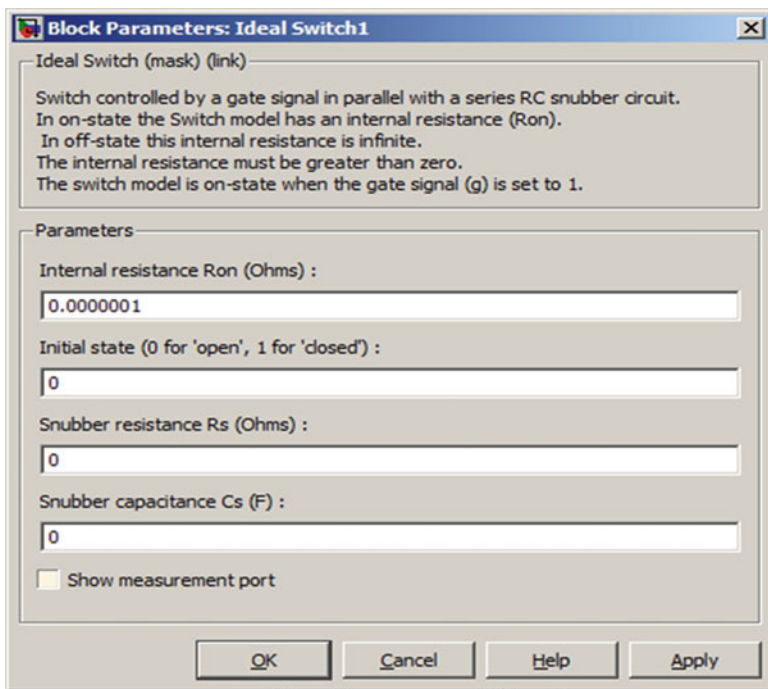


Fig. 2.32 Block parameters of ideal switch

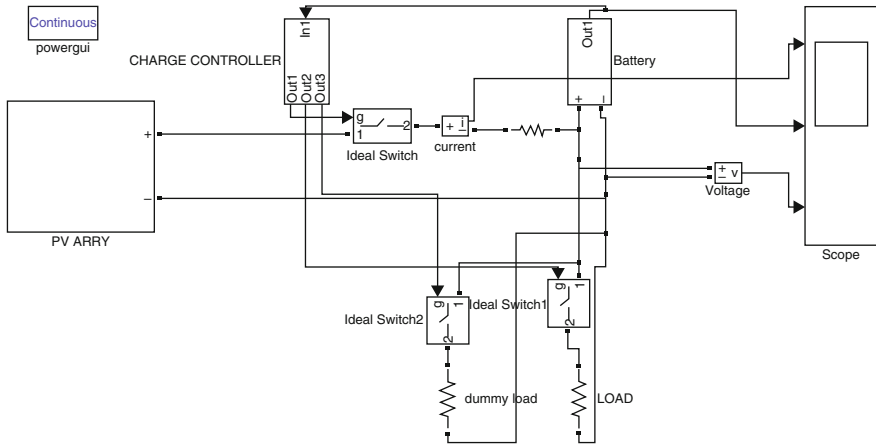


Fig. 2.33 Complete circuit

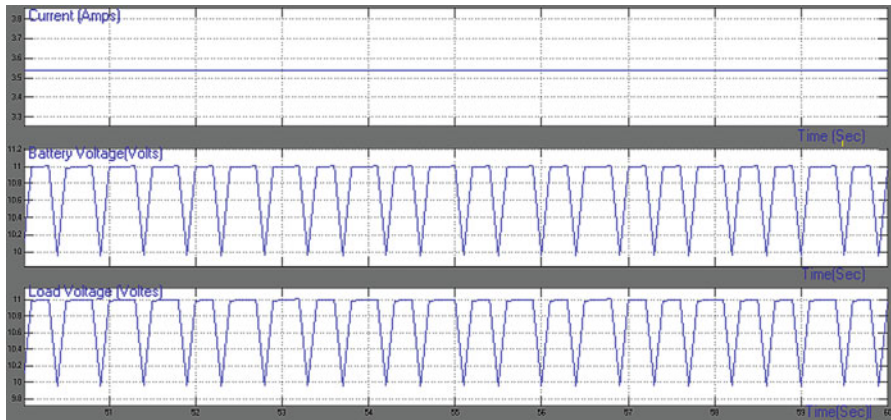


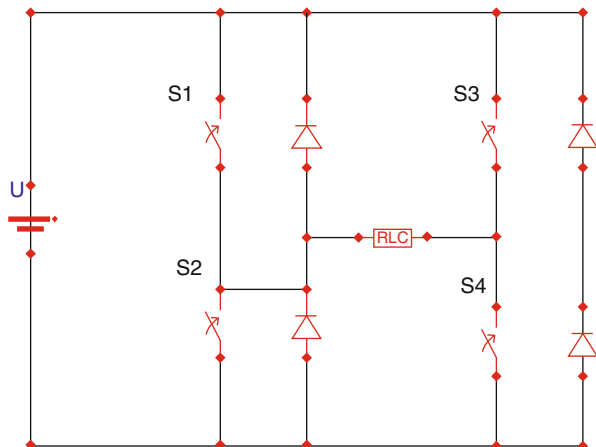
Fig. 2.34 Scope wave forms of complete circuit

## 2.8 Inverter

Inverters are used to convert DC current into AC currents in PV systems. Different types of inverters produce a different “quality” of electricity. So, the user must match the power quality required by your loads with the power quality produced by the inverter. Major discrepancies exist between power generation with PV modules and the requirements of the public grid. The job of the inverter is to connect the systems with each other and to feed the solar power into the grid with the highest possible efficiency.

The simplest inverter can be accomplished with a circuit similar to that shown in Fig. 2.35. The ideal switches in the circuit can be selected depending on the power

**Fig. 2.35** Simple inverter circuit



and voltage requirements. A simple control strategy to get the inverter output is to turn on and off the switches at the required AC frequency to obtain a square wave voltage but it consists of high harmonic currents and voltages. It can be reduced by using high frequency pulse width modulation techniques to diminish harmonic distortion and provide load voltage control. Because, harmonic content can cause overheating in the case of motor loads due to higher copper losses as well as uneven magnetic fields affecting overall operation. Sensitive electronic loads may also display erratic operation. Today, advanced control schemes and creative topologies allow the creation of AC with very low harmonic distortion; three phase designs are also possible by incorporating additional switches.

The efficiency indicates the percentage of the available solar power that is actually converted and fed into the utility grid. Modern inverters currently consume between 4 % and 8 % of the converted energy in the conversion process, which corresponds to an overall efficiency of 92–94 %. Further reducing this already low energy consumption is a major technical challenge, and one which can only be achieved with new and innovative designs. The solar PV inverters can be classified into (i) Centralized inverters (ii) String inverters (iii) Multi string inverter and (iv) Module integrated inverter.

### 2.8.1 Centralized Inverters

Earlier centralized inverters are the most common form of power electronics used in PV systems. In this model a single, large inverter is connected to many PV modules wired in series to form strings with up to 600 V/1,000 V of open-circuit voltage. All the solar PV modules are connected in strings, generating a sufficient high voltage to avoid amplification and the strings are connected in parallel to support high power to output. The conversion efficiency of many central inverters is

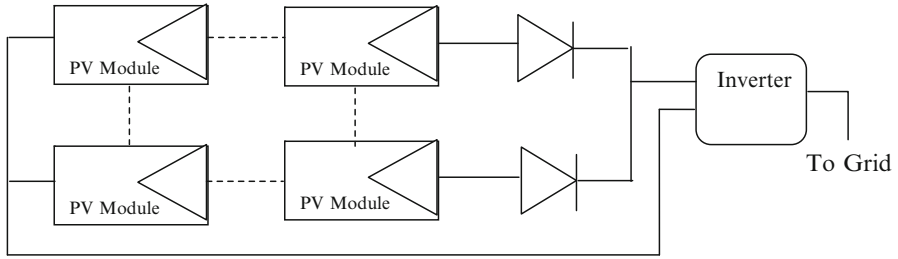


**Fig. 2.36** Centralized inverters

95 % or higher, and they feature a relatively low unit cost per watt. However, central inverters have multiple drawbacks.

This main disadvantage of this topology is the involvement of high voltage DC cable from the strings to the inverter and losses in string diodes. This structure is also limited from Maximum Power Point (MPP) Tracking and controlling mismatch between strings so individual PVs, resulting in low efficiency and reliability. This topology is not flexible and this makes it less appealing in mass production. With all these issues, this technology is not used in new solar PV systems installation. Central inverters (Fig. 2.36) cannot monitor the performance of individual PV modules, so damaged or otherwise compromised modules often go undetected. Finally, central inverters limit the design and site selection of PV systems, particularly in residential applications. They require co-planar module layouts and a lack of partial shading from chimneys, trees, vent pipes, etc. PV installers may opt out of half or more of potential sites due to these restrictions.

The conversion efficiency of many central inverters is 95 % or higher, and they feature a relatively low unit cost per watt. Generally for high voltage PV systems central inverters are preferred mainly because for systems ranging from 5 kW to 1 MW, incentives are provided by government agencies. Certain centralized inverters use common MPPT and IGBT based topology for enhancing power quality. In some power plants, central inverters were arranged in master slave configurations in order to use the most efficient combination of inverters according to total PV array output. Presently central inverters can be installed along with the DC-DC Optimizers. DC-DC optimizers supplement a central inverter with individual DC-DC converters installed for each PV module (Fig. 2.37). DC-DC optimizers can be wired serially in strings and also it can be wired in parallel. The central inverter still converts the combined DC output from across the array to grid-compatible AC power, but the DC-DC optimizers perform MPPT at the module level. This allows each module to produce its full output without being held back by any under-performing modules in the array. DC-DC optimizers also permit module-level communications and performance monitoring. However, DC-DC optimizers retain a key disadvantage of central inverters—a failure of the central inverter still results in a complete loss of system output. Furthermore, some DC-DC optimizer systems also require a separate command-and-control device to operate, creating one more point of potential system failure in addition to the central

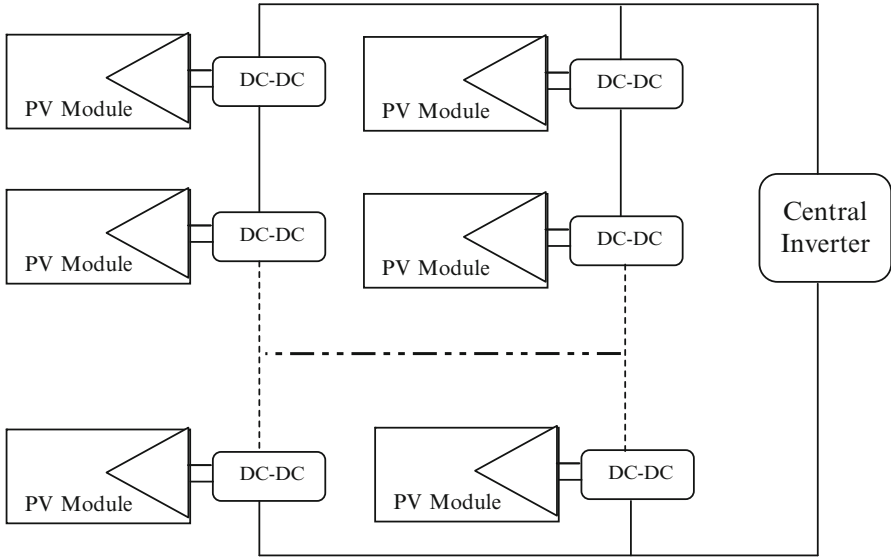


**Fig. 2.37** Central inverter with one DC-DC optimizer per module

inverter. With additional equipment to purchase and install, DC-DC optimizers add to the initial cost of a PV system. The added module-level hardware also imposes a penalty on overall system-level efficiency by introducing an additional stage of loss power conversion.

### 2.8.2 String Inverters

This topology having been introduced to the market for about 10 years, this structure remains a favorite structure in new installation. However, in a common scenario of partial shading, MPP tracking may still not be sufficient to achieve a certain efficiency requirement. Currently, the most successful technology is the string inverter. Most of these inverters use either Metal Oxide Field Effect Transistors (MOSFET) or Insulated Gate Bipolar Transistor (IGTB) semiconductors instead of thyristors to perform self-commutated switching actions. High input voltages are possible to avoid voltage amplification stages, yet smaller voltages are possible (e.g. AC module) by incorporating additional DC-DC conversion or line frequency transformers at the output. Figure 2.38 has a string of inverters connected in series with an AC module. While still avoiding high voltage amplification, this structure has improved performance with no diode loss in series, separate MPP tracking for each string and lower cost with mass productions. It is possible to have less PVs in string with voltage amplification by DC-DC converter or a line frequency transformer, which increases total area.



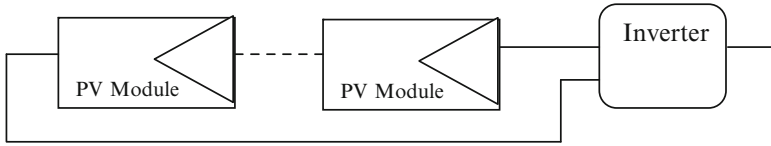


Fig. 2.38 String inverters

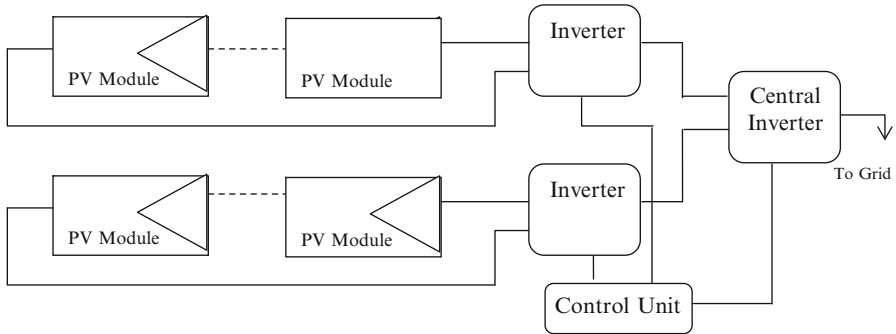


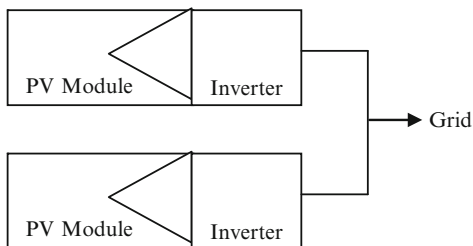
Fig. 2.39 Multi-string inverters

### 2.8.3 Multi-string Inverters

In this structure as shown in Fig. 2.39, DC-DC converter is implemented for each string for MPP tracking and power combination of different string to a DC bus. Multi-string inverter features the optimal MPP tracking for a single string of PVs. A big power stage works as a grid connected half bridge inverter without transformer. The multi-string inverter is useful when PV strings of different rated power, different orientation are combined. The DC-DC part can be implemented with high-frequency pulse width modulation (PWM) converter to reduce implementation area.

### 2.8.4 Module Integrated Inverter/Micro-inverters

Micro inverters (Fig. 2.40) are a complete, environmentally protected unit consisting of solar cells, optics, inverter, and other components, designed to generate AC power when exposed to sunlight. Module-level micro-inverters were first introduced to the PV market in the 1990s but now they progressed to the point and it became the alternative solution to the central inverters most commonly used today in PV systems. It is predicted that within a few years most PV modules will feature some form of module-level power electronics. The micro-inverter,

**Fig. 2.40** Micro-inverters

also called AC module is the integration of PV and inverter into one electrical device. In an AC module, a micro-inverter is directly integrated with a PV panel, yielding a module that natively generates grid-compatible AC power. Micro inverter simplify system design, allowing any number and combination of modules to connect directly to the grid, and provide enhanced safety by eliminating all exposed DC wiring from the system altogether.

### 2.8.5 Inverter Topology

Inverters can be classified by their output waveform in four categories: square wave, modified square wave, also called quasi-square wave, multilevel and sine wave (synthesized from a high frequency PWM). The square and quasi-square wave inverters are not recommended due to their poor quality waveform. Multilevel and sine wave inverters are considered the state of the art technology. The Multilevel inverter is based on low frequency and the sine wave inverter is based on high switching frequency. Multilevel inverters are the best available solution for high power applications. However, for medium and low power applications, there is not a clear tradeoff to make it more appealing than sine wave inverters, or vice versa. High frequency inverters favor compactness and reduced cost, while low frequency ones are claimed to have the best efficiency and robustness. The final choice of one inverter instead of the other better depends on the application. In our application of stand-alone renewable energy systems (SARES), multilevel inverters have great potential with its reliability, surge power capacity and efficiency.

## 2.9 MATLAB/SIMULINK Model of Inverter

For a solar PV output of 2.7 V DC, we design a boost converter with output voltage = 8 V, supply current = 1 A. Switching Frequency = 25 KHz such that the variation in inductor current is not more than 40 % of average inductor current for all operating conditions. The output ripple should be not more than 2 %.

**DC-DC Converter (Boost)**

In a boost converter, the output voltage is related to input voltage by the formula

$$v_o = \frac{V_{IN}}{(1 - k)}$$

Switching frequency = 25 kHz

$V_{in} = 2.7$  V To obtain an output of 8 V and load current of 1 A,

$$8 = \frac{2.7}{(1 - k)} \quad K = 0.6$$

$$\Delta V_C = \frac{I_O K}{CF} \quad \Delta I = \frac{V_S * K}{LF}$$

The tolerable limits of voltage and current ripple are 20 % and 40 % respectively.

$$I_O = 0.44 \text{ A} \quad \Delta V_C = 0.02 * 8 = 0.16, \quad \Delta I = 0.40$$

$$C = \frac{I_O * K}{\Delta V_C * F} = \frac{0.44 * 0.66}{16 * 25K} = 72.6 \mu\text{F} \quad L = \frac{V_S * K}{\Delta I * F} = \frac{2.7 * 0.66}{0.40 * 25K} = 0.2 \text{ mH}$$

**Single-Phase Inverter**

Input Voltage = 8 V DC

Reference Wave:

Amplitude = 1 V

Frequency = 50 Hz

$$= 2 * 3.14 * 50$$

$$= 314 \text{ radians}$$

Carrier Wave:

Time period = [0 0.25e-4 0.5e-4 0.75e-4 1e-4]

Amplitude = [0 1.2 0 -1.2 0]

**2.9.1 SIMULINK Model**

For inverter development, the power system blockset provides the required components such as a full-bridge, batteries, resistors, inductors, capacitors etc. The pulse generation circuit is modeled as shown in Fig. 2.41.

The single phase inverter designed using IGBT, diode and ideal switch is presented in Fig. 2.42. The block parameters used in this SIMULINK implementation are illustrated in Figs. 2.43, 2.44, 2.45, and 2.46. The input voltage was set to 2.7 V based on the design specifications in the DC voltage source block. The internal resistance of the ideal switch was set to 0.001  $\Omega$  with the initial state 'open'. The diode's internal resistance was also maintained at 0.001  $\Omega$  with a forward voltage of 0.8 V.

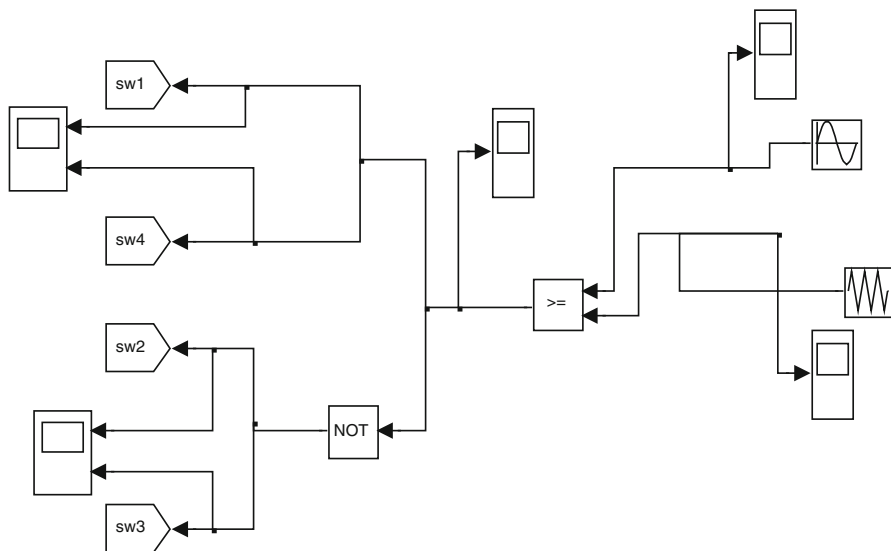


Fig. 2.41 Pulse generation circuit

The output voltage waveform is shown in Fig. 2.47. The boost converter was designed for a 2.7 V input from solar PV panel with  $L = 0.2 \text{ mH}$  and  $C = 72.6 \mu\text{F}$ . A single phase full-bridge inverter (PWM) circuit was used to convert the boosted DC voltage to alternating voltage. The above model can be conveniently used for integrating the Solar PV system to grid system. The inverter system modeled with MATLAB/SIMULINK was achieved using the power system and standard SIMULINK block sets. The system was analyzed by sending the required signal to scopes and the workspace, which allowed for analysis and design of the inverter model.

### 2.10 Maximum Power Point Tracking

Maximum Power Point Tracking, frequently referred to as MPPT, operates Solar PV modules in a manner that allows the modules to produce all the power they are capable of generating. MPPT is not a mechanical tracking system but it works on a particular tracking algorithm and it based on a control system. MPPT can be used in conjunction with a mechanical tracking system, but the two systems are completely different. MPPT algorithms are used to obtain the maximum power from the solar array based on the variation in the irradiation and temperature. The voltage at which PV module can produce maximum power is called ‘maximum power point’ (or peak power voltage). Maximum power varies with solar radiation, ambient temperature and solar cell temperature.

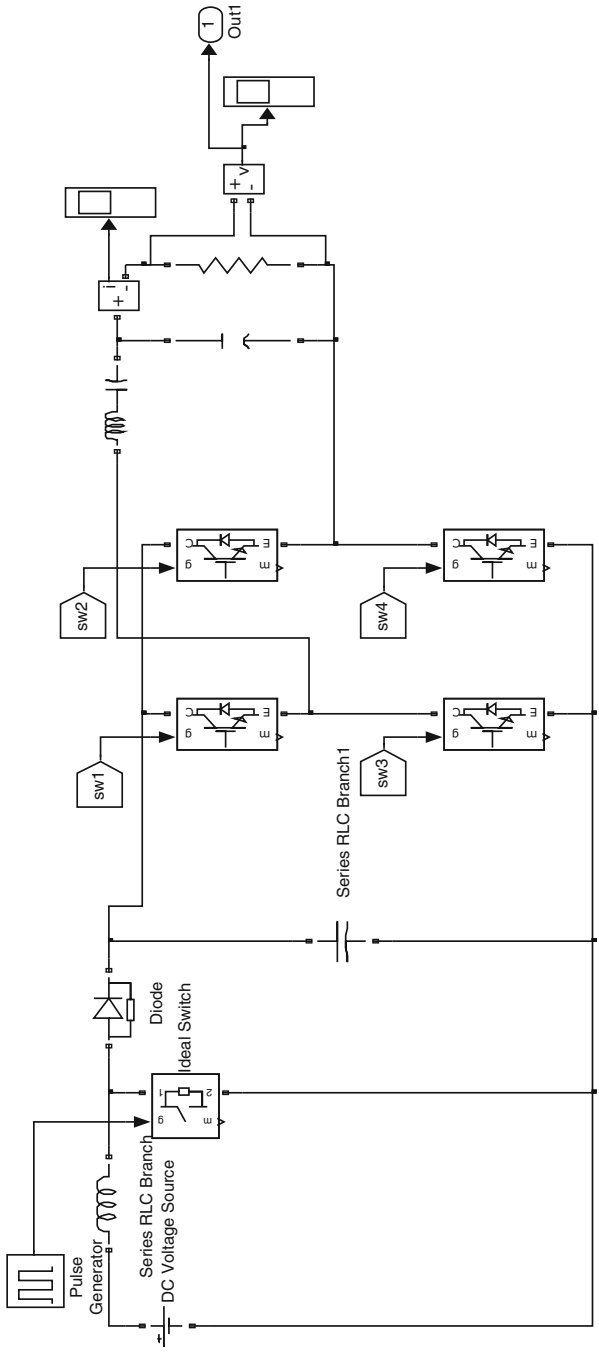


Fig. 2.42 Boost converter and single-phase inverter circuit

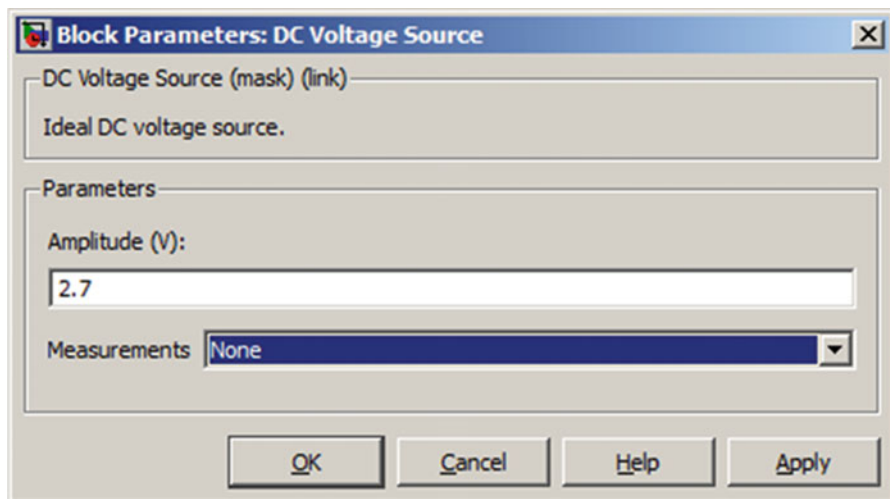


Fig. 2.43 Block parameters of DC voltage source

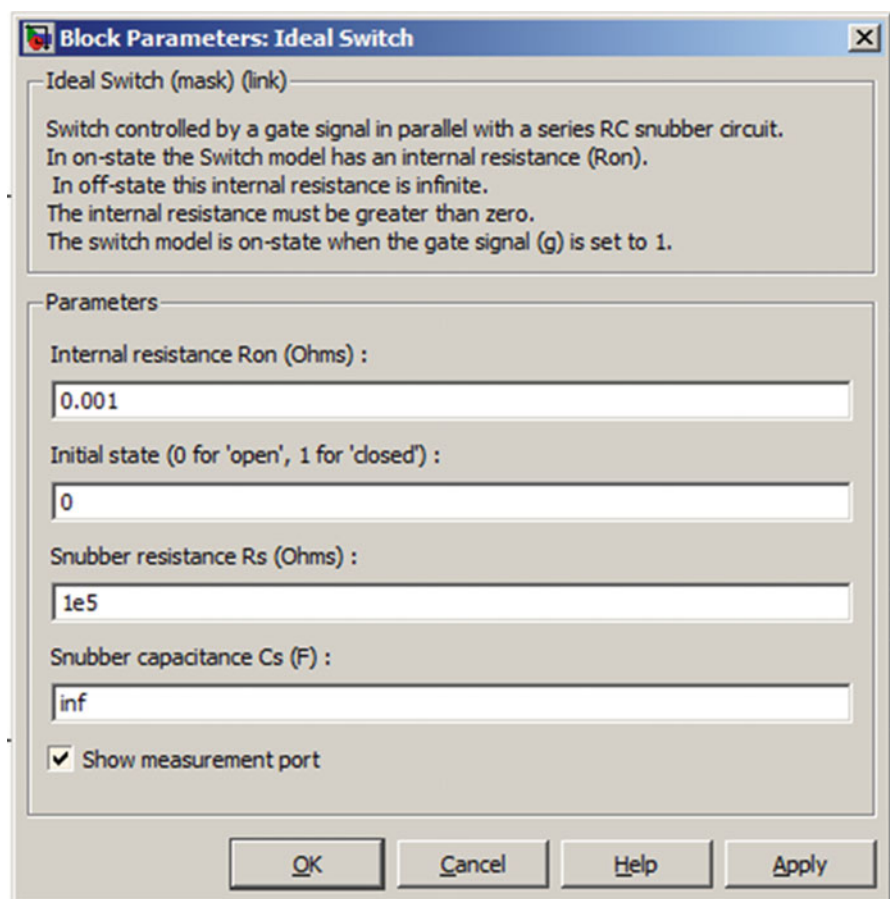


Fig. 2.44 Block parameters of ideal switch

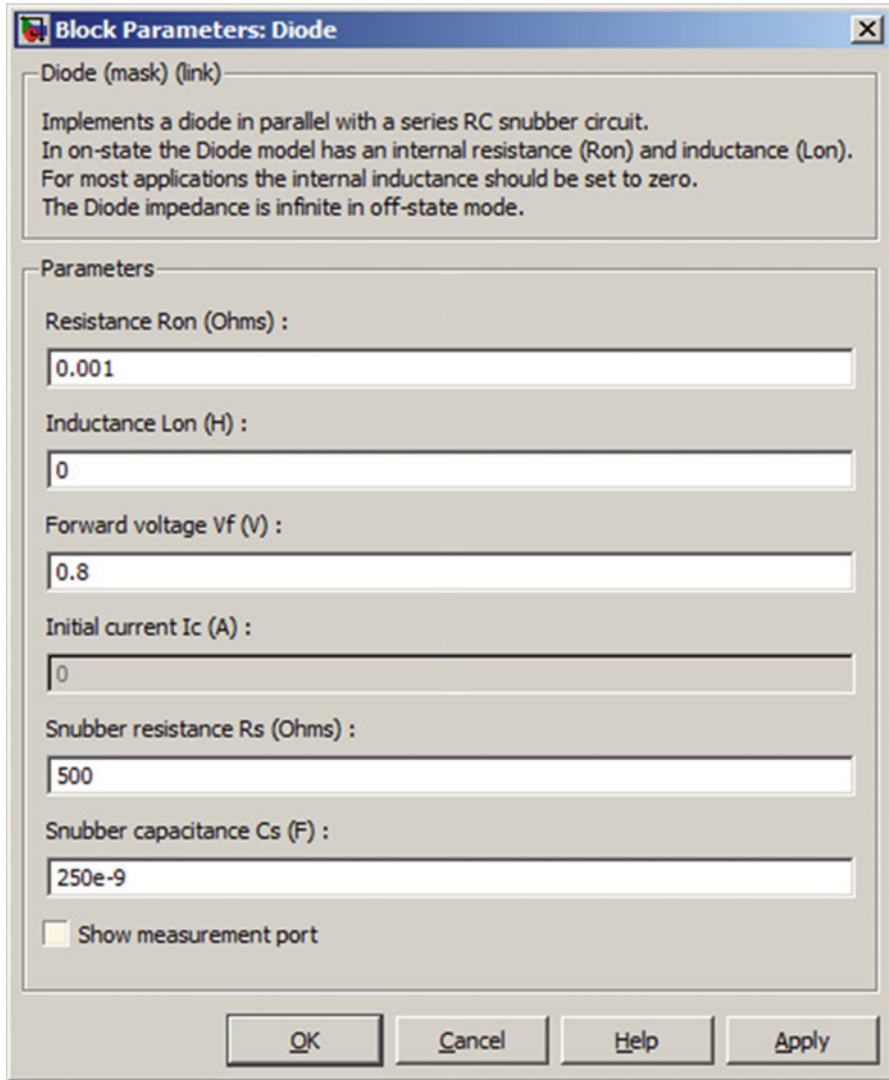


Fig. 2.45 Block parameters of diode

Typical PV module produces power with maximum power voltage of around 17 V when measured at a cell temperature of 25 °C, it can drop to around 15 V on a very hot day and it can also rise to 18 V on a very cold day. The major principle of MPPT is to extract the maximum available power from PV module by making them operate at the most efficient voltage. MPPT Algorithm is based on the simple logic that, MPPT calculates the output of PV module, compares it to battery voltage then

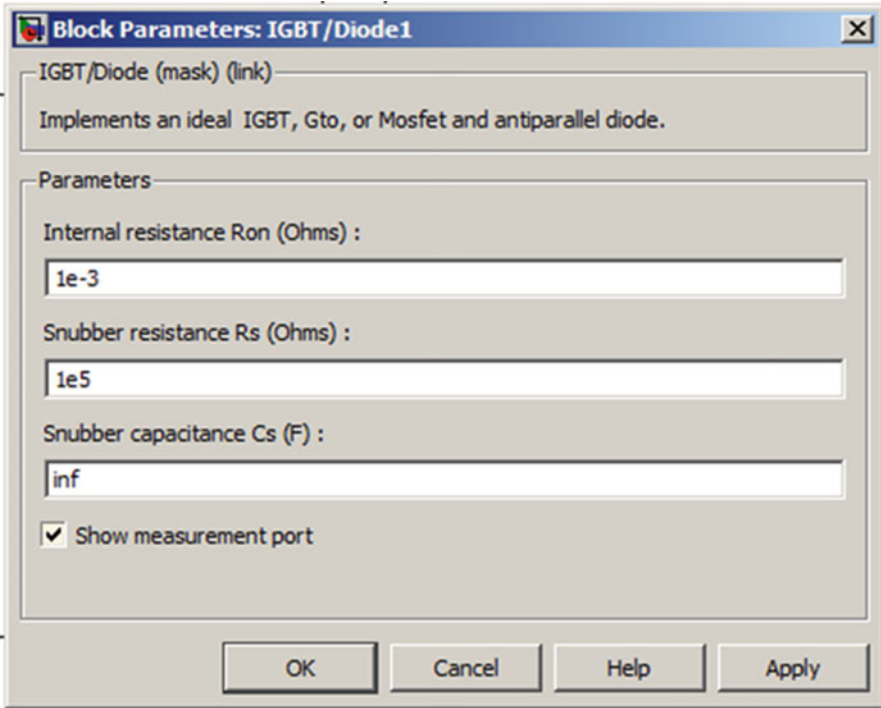


Fig. 2.46 Block parameters of IGBT

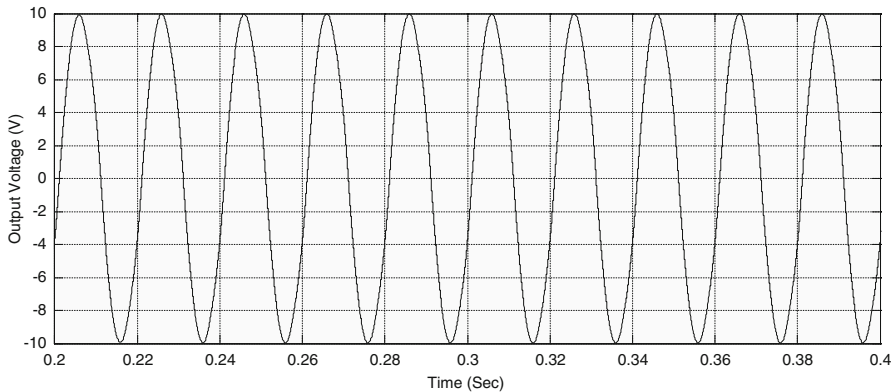


Fig. 2.47 Scope output for inverter model

fixes what is the optimum power that PV module can produce to charge the battery and converts it to the optimum voltage to get maximum current into battery. It can also supply power to a DC load, which is connected directly to the battery. MPPT is mostly useful during cloudy days and when the battery is deeply discharged.



### **2.10.1 MPPT Techniques**

Over the past decades many methods to find the MPP have been developed. These techniques differ in many aspects such as required sensors, complexity, cost, range of effectiveness, convergence speed, correct tracking when irradiation and/or temperature change, hardware needed for the implementation or popularity, among others. Some of the most popular MPPT techniques are:

1. Perturb and Observe (hill climbing method).
2. Incremental Conductance method.
3. Fractional short circuit current.
4. Fractional open circuit voltage.
5. Fuzzy logic.
6. Neural networks.
7. Ripple Correlation Control.
8. Current Sweep.
9. DC-link capacitor droop control.
10. Load current or load voltage maximization.
11.  $dP/dV$  or  $dP/dI$  Feedback control.

Among several techniques mentioned, the Perturb and Observe (P&O) method and the Incremental Conductance (InCond) algorithms are the most commonly applied algorithms. Other techniques based on different principles include fuzzy logic control, neural network, fractional open circuit voltage or short circuit current, current sweep, etc. Most of these methods yield a local maximum and some, like the fractional open circuit voltage or short circuit current, give an approximated MPP, rather than an exact output. In normal conditions the V-P curve has only one maximum. However, if the PV array is partially shaded, there are multiple maxima in these curves. Both P&O and InCond algorithms are based on the “hill-climbing” principle, which consists of moving the operation point of the PV array in the direction in which the power increases. Hill-climbing techniques are the most popular MPPT methods due to their ease of implementation and good performance when the irradiation is constant. The advantages of both methods are simplicity and requirement of low computational power. The drawbacks are: oscillations occur around the MPP and they get lost and track the MPP in the wrong direction during rapidly changing atmospheric conditions.

#### **2.10.1.1 Perturb and Observe**

In the P&O method only one voltage sensor is used to sense the PV array voltage and hence the cost of implementation is less. The algorithm involves a perturbation on the duty cycle of the power converter and a perturbation in the operating voltage of the DC-link between the PV array and the power converter. Perturbing the duty cycle of the power converter implies modifying the voltage of the DC-link

between the PV array and the power converter. In this method, the sign of the last perturbation and the sign of the last increment in the power are used to decide the next perturbation. As can be seen in Fig. 2.48, on the left of the MPP incrementing the voltage increases the power whereas on the right decrementing the voltage decreases the power. If there is an increment in the power, the perturbation should be kept in the same direction and if the power decreases, then the next perturbation should be in the opposite direction. Based on these facts, the algorithm is implemented as show in the flowchart in Fig. 2.49 and the process is repeated until the MPP is reached. The operating point oscillates around the MPP.

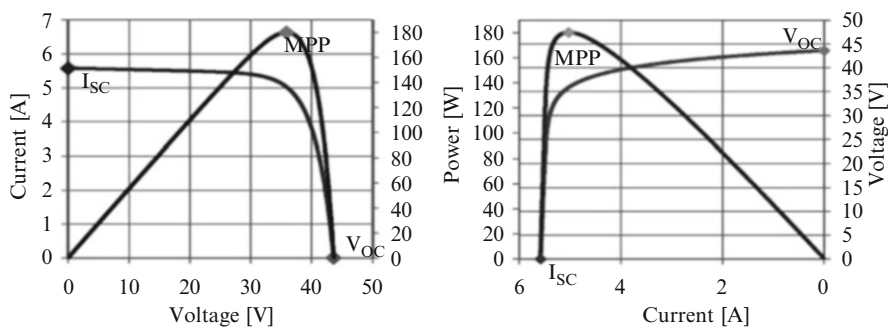


Fig. 2.48 PV panel characteristic curves

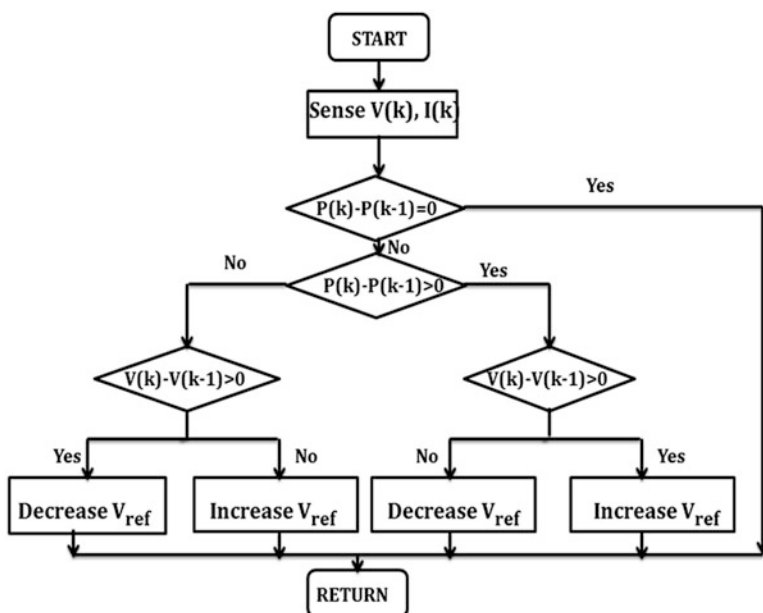


Fig. 2.49 Flowchart of the perturb and observe algorithm

The time complexity of this algorithm is very less but on reaching very close to the MPP it doesn't stop at the MPP and keeps on perturbing on both the directions. To avoid such a condition, an appropriate error limit can be set or a wait function can be used to stop the increase in time complexity of the algorithm. However the method does not take account of the rapid change of irradiation level (due to which MPPT changes) and considers it as a change in MPP due to perturbation and ends up calculating the wrong MPP. To avoid this problem we can use incremental conductance method.

### 2.10.1.2 Incremental Conductance

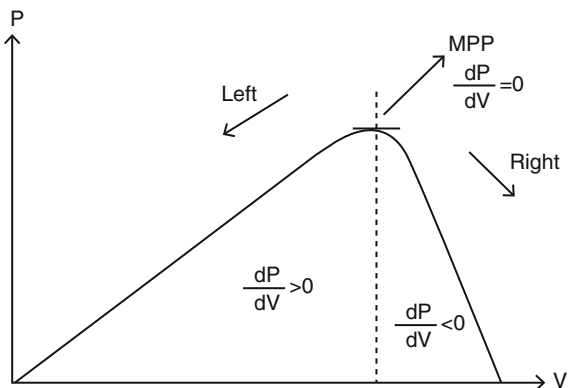
The incremental conductance algorithm uses two voltage and current sensors to sense the output voltage and current of the PV array. In incremental conductance method the array terminal voltage is always adjusted according to the MPP voltage it is based on the incremental and instantaneous conductance of the PV module.

Figure 2.50 shows that the slope of the P-V array power curve is zero at The MPP, increasing on the left of the MPP and decreasing on the Right hand side of the MPP. The basic equations of this method are as follows.

$$\begin{aligned}
 \frac{dI}{dV} &= -\frac{I}{V} && \text{At MPP} \\
 \frac{dI}{dV} &> -\frac{I}{V} && \text{Left of MPP} \\
 \frac{dI}{dV} &< -\frac{I}{V} && \text{Right of MPP}
 \end{aligned}
 \tag{2.11}$$

where I and V are P-V array output current and voltage respectively. The left hand side of equations represents incremental conductance of P-V module and the right hand side represents the instantaneous conductance. When the ratio of change in output conductance is equal to the negative output conductance, the solar array

**Fig. 2.50** Basic idea of incremental conductance method on a P-V curve of solar module



will operate at the maximum power point. This method exploits the assumption of the ratio of change in output conductance is equal to the negative output Instantaneous conductance. We have,

$$P = VI$$

Applying the chain rule for the derivative of products yields to

$$\partial P/\partial V = [\partial(VI)]/\partial V \tag{2.12}$$

At MPP, as  $\partial P/\partial V = 0$

The above equation could be written in terms of array voltage  $V$  and array current  $I$  as

$$\partial P/\partial V = -I/V \tag{2.13}$$

The MPPT regulates the PWM control signal of the DC – to – DC boost converter until the condition:  $(\partial I/\partial V) + (I/V) = 0$  is satisfied. In this method the peak power of the module lies at above 98 % of its incremental conductance. The Flow chart of incremental conductance MPPT is shown in Fig. 2.51.

In both P&O and InCond schemes, the speed of occurrence of MPP depends on the size of the increment of the reference voltage. The drawbacks of these

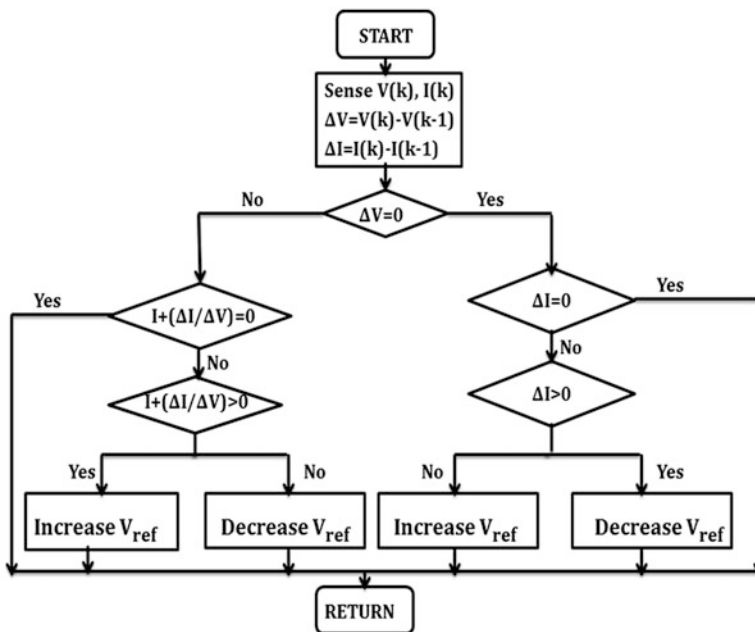


Fig. 2.51 Flow chart for incremental conductance algorithm

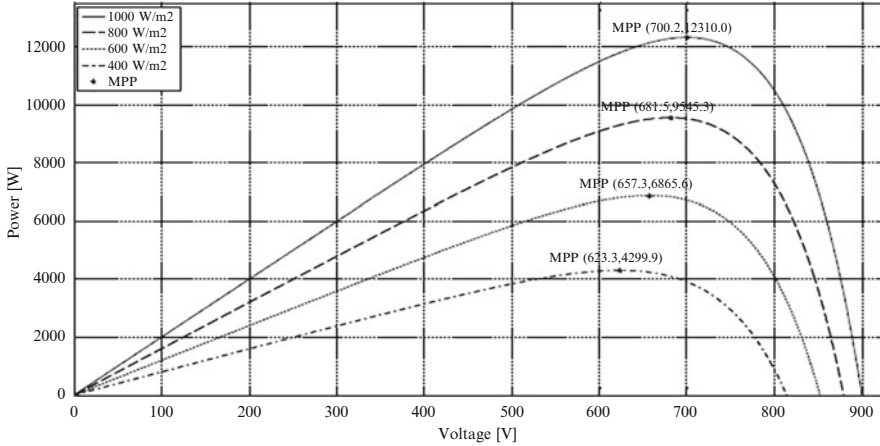


Fig. 2.52 P-V curve depending on the irradiation

techniques are: The first drawback is that they can easily lose track of the MPP if the irradiation changes rapidly. In case of step changes they track the MPP very well, because the change is instantaneous and the curve does not keep on changing. However, when the irradiation changes following a slope, the curve in which the algorithms are based changes continuously with the irradiation, as can be seen in Fig. 2.52, so the changes in the voltage and current are not only due to the perturbation of the voltage. As a consequence it is not possible for the algorithms to determine whether the change in the power is due to its own voltage increment or due to the change in the irradiation.

The other drawback of both methods is the oscillations of the voltage and current around the MPP in the steady state. This is due to the fact that the control is discrete and the voltage and current are not constantly at the MPP but oscillating around it. The size of the oscillations depends on the size of the rate of change of the reference voltage. The greater the oscillation, higher is the amplitude of the oscillations. However, speed of the MPP occurrence also depends on this rate of change and this dependence is inversely proportional to the size of the voltage increments. The traditional solution is a trade off: if the increment is small the oscillations decrease, then the MPP is reached slowly and vice versa, so a compromise solution has to be found.

### 2.10.1.3 Fractional Open-Circuit Voltage

The near linear relationship between  $V_{MPP}$  and  $V_{OC}$  of the PV array, under varying irradiance and temperature levels, has given rise to the fractional  $V_{OC}$  method.

$$V_{MPP} \approx k_1 V_{OC} \tag{2.14}$$

where  $k_1$  is a constant of proportionality. Since  $k_1$  is dependent on the characteristics of the PV array being used, it usually has to be computed beforehand by empirically determining  $V_{MPP}$  and  $V_{OC}$  for the specific PV array at different irradiance and temperature levels. The factor  $k_1$  has been reported to be between 0.71 and 0.78. Once  $k_1$  is known,  $V_{MPP}$  can be computed using (2.14) with  $V_{OC}$  measured periodically by momentarily shutting down the power converter. However, this incurs some disadvantages, including temporary loss of power. To prevent this, pilot cells are used from which  $V_{OC}$  can be obtained. These pilot cells must be carefully chosen to closely represent the characteristics of the PV array. Once  $V_{MPP}$  has been approximated, a closed loop control on the array power converter can be used to asymptotically reach this desired voltage. Since (2.14) is only an approximation, the PV array technically never operates at the MPP. Depending on the application of the PV system, this can sometimes be adequate. Even if fractional  $V_{OC}$  is not a true MPPT technique, it is very easy and cheap to implement as it does not necessarily require DSP or microcontroller control. However,  $k_1$  is no more valid in the presence of partial shading (which causes multiple local maxima) of the PV array and proposes sweeping the PV array voltage to update  $k_1$ . This obviously adds to the implementation complexity and incurs more power loss.

#### 2.10.1.4 Fractional Short-Circuit Current

Fractional  $I_{SC}$  results from the fact that, under varying atmospheric conditions,  $I_{MPP}$  is approximately linearly related to the  $I_{SC}$  of the PV array.

$$I_{MPP} \approx k_2 I_{SC} \quad (2.15)$$

where  $k_2$  is a proportionality constant. Just like in the fractional  $V_{OC}$  technique,  $k_2$  has to be determined according to the PV array in use. The constant  $k_2$  is generally found to be between 0.78 and 0.92. Measuring  $I_{SC}$  during operation is problematic. An additional switch usually has to be added to the power converter to periodically short the PV array so that  $I_{SC}$  can be measured using a current sensor. This increases the number of components and cost. Power output is not only reduced when finding  $I_{SC}$  but also because the MPP is never perfectly matched as suggested by (2.15). The variable  $k_2$  can be compensated such that the MPP is better tracked while atmospheric conditions change. To guarantee proper MPPT in the presence of multiple local maxima, the PV array voltage from open-circuit to short-circuit periodically sweeps to update  $k_2$ . Most of the PV systems using fractional  $I_{SC}$  in the literature use a DSP, while a few systems use a simple current feedback control loop instead.

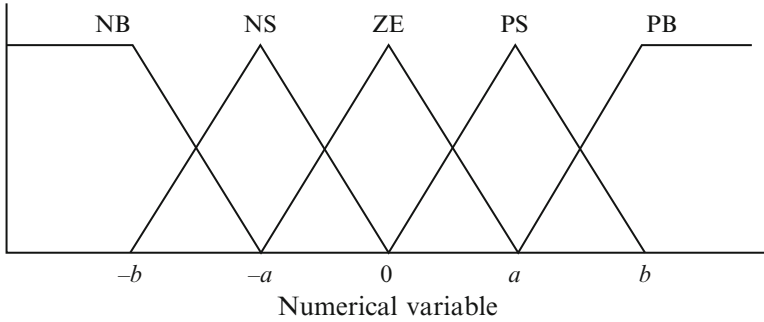


Fig. 2.53 Membership function for inputs and output of fuzzy logic controller

**2.10.1.5 Fuzzy Logic Control**

Microcontrollers have made using fuzzy logic control popular for MPPT over last decade. Fuzzy logic controllers have the advantages of working with imprecise inputs, not needing an accurate mathematical model, and handling nonlinearity. Fuzzy logic control generally consists of three stages: fuzzification, rule base table lookup, and defuzzification. During fuzzification, numerical input variables are converted into linguistic variables based on a membership function similar to Fig. 2.53. In this case, five fuzzy levels are used: NB (Negative Big), NS (Negative Small), ZE (Zero), PS (Positive Small), and PB (Positive Big).

In some cases seven fuzzy levels are also used probably for more accuracy. In Fig. 2.53,  $a$  and  $b$  are based on the range of values of the numerical variable. The membership function is sometimes made less symmetric to give more importance to specific fuzzy levels. The inputs to a MPPT fuzzy logic controller are usually an error  $E$  and a change in error  $\Delta E$ . The user has the flexibility of choosing how to compute  $E$  and  $\Delta E$ . Since  $dP/dV$  vanishes at the MPP, approximation can be applied as follows,

$$E(n) = \frac{P(n) - P(n - 1)}{V(n) - V(n - 1)} \tag{2.16}$$

and

$$\Delta E(n) = E(n) - E(n - 1) \tag{2.17}$$

Equivalently,  $e = I/V + dI/dV$  is often used. Once  $E$  and  $\Delta E$  are calculated and converted to the linguistic variables, the fuzzy logic controller output, which is typically a change in duty ratio  $\Delta D$  of the power converter, can be looked up in a rule base table such as Table 2.5. The linguistic variables assigned to  $\Delta D$  for the different combinations of  $E$  and  $\Delta E$  are based on the power converter being used and also on the knowledge of the user. The rule base shown in Table 2.5 is based on a boost converter. If for example, the operating point is far to the left of the MPP,

**Table 2.5** Fuzzy rule base

E	$\Delta E$				
	NB	NS	ZE	PS	PB
NB	ZE	ZE	NB	NB	NB
NS	ZE	ZE	NS	NS	NS
ZE	NS	ZE	ZE	ZE	PS
PS	PS	PS	PS	ZE	ZE
PB	PB	PB	PB	ZE	ZE

that is  $E$  is PB, and  $\Delta E$  is ZE, then we want to increase the duty ratio largely, that is  $\Delta D$  should be PB to reach the MPP. In the defuzzification stage, the fuzzy logic controller output is converted from a linguistic variable to a numerical variable still using a membership function as shown in Fig. 2.53. This provides an analog signal that will control the power converter to the MPP. MPPT fuzzy logic controllers have been shown to perform well under varying atmospheric conditions. However, their effectiveness depends a lot on the knowledge of the user or control engineer in choosing the right error computation and coming up with the rule base table.

### 2.10.1.6 Neural Network

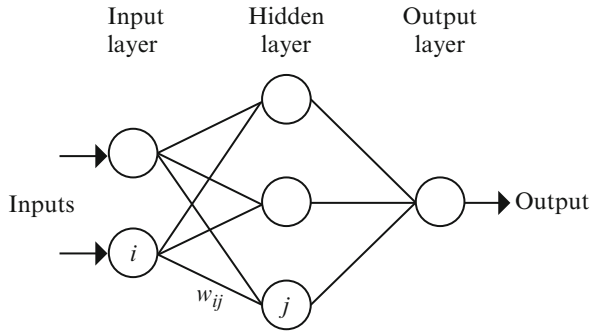
Along with fuzzy logic controllers another technique of implementing MPPT are the neural networks, which are also well adapted for microcontrollers. Neural networks commonly have three layers: input, hidden, and output layers as shown in Fig. 2.54. The number nodes in each layer vary and are user-dependent. The input variables can be PV array parameters like  $V_{OC}$  and  $I_{SC}$ , atmospheric data like irradiance and temperature, or any combination of these. The output is usually one or several reference signal(s) like a duty cycle signal used to drive the power converter to operate at or close to the MPP. How close the operating point gets to the MPP depends on the algorithms used by the hidden layer and how well the neural network has been trained. The links between the nodes are all weighted. The link between nodes  $i$  and  $j$  is labeled as having a weight of  $w_{ij}$  in Fig. 2.54. To accurately identify the MPP, the  $w_{ij}$ 's have to be carefully determined through a training process, whereby the PV array is tested over months or years and the patterns between the input(s) and output(s) of the neural network are recorded. Since most PV arrays have different characteristics, a neural network has to be specifically trained for the PV array with which it will be used. The characteristics of a PV array also change with time, implying that the neural network has to be periodically trained to guarantee accurate MPPT.

### 2.10.1.7 Ripple Correlation Control

When a PV array is connected to a power converter, the switching action of the power converter imposes voltage and current ripple on the PV array. As a consequence, the PV array power is also subject to ripple. Ripple correlation control (RCC) makes use of ripple to perform MPPT. RCC correlates the time derivative of



**Fig. 2.54** Example of neural network



the time-varying PV array power  $p$  with the time derivative of the time-varying PV array current  $i$  or voltage  $v$  to drive the power gradient to zero, thus reaching the MPP. Based on the PV array characteristics, if  $v$  or  $i$  is increasing ( $v > 0$  or  $i > 0$ ) and  $p$  is increasing ( $p > 0$ ), then the operating point is below the MPP ( $V < V_{MPP}$  or  $I < I_{MPP}$ ). On the other hand, if  $v$  or  $i$  is increasing and  $p$  is decreasing ( $p < 0$ ), then the operating point is above the MPP ( $V > V_{MPP}$  or  $I > I_{MPP}$ ). Combining these observations, we see that  $\dot{p}\dot{v}$  or  $\dot{p}\dot{i}$  are positive to the left of the MPP, negative to right of the MPP, and zero at the MPP. When the power converter is a boost converter, increasing the duty ratio increases the inductor current, which is the same as the PV array current, but decreases the PV array voltage. Therefore, the duty ratio control input is

$$d(t) = -k_3 \int \dot{p}\dot{v} dt \tag{2.18}$$

or

$$d(t) = k_3 \int \dot{p}\dot{i} dt \tag{2.19}$$

where  $k_3$  is a positive constant. Controlling the duty ratio in this fashion assures that the MPP will be continuously tracked, making RCC a true MPP tracker. The derivatives in (2.18) and (2.19) are usually undesirable, the AC-coupled measurements of the PV array current and voltage can be used instead since they contain the necessary phase information. The derivatives can also be approximated by high-pass filters with cutoff frequency higher than the ripple frequency. A different and easy way of obtaining the current derivative in (2.19) is to sense the inductor voltage, which is proportional to the current derivative. The non-idealities in the inductor (core loss, resistance) have a small effect since the time constant of the inductor is much larger than the switching period in a practical converter. Equation (2.19) can fail due to the phase shift brought about by the intrinsic capacitance of the PV array at high switching frequencies. However, correlating power and voltage as in (2.18) is barely affected by the intrinsic capacitance.

### 2.10.1.8 Current Sweep

The current sweep method uses a sweep waveform for the PV array current such that the  $I$ - $V$  characteristic of the PV array is obtained and updated at fixed time intervals. The  $V_{MPP}$  can then be computed from the characteristic curve at the same intervals. The function chosen for the sweep waveform is directly proportional to its derivative as in (2.20),

$$f(t) = k_4 \frac{df(t)}{dt} \quad (2.20)$$

where  $k_4$  is the proportionality constant. The PV array power is thus given by

$$p(t) = v(t)i(t) = v(t)f(t) \quad (2.21)$$

At the MPP,

$$\frac{dp(t)}{dt} = v(t) \frac{df(t)}{dt} + f(t) \frac{dv(t)}{dt} = 0 \quad (2.22)$$

Substituting (2.20) in (2.22) gives

$$\frac{dp(t)}{dt} = \left[ v(t) + k_4 \frac{dv(t)}{dt} \right] \frac{df(t)}{dt} = 0 \quad (2.23)$$

The differential equation in (2.20) has the following solution

$$f(t) = C e^{t/k_4} \quad (2.24)$$

$C$  is chosen to be equal to the maximum PV array current  $I_{max}$  and  $k_4$  to be negative, resulting in a decreasing exponential function with time constant  $\tau = -k_4$ . Equation (2.24) leads to

$$f(t) = I_{max} e^{-t/\tau} \quad (2.25)$$

The current in (2.25) can be easily obtained by using some current discharging through a capacitor. Since the derivative of (2.25) is nonzero, (2.23) can be divided throughout by  $df(t)/dt$  and, with  $f(t) = i(t)$ , (2.23) simplifies to

$$\frac{dp(t)}{di(t)} = v(t) + k_4 \frac{dv(t)}{dt} = 0 \quad (2.26)$$

Once  $V_{MPP}$  is computed after the current sweep, (2.26) can be used to double check whether the MPP has been reached. In literature it is been observed that the current sweep takes about 50 ms, implying some loss of available power.

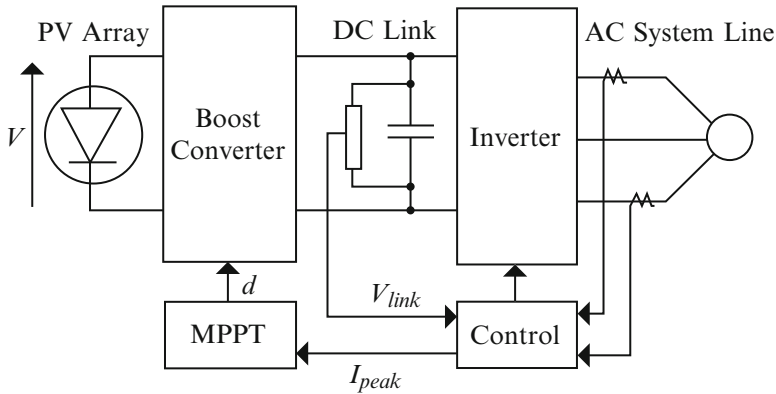


Fig. 2.55 Topology for DC-link capacitor droop control

### 2.10.1.9 DC Link Capacitor Droop Control

DC-link capacitor droop control is a MPPT technique that is specifically designed to work with a PV system that is connected in parallel with an AC system line as shown in Fig. 2.55. The duty ratio of an ideal boost converter is given by

$$d = 1 - V/V_{link} \tag{2.27}$$

where  $V$  is the voltage across the PV array and  $V_{link}$  is the voltage across the DC-link. If  $V_{link}$  is kept constant, increasing the current going in the inverter increases the power coming out of the boost converter and consequently increases the power coming out of the PV array. While the current is increasing, the voltage  $V_{link}$  can be kept constant as long as the power required by the inverter does not exceed the maximum power available from the PV array. If that is not the case,  $V_{link}$  starts drooping. Right before that point, the current control command  $I_{peak}$  of the inverter is at its maximum and the PV array operates at the MPP. The AC system line current is feedback to prevent  $V_{link}$  from drooping and  $d$  is optimized to bring  $I_{peak}$  to its maximum, thus achieving MPPT. DC-link capacitor droop control does not require the computation of the PV array power, but its response deteriorates when compared to a method that detects the power directly; this is because its response directly depends on the response of the DC voltage control loop of the inverter. This control scheme can be easily implemented with analog operational amplifiers and decision making logic units.

### 2.10.1.10 Load Current or Load Voltage Maximization

The purpose of MPPT techniques is to maximize the power coming out of a PV array. When the PV array is connected to a power converter, maximizing

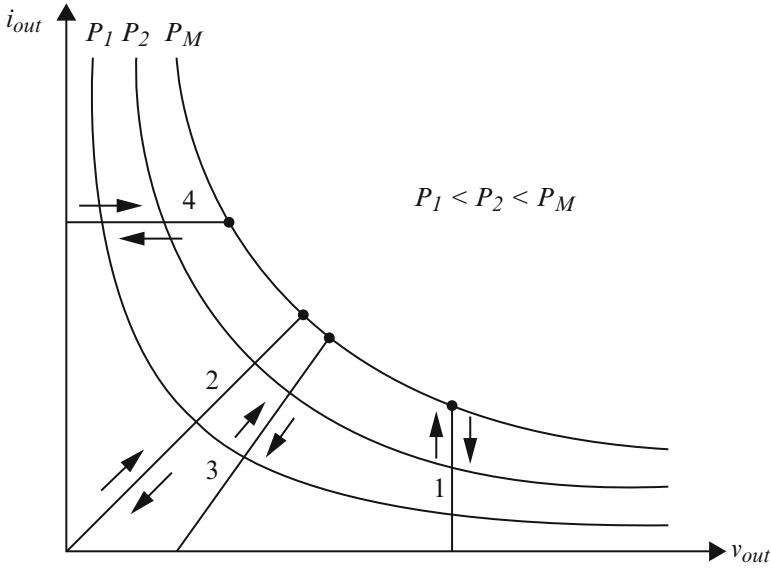


**Fig. 2.56** Different load types: 1-voltage-source, 2-resistive, 3-resistive and voltage-source, 4-current-source

the PV array power also maximizes the output power at the load of the converter. Conversely, maximizing the output power of the converter should maximize the PV array power, assuming a lossless converter. Most loads can be of voltage source type, current-source type, resistive type, or a combination of these, as shown in Fig. 2.56. From this figure, it is clear that for a voltage-source type load, the load current  $i_{out}$  should be maximized to reach the maximum output power  $P_M$ . For a current-source type load, the load voltage  $v_{out}$  should be maximized. For the other load types, either  $i_{out}$  or  $v_{out}$  can be used. This is also true for nonlinear load types as long as they do not exhibit negative impedance characteristics. Therefore, for almost all loads of interest, it is adequate to maximize either the load current or the load voltage to maximize the load power. Consequently, only one sensor is needed. In most PV systems, a battery is used as the main load or as a backup. Since a battery can be thought of as a voltage-source type load, the load current can be used as the control variable. A positive feedback can also be used to control the power converter such that the load current is maximized and the PV array operates close to the MPP. Operation exactly at the MPP is almost never achieved because this MPPT method is based on the assumption that the power converter is lossless.

#### 2.10.1.11 $dP/dV$ or $dP/dI$ Feedback Control

With DSP and microcontroller being able to handle complex computations, an obvious way of performing MPPT is to compute the slope ( $dP/dV$  or  $dP/dI$ ) of the

PV power curve and feed it back to the power converter with some control to drive it to zero. There are several methods to compute the slope.  $dP/dV$  can be computed and its sign can be stored for the past few cycles. Based on these signs, the duty ratio of the power converter is either incremented or decremented to reach the voltage-source, 4-current-source. A dynamic step size is used to improve the transient response of the system. Linearization based method can also be used to compute  $dP/dV$ . Sometimes sampling and data conversion with subsequent digital division of power and voltage are also applied to approximate  $dP/dV$ .  $dP/dI$  can then be integrated together with an adaptive gain to improve the transient response. The PV array voltage is periodically incremented or decremented and  $\Delta P/\Delta V$  is compared to a marginal error until the MPP is reached. Convergence to the MPP was shown to occur in tens of milliseconds.

With so many MPPT techniques available to PV system users, it might not be obvious for the latter to choose which one better suits their application needs. The main aspects of the MPPT techniques to be taken into consideration are highlighted in the following subsections.

### Implementation

The ease of implementation is an important factor in deciding which MPPT technique to use. However, this greatly depends on the end-users' knowledge. Some might be more familiar with analog circuitry, in which case, fractional  $I_{SC}$  or  $V_{OC}$ , RCC, and load current or voltage maximization are good options. Others might be willing to work with digital circuitry, even if that may require the use of software and programming. Then, their selection should include hill-climbing/P&O, IncCond, fuzzy logic control, neural network, and  $dP/dV$  or  $dP/dI$  feedback control. Furthermore, a few of the MPPT techniques only apply to specific topologies. For example, the DC-link capacitor droop control works with the system shown in Fig. 2.55 and the OCC MPPT works with a single-stage inverter.

### Sensors

The number of sensors required to implement MPPT also affects the decision process. Most of the time, it is easier and more reliable to measure voltage than current. Moreover, current sensors are usually expensive and bulky. This might be inconvenient in systems that consist of several PV arrays with separate MPP trackers. In such cases, it might be wise to use MPPT methods that require only one sensor or that can estimate the current from the voltage. It is also uncommon to find sensors that measure irradiance levels, as needed in the linear current control and the  $I_{MPP}$  and  $V_{MPP}$  computation methods.

## Multiple Local Maxima

The occurrence of multiple local maxima due to partial shading of the PV array (s) can be a real hindrance to the proper functioning of a MPP tracker. Considerable power loss can be incurred if a local maximum is tracked instead of the real MPP. As mentioned previously, the current sweep and the state-based methods should track the true MPP even in the presence of multiple local maxima. However, the other methods require an additional initial stage to bypass the unwanted local maxima and bring operation to close the real MPP.

## Costs

It is hard to mention the monetary costs of every single MPPT technique unless it is built and implemented. However, a good costs comparison can be made by knowing whether the technique is analog or digital, whether it requires software and programming, and the number of sensors. Analog implementation is generally cheaper than digital, which normally involves a microcontroller that needs to be programmed. Eliminating current sensors considerably drops the costs.

## Applications

Different MPPT techniques discussed above will suit different applications. For example, in space satellites and orbital stations that involve large amount of money, the costs and complexity of the MPP tracker are not as important as its performance and reliability. The tracker should be able to continuously track the true MPP in minimum amount of time and should not require periodic tuning. In this case, hill climbing/P&O, IncCond, and RCC are appropriate. Solar vehicles would mostly require fast convergence to the MPP. Fuzzy logic control, neural network, and RCC are good options in this case. Since the load in solar vehicles consists mainly of batteries, load current or voltage maximization should also be considered. The goal when using PV arrays in residential areas is to minimize the payback time and to do so, it is essential to constantly and quickly track the MPP. Since partial shading (from trees and other buildings) can be an issue, the MPPT should be capable of bypassing multiple local maxima. Therefore, the two-stage IncCond and the current sweep methods are suitable. Since a residential system might also include an inverter, the OCC MPPT can also be used. PV systems used for street lighting only consist in charging up batteries during the day. They do not necessarily need tight constraints; easy and cheap implementation might be more important, making fractional  $V_{OC}$  or  $I_{SC}$  viable. Table 2.6 summarizes the major characteristics of all the MPPT techniques.

**Table 2.6** Characteristics of MPPT techniques

MPPT technique	PV array dependent?	True MPPT?	Analog or digital?	Periodic tuning?	Convergence speed	Implementation complexity	Sensed parameters
Hill-climbing/P&O	No	Yes	Both	No	Varies	Low	Voltage, current
IncCond	No	Yes	Digital	No	Varies	Medium	Voltage, current
Fractional $V_{OC}$	Yes	No	Both	Yes	Medium	Low	Voltage
Fractional $I_{SC}$	Yes	No	Both	Yes	Medium	Medium	Current
Fuzzy logic control	Yes	Yes	Digital	Yes	Fast	High	Varies
Neural network	Yes	Yes	Digital	Yes	Fast	High	Varies
RCC	No	Yes	Analog	No	Fast	Low	Voltage, current
Current sweep	Yes	Yes	Digital	Yes	Slow	High	Voltage, current
DC-link capacitor droop control	No	No	Both	No	Medium	Low	Voltage
Load $I$ or $V$ maximization	No	No	Analog	No	Fast	Low	Voltage, current
$dP/dV$ or $dP/dI$ feedback control	No	Yes	Digital	No	Fast	Medium	Voltage, current
Array reconfiguration	Yes	No	Digital	Yes	Slow	High	Voltage, current
Linear current control	Yes	No	Digital	Yes	Fast	Medium	Irradiance
$I_{MPP}$ & $V_{MPP}$ computation	Yes	Yes	Digital	Yes	N/A	Medium	Irradiance, temperature
State-based MPPT	Yes	Yes	Both	Yes	Fast	High	Voltage, current
OCC MPPT	Yes	No	Both	Yes	Fast	Medium	Current
BFV	Yes	No	Both	Yes	N/A	Low	None
LRCM	Yes	No	Digital	No	N/A	High	Voltage, current
Slide control	No	Yes	Digital	No	Fast	Medium	Voltage, current

### ***2.10.2 MATLAB/SIMULINK Implementation of Perturb and Observe Method***

The detailed block diagram of the P&O algorithm mentioned above is constructed using MATLAB/SIMULINK and the model is shown in Fig. 2.57. Here the voltage and current inputs are sensed to compute power as shown. A saturation limit is set to monitor the increase or decrease in voltage in order to avoid oscillations in the MPP.

### ***2.10.3 MATLAB/SIMULINK Model of the Incremental Conductance Method***

The MATLAB/SIMULINK model of the incremental conductance method is shown in Fig. 2.58.

The duty cycle in both P&O and the InCond algorithms can be adjusted as shown in Fig. 2.59.

### ***2.10.4 PV Module with MPPT Techniques***

The SIMULINK model for the MPPT algorithm using incremental conductance (If P&O algorithm is required the block can be replaced accordingly) is shown in Fig. 2.60. The PV module is added from Fig. 2.9.



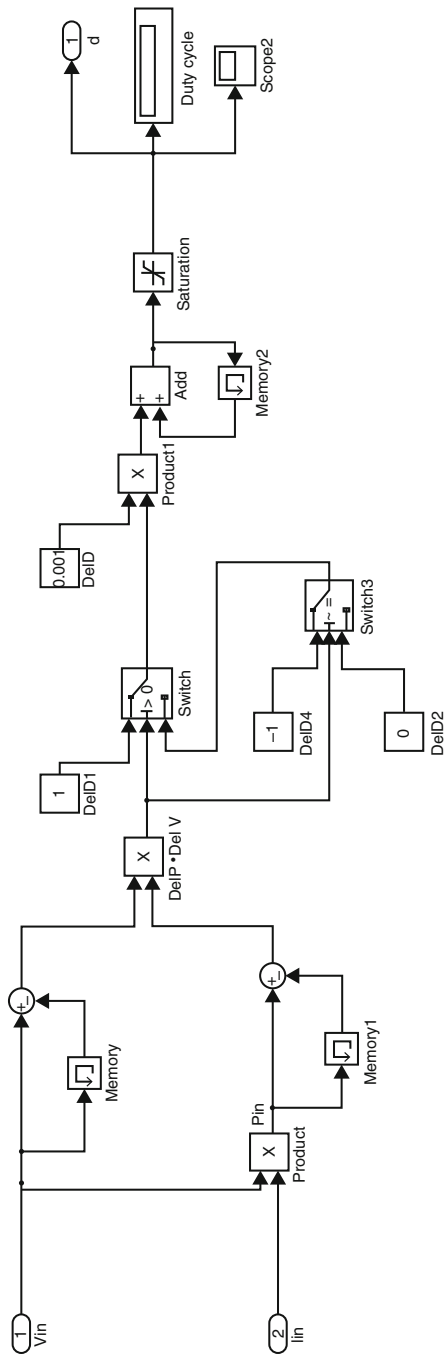


Fig. 2.57 SIMULINK model of the perturb and observe method

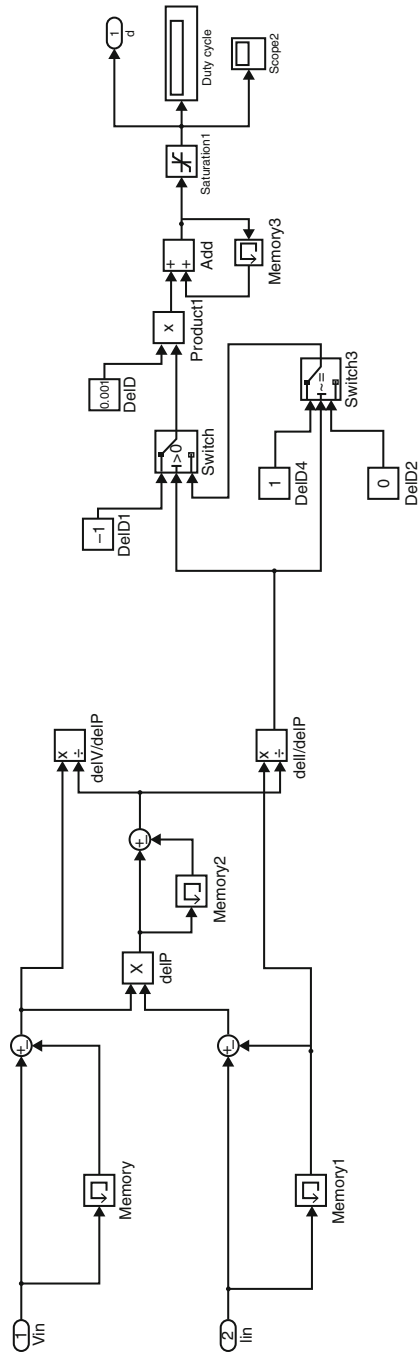


Fig. 2.58 SIMULINK model of incremental conductance method

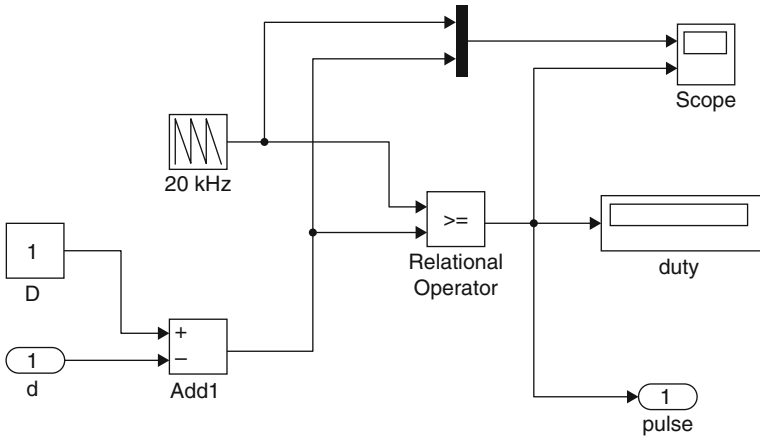


Fig. 2.59 SIMULINK model for adjusting the duty cycle

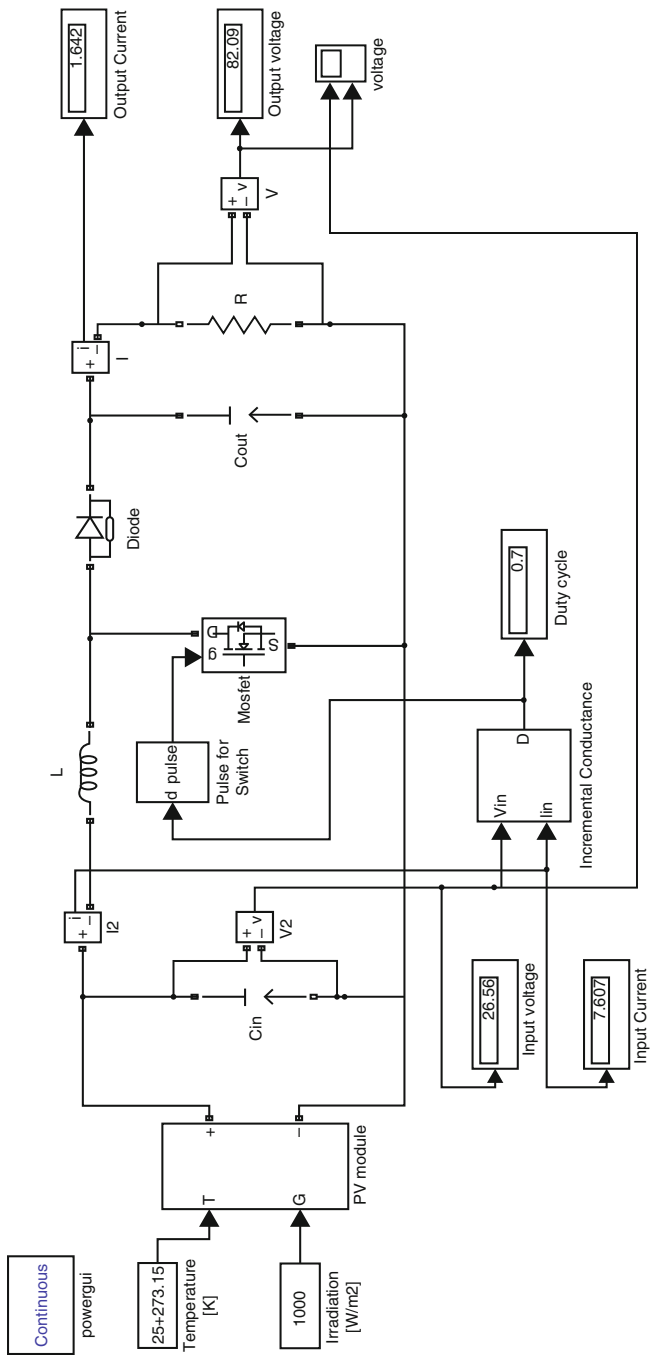
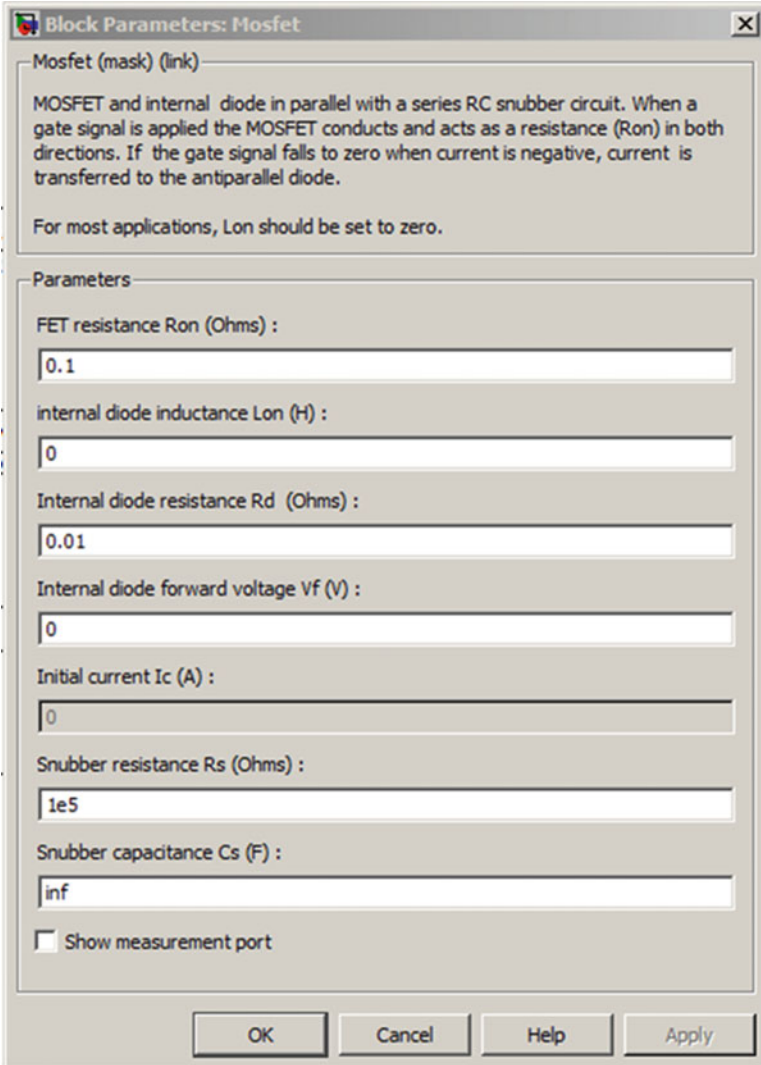


Fig. 2.60 Overall SIMULINK model

### 2.10.4.1 Blockset Used

#### MOSFET Block

The properties of the MOSFET block are shown below. The FET resistance is set to  $0.1 \Omega$  and the internal diode resistance is  $0.01 \Omega$ .



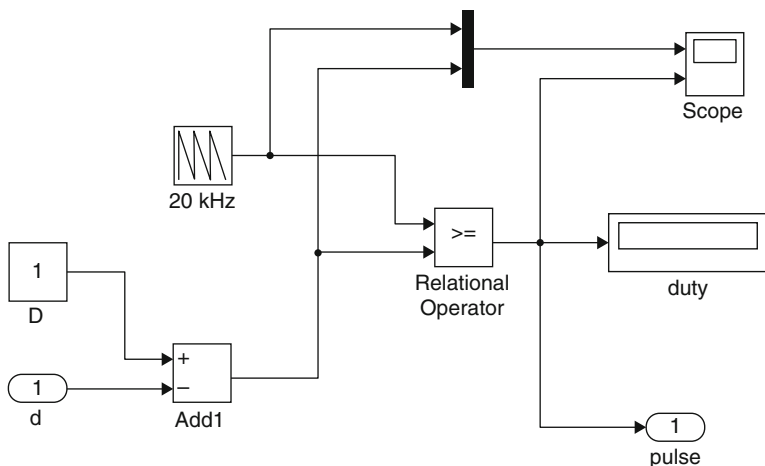


Fig. 2.61 Pulse to switch module

Pulse for Switch

The pulse for switch module is constructed using relational operator as shown in Fig. 2.61.

The parameters used in the model has the following specifications

Parameters	Value
$C_{in}$	1,000 $\mu F$
L	0.011 H
$C_{out}$	60 $\mu F$
R	50 $\Omega$
Switching frequency, $F_s$	20 kHz

2.10.4.2 Simulation Results

Figures 2.62 and 2.63 show the voltage versus time curve without the MPPT technique at temperature 25 °C with irradiation levels 1,000 W/m<sup>2</sup> and 600 W/m<sup>2</sup>. It is inferred that the output voltage obtained without MPPT technique had perturbations before obtaining the required output and the output voltage was not of the desired value. The P&O method was applied and the output was observed as shown in Figs. 2.64 and 2.65 for irradiation levels 1,000 W/m<sup>2</sup> and 600 W/m<sup>2</sup>. It is inferred that using the perturb and observe technique, when the irradiation is constant, it oscillates around the MPP value. The amplitude of the oscillations depends directly on the size of increment in the reference voltage,  $\Delta V_{ref}$ . Also, when the irradiation is constant, the corresponding MPP voltage is reached after a delay, which depends on the size of  $\Delta V_{ref}$ . The P&O block was replaced using the

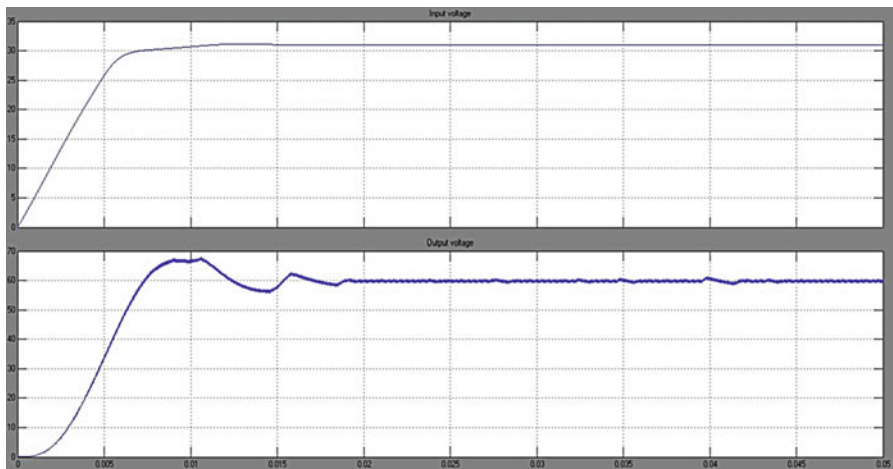


**Fig. 2.62** Voltage versus time curve without MPPT technique at temperature 25 °C and irradiance 1,000 W/m<sup>2</sup>

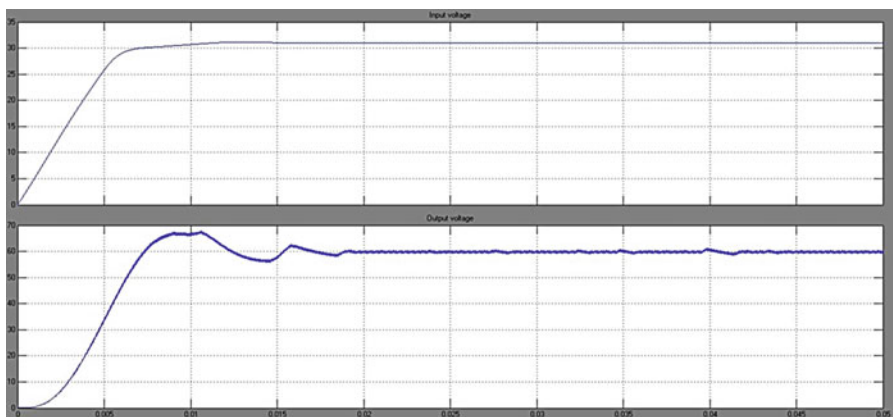


**Fig. 2.63** Voltage versus time curve without MPPT technique at temperature 25 °C and irradiance 600 W/m<sup>2</sup>

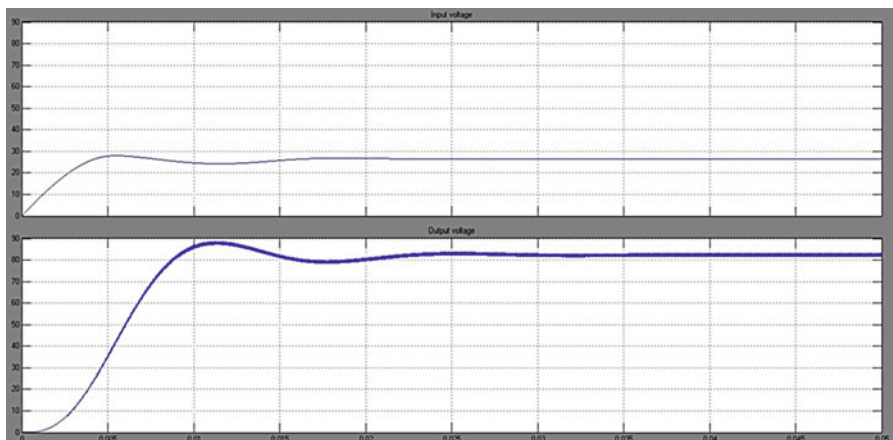


**Fig. 2.64** Voltage versus time curve with P&O MPPT technique with temperature 25 °C and irradiance 1,000 W/m<sup>2</sup>

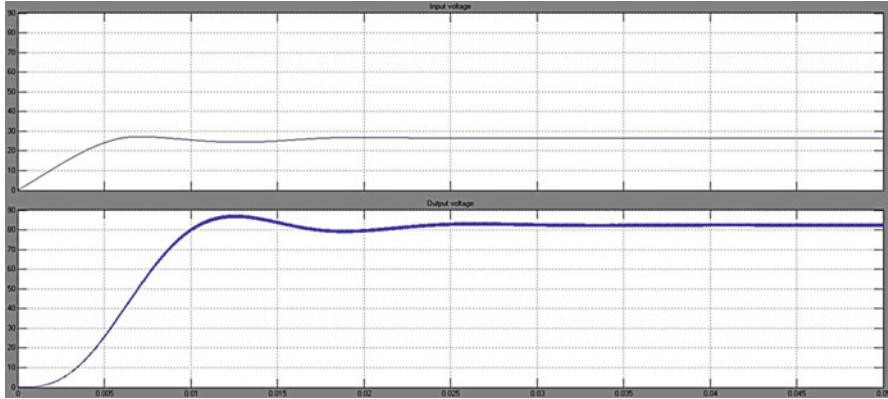


**Fig. 2.65** Voltage versus time curve with P&O MPPT technique with temperature 25 °C and irradiance 600 W/m<sup>2</sup>

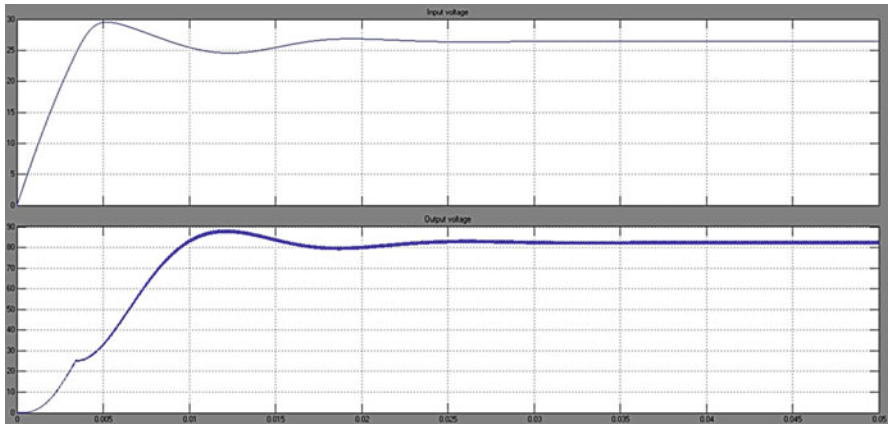


**Fig. 2.66** Voltage versus time curve with In Cond MPPT technique with temperature 25 °C and irradiance 1,000 W/m<sup>2</sup>

InCond technique and the output was observed as shown in Figs. 2.66 and 2.67. The results are almost practically the same. Simulations were carried out by varying the irradiation levels from 1,000 W/m<sup>2</sup> to 600 W/m<sup>2</sup>. Figure 2.68 shows the Voltage versus Time curve with P&O MPPT technique and Fig. 2.69 shows the Voltage versus Time curve with In Cond MPPT technique. In this case the tracking is adequate, which demonstrates that irradiation step changes do not pose a challenge to the hill-climbing algorithms and are not suitable for testing MPPT. As expected, the convergence speed, i.e. how fast the steady state is reached, and the amplitude of the oscillations are a trade off, as both cannot be improved at the same time: if one is reduced the other increases, because both depend directly on the size of the voltage increment.



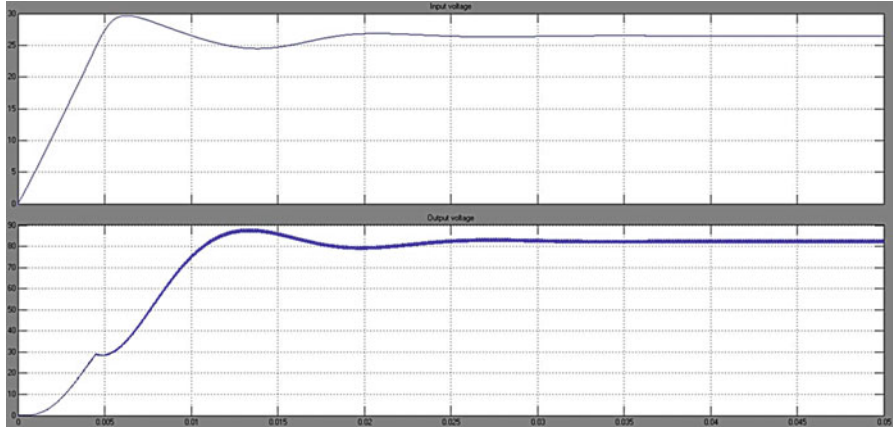


**Fig. 2.67** Voltage versus time curve with In Cond MPPT technique with temperature 25 °C and irradiance 600 W/m<sup>2</sup>

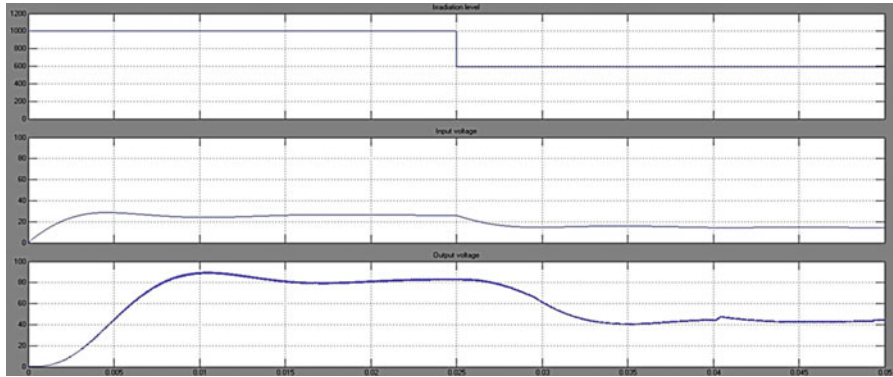


**Fig. 2.68** Voltage versus time curve with P&O MPPT technique with temperature 25 °C and variation in irradiation from 1,000 W/m<sup>2</sup> to 600 W/m<sup>2</sup>

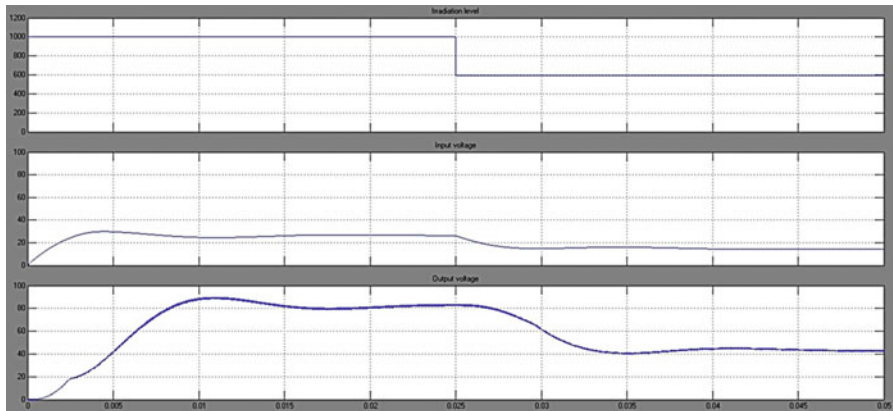


**Fig. 2.69** Voltage versus time curve with In Cond MPPT technique with temperature 25 °C and variation in irradiation from 1,000 W/m<sup>2</sup> to 600 W/m<sup>2</sup>

## 2.11 Summary

Solar PV is used primarily for grid-connected electricity to operate residential appliances, commercial equipment, lighting and air conditioning for all types of buildings. Through stand-alone systems and the use of batteries, it is also well suited for remote regions where there is no electricity source. Solar PV panels can be ground mounted, installed on building rooftops or designed into building materials at the point of manufacturing. This chapter discussed the solar PV array, batteries, charge controllers, inverters, power conditioning unit and MPPT techniques along with their MATLAB/SIMULINK modules. The future will see everyday objects such as clothing, the rooftops of cars and even roads themselves turned into power-generating solar collectors.

### Review Questions

1. Mention the major components of a PV system.
2. Differentiate between grid connected and stand-alone PV systems.
3. What is the need for batteries in stand-alone PV systems?
4. What are the considerations for installing PV arrays on rooftops?
5. List the consequences of shading in PV arrays.
6. How are stand-alone PV systems sized?
7. Differentiate between PWM charge controller and MPPT charge controller.
8. Develop a MATLAB/SIMULINK model for a PV system using micro inverters.
9. Design a full bridge inverter using MATLAB/SIMULINK.
10. Design and simulate a PV module using fuzzy based MPPT algorithm using MATLAB/SIMULINK.

### Bibliography

- Ahmed MM, Sulaiman M (2003) Design and proper sizing of solar energy schemes for electricity production in Malaysia. National Power and Energy Conference 2003, pp 268–271
- Akhter R, Hoque A (2008) Analysis of a PWM boost inverter for solar home application. World Acad Sci Eng Technol 23
- Anegawa T (2010) Characteristics of CHAdEMO quick charging system. In: Proceedings of the EVS-25 Shenzhen, 5–9 Nov 2010
- Ardente F, Beccali G, Cellura M (2004) Life cycle assessment of a solar thermal collector. Science Direct
- Atlas H, Sharaf AM (2007) A photovoltaic array simulation model for matlab-simulink GUI environment. In: Proceedings of IEEE international conference on clean electrical power, ICCEP 2007, Capri
- AVA Solar website (2008) IEEE standard for interconnecting distributed resources with electric power systems, New York: IEEE, IEEE Std.1547–2003. <http://www.avasolar.com>. Accessed June 2008.

- Ayob SM, Yee CH, Muhamad ND, Jusoh A (2005) A new hybrid multilevel inverter topology with harmonics profile improvement. *IEEE Trans Power Electron Drives Syst*, ISSN: 0-7803-9296-5/05, pp 999–1002
- Baldsing et al (1991) Lead-acid batteries for remote area energy storage. CSIRO Australia, Jan 1991
- Banerjee S, Jeevanathan (2010) Modeling of PV array and performance enhancement by MPPT algorithm. *Int J Comput Appl* 7:35–39 (0975–8887)
- Bechtel National (1980) Handbook for battery energy storage in photovoltaic power systems, Final report, SAND80-7022, Feb 1980
- Borowy BS, Salameh ZM (1996) Methodology for optimally sizing the combination of a battery bank and PV array in a wind/PV hybrid system. *IEEE Trans Energy Conv* 11(2):367–375
- “Buck Converter Design Example”, Microchip WebSeminar, Microchip Technology Incorporated. All Rights Reserved (2006). Microchip Web Sites: [www.microchip.com/smps](http://www.microchip.com/smps)
- Calais M, Agelidis V (1998) Multilevel converters for single phase grid connected photovoltaic systems, an overview. *IEEE Int Symp Ind Electron* 7–10:224–229
- Cavalcanti MC, de Oliveira KC, Neves FAS, Azevedo GMS (2010) Modulation techniques to eliminate leakage currents in transformer less three-phase photovoltaic systems. *IEEE Trans Ind Electron* 57(4)
- Chang HC, Liaw CM (2009) Development of compact switched reluctance motor drive for EV propulsion with voltage-boosting and PFC charging capabilities. *IEEE Trans Veh Technol* 58:3198–3215
- Chen A, He X (2006) Research on hybrid-clamped multilevel inverter topologies. *IEEE Trans Ind Electron* 53(6):1898–1906
- Chowdhury AA, Koval DO (2005) Impact of photovoltaic power sources on a power system’s capacity reliability levels. *I&CPS*
- Chowdhury BH, Rahman S (1988) Is central power station photovoltaic power dispatchable? *IEEE Trans Energy Convers* 3(42):747–754
- Conti S, Raiti S, Tina G, Vagliasindi U (2003) Integration of multiple PV units in urban power distribution systems. *Sol Energy* 75:87–94
- Corzine KA, Wielebski MW, Peng FZ, Wang J (2004) Control of cascaded multilevel inverter. *IEEE Trans Power Electron* 19(3):732–738
- Davidson J, *The new solar electric home*, 20th printing 2001
- Duffie JA, Beckman WA (2006) *Solar engineering of thermal processes*, 3rd edn. Wiley, New York
- Dunlop JP (1997) Batteries and charge control in stand alone photovoltaic systems, Jan 1997
- Dunlop J, Bower W, Harrington S (1991) Performance of batter charge controllers: first year test report. In: *Proceedings of the 22nd IEEE photovoltaic specialists conference*, Las Vegas, Nevada, 7–11 Oct 1991
- Egan MG, O’Sullivan DL, Hayes JG (2007) Power-factor-corrected single-stage inductive charger for electric vehicle batteries. *IEEE Trans Ind Electron* 54:1217–1226
- Enslin JHR, Snyman DB (1991) Combined low-cost, high-efficient inverter, peak power tracker and regulator for PV applications. *IEEE Tran Power Electron* 6(1):73–82
- Esrat T, Chapman PL (2007) Comparison of photovoltaic array maximum power point tracking techniques. *IEEE Trans Energy Convers* 22(2):439–449
- Exide Management and Technology Company (1981) Handbook of secondary storage batteries and charge controllers in photovoltaic systems – final report, for Sandia National Laboratories, SAND81-7135, Aug 1981
- Ghani ZA, Hannan MA, Mohamed A (2012) Simulation model linked PV inverter implementation utilizing dSPACE DS1104 controller. Elsevier
- Gounden NA, Peter SA, Nallandula H, Krithiga S (2009) Fuzzy logic controller with MPPT using line-commutated inverter for three-phase grid-connected photovoltaic systems. *Renew Energy* 34:909–915

- Hagbini S, Khan K (2010) Integrated chargers for EV's and PHEV's: examples and new solutions. In: Proceedings of ICEM, pp 1–6, Sept 2010
- Haiwen Liu, Leon M Tolbert, Surin Khomfoi, Burak Ozpineci, Zhong Du (2008) Hybrid cascaded multilevel inverter with PWM control method. IEEE, pp 162–166
- Harrington S, Dunlop J (1992) Battery charge controller characteristics in photovoltaic systems. In: Proceedings of the 7th annual battery conference on advances and applications. Long Beach, California, 21 Jan 1992
- Hart DW (1997) Introduction to power electronics. Prentice Hall, New Jersey  
[http://inventors.about.com/od/pstartinventions/ss/photovoltaic\\_cel\\_8.htm](http://inventors.about.com/od/pstartinventions/ss/photovoltaic_cel_8.htm)  
<http://www.solarbuzz.com/Technologies.htm>  
<http://www.ren21.net>. Accessed June 2008
- Huan-Liang Tsai, Ci-Siang Tu, Yi-Jie Su *Member, IAENG* (2008) Development of generalized photovoltaic model using MATLAB/SIMULINK. In: Proceedings of the world congress on engineering and computer science 2008 WCECS, 22–24 Oct 2008
- Hussein KH, Muta I, Hoshino T, Osakada M (1995) Maximum photovoltaic power tracking: an algorithm for rapidly changing atmospheric conditions. IEE Proc Gener Trans Distrib 142 (1):59
- IEEE recommended practice for utility interface of photovoltaic system, IEEE Std. 929–2000
- Institute of Electrical and Electronics Engineers (1987) IEEE recommended practice for installation and operation of lead-acid batteries for photovoltaic (PV) systems. ANSI/IEEE Std. 937–1987, New York
- Institute of Electrical and Electronics Engineers (1990) IEEE recommended practice for installation and operation of nickel-cadmium batteries for photovoltaic (PV) systems. ANSI/IEEE Std. 1145–1990, New York
- International Rectifier Application Note AN-978  
 IR2112 Datasheet
- Jäger-Waldau A (2007) PV status report 2007: research, solar cell production and market implementation of photovoltaics. European Commission Directorate General Joint Research Center. [http://re.jrc.ec.europa.eu/refsys/pdf/PV\\_StatusReport\\_2007.pdf](http://re.jrc.ec.europa.eu/refsys/pdf/PV_StatusReport_2007.pdf). Accessed June 2008
- Jenkins N (1995) Photovoltaic systems for small scale remote power supplies. Power Eng J 9 (2):89–96
- Jewell WT, Uaruh TD (1990) Limits on cloud-induced fluctuations in photovoltaic generation. IEEE Trans Energy Convers 5(1):8–14
- Jiang A et al (2005) Maximum power tracking for photovoltaic power systems. Tamkang J Sci Eng 8(2):147–153
- Jianye Rao, Yongdong Li (2008) High-performance control strategies and applications of a new hybrid cascaded multilevel inverter. ISSN: 978-14244-2279-1/08, pp 1–5
- Kannan R, Leong K, Osman R (2005) “Life Cycle Assessment” study of solar PV systems: an example of a 2.7 kWp distributed solar PV system in Singapore. Science Direct
- Kern EC, Gulachenski EM, Kern GA (1989) Cloud effects on distributed photovoltaic generation: slow transients at the Gardner, Massachusetts photovoltaic experiment. IEEE Trans Energy Convers 4(2):184–190
- Khomfoi S, Aimsaard C (2009) A 5-level cascaded hybrid multilevel inverter for interfacing with renewable energy resources. IEEE, 978-1-4244-3388-9
- Khomfoi S, Praisuwanna N (2010) A hybrid cascaded multilevel inverter for interfacing with renewable energy resources. IEEE, 978-1-4244-5393-1/10/2010
- Kiehne HA (1989) Battery technology handbook. Marcel Dekker, New York
- Kleinkauf W, Cramer G, Ibrahim M (2005) PV systems technology: state of the art developments and trends in remote electrification. SMA Technologies AG
- Koutroulis E et al (2001) Development of a microcontroller-based photovoltaic maximum power tracking control system. IEEE Trans Power Electron 16(1):46–54
- Kutkut NH, Divan DM, Novotny DW, Marion RH (1998) Design considerations and topology selection for a 120-kW IGBT converter for EV fast charging. IEEE Trans Power Electron 13:169–178

- Ladner-Garcia HP, O'Neill-Carrillo E (2008) Demonstrative PV systems for an isolated system. In: Proceedings of the 10th IASTED international conference on power and energy systems
- Liang TJ, Kuo YC, Chen JF (2001) Single-stage photovoltaic energy conversion system. *Proc Inst Elect Eng* 148(4):339–344
- Linden D (1984) Handbook of batteries and fuel cells. McGraw Hill, New York
- Luque A, Hegedus S (2003) Handbook of photovoltaic science and engineering. Wiley, New York
- Maimone G (2010) Application note. Selecting L and C components in the power stage of the MC34700 switching regulators. Freescale Semiconductor, AN4067 Rev. 1.0, 11/2010
- Markvart T, Castañer L (2003) Practical handbook of photovoltaics: fundamentals and applications. Elsevier Advanced Technology, Oxford
- Musavi F, Eberle W, Dunford WG (2010) Efficiency evaluation of single-phase solutions for AC-DC PFC boost converters for plug-in hybrid electric vehicle battery chargers. In: Proceedings of IEEE VPPC, pp 1–6, Sept 2010
- Navigant Consulting (2006) A review of PV inverter technology cost and performance projections NREL/SR-620-38771, Jan 2006. [www.nrel.gov](http://www.nrel.gov). Accessed June 2008
- Orosco R, Vazquez N (2000) Discrete sliding mode control for DC/DC converters. *Power Electronics Congress* 231–236
- Ozpineci B, Chinthavali MS, Tolbert LM, Kashyap A, Mantooth HA (2009) A 55 kW three-phase inverter with Si IGBTs and SiC Schottky diodes. *IEEE Trans Ind Appl* 45(1):278–285
- Qin YC, Mohan N, West R, Bonn R (2002) Status and needs of power electronics for photovoltaic inverters. SAND2002-1535, Unlimited Release, June 2002
- Ramakumar R (1993) Photovoltaic systems. *Proc IEEE* 81(3):365–376
- Rashid MH (2006) Power electronics devices, circuits and applications. Academic Press, San Diego
- Saravana Ilango G, Srinivasa Rao P, Karthikeyan A, Nagamani C Single-stage sine-wave inverter for an autonomous operation of solar Photo voltaic energconversion system
- Solero L (2001) Nonconventional on-board charger for electric vehicle propulsion batteries. *IEEE Trans Veh Technol* 50:144–149
- Teodorescu R, Blaabjerg F, Pedersen JK, Cengcelci E, Enjeti PN (2002) Multilevel inverter by cascaded industrial VSI. *IEEE Trans Ind Electron* 49(4):832–834
- Vinal GW (1954) Storage batteries, 4th edn. Wiley, New York
- Waldau A (2007) PV status report 2007\_Research, solar cell production and market implementation of photovoltaics
- Xue Y, Chang L, Kjaer S, Bordonau J, Shimizu T (2004) Topologies of single-phase inverters for small distributed power generators: an overview. *IEEE Trans Power Electron* 19(5):1305–1314



<http://www.springer.com/978-3-319-14940-0>

Solar PV and Wind Energy Conversion Systems  
An Introduction to Theory, Modeling with MATLAB/SIMULINK,  
and the Role of Soft Computing Techniques  
Sumathi, S.; Ashok Kumar, L.; Surekha, P.  
2015, XXIV, 790 p. 677 illus., 334 illus. in color.,  
Hardcover  
ISBN: 978-3-319-14940-0